Neuroscience and Biobehavioral Reviews 118 (2020) 538–567

Contents lists available at ScienceDirect

Neuroscience and Biobehavioral Reviews

journal homepage: www.elsevier.com/locate/neubiorev

Review article

Dosage-sensitive genes in autism spectrum disorders: From neurobiology to therapy

Sehrish Javed, Tharushan Selliah, Yu-Ju Lee, Wei-Hsiang Huang *

Centre for Research in Neuroscience, Department of Neurology and Neurosurgery, The Research Institute of the McGill University Health Centre, Montréal, Québec, Canada

ARTICLE INFO

Keywords:
Autism
Copy number variants
Dose-sensitive genes
Epilepsy
Mouse models
Neurodevelopment
Obesity
Repetitive behavior
Social interaction

ABSTRACT

Autism spectrum disorders (ASDs) are a group of heterogenous neurodevelopmental disorders affecting 1 in 59 children. Syndromic ASDs are commonly associated with chromosomal rearrangements or dosage imbalance involving a single gene. Many of these genes are dosage-sensitive and regulate transcription, protein homeostasis, and synaptic function in the brain. Despite vastly different molecular perturbations, syndromic ASDs share core symptoms including social dysfunction and repetitive behavior. However, each ASD subtype has a unique pathogenic mechanism and combination of comorbidities that require individual attention. We have learned a great deal about how these dosage-sensitive genes control brain development and behaviors from genetically-engineered mice. Here we describe the clinical features of eight monogenic neurodevelopmental disorders caused by dosage imbalance of four genes, as well as recent advances in using genetic mouse models to understand their pathogenic mechanisms and develop intervention strategies. We propose that applying newly developed quantitative molecular and neuroscience technologies will advance our understanding of the unique neurobiology of each disorder and enable the development of personalized therapy.

1. Introduction

Autism spectrum disorders (ASDs) are early-onset neurodevelopmental disorders characterized by two core behavioral features: impaired social interaction and stereotyped behaviors. By definition, impaired social interaction comprises of problems in maintaining reciprocal social or emotional interactions, maintaining relationships, and nonverbal communication. As for the stereotyped behaviors, at least two of the following symptoms must be present: stereotyped or repetitive speech, use of objects or motor movement, adherence to routines, ritualized patterns of behavior, inflexibility in behavior, and highly restricted interests (DSM-5, 2013). The strong genetic component of ASDs was demonstrated by twin studies that found that the individual risk for ASDs dramatically increases with genetic relatedness. Specifically, monozygotic twins show a 70–90 % concordance rate, several-fold higher than the concordance rate of dizygotic twins (0–10 %) (Folstein and Rutter, 1977; Sandin et al., 2014; Steffenburg et al., 1989). A child with an affected sibling is 25-fold more likely to be diagnosed with ASDs than the general population (Jorde et al., 1991). Clinically, ASDs are categorized into idiopathic and syndromic ASDs. Idiopathic ASD patients show the core behavioral features and represent the majority (90~95 %) of ASD cases (de la Torre-Ubieta et al., 2016d). Idiopathic ASDs are likely caused by multiple common genetic variants, each has a small effect on ASD risk (Gaugler et al., 2014). An example is *de novo* copy number variants (CNVs) that account for 5–8 % of idiopathic ASDs (Gilman et al., 2011; Levy et al., 2011; Sanders et al., 2011). CNVs are unbalanced genomic rearrangements such as chromosomal deletion and duplication spanning anywhere between 100 base pairs (bp) to 5 megabase pairs (Mb) (Carvalho and Lupski, 2016; Sebat et al., 2007, 2004). Therefore, CNVs often affect tens to hundreds of genomic loci, each carry an unknown contribution to ASD risk and present a critical challenge to experimentally dissect the clinical contribution of each locus (de la Torre-Ubieta et al., 2016d). As a result, we have little knowledge of its etiology and therapeutic options are limited (Ghosh et al., 2013; Lovaas, 1987).

Clear progress in understanding the etiology of ASDs stems from studying the genetically-defined syndromic ASDs that collectively account for 5% of ASD cases (Tammimies et al., 2015). In addition to the core features of ASDs, syndromic ASDs show comorbidities ranging from facial dysmorphia, language deficits, obesity, epilepsy, to motor

* Corresponding author.
E-mail address: wei-hsiang.huang@mcgill.ca (W.-H. Huang).

https://doi.org/10.1016/j.neubiorev.2020.08.009
Received 6 May 2020; Received in revised form 26 July 2020; Accepted 17 August 2020
Available online 25 August 2020

problems (Table 1). Genetically, syndromic ASDs are caused by a small number of highly penetrant rare genetic variants. Importantly, CNVs and point mutations are the main causes of syndromic ASDs (Sztainberg and Zoghbi, 2016). The penetrance of these disease features is variable but is often associated with dosage imbalance in single genes (Durand et al., 2007; Slager et al., 2003). This offers an excellent opportunity to decipher the neurobiological mechanism by which gene dosage imbalance affects brain development and function. A hallmark of the monogenic CNV disorders is that deletion and duplication of the same genes result in clinically distinct syndromes that share common endpoints including autistic features, epilepsy, and cognitive deficits. Here, we summarize genetics and clinical features of four pairs of monogenic ASDs caused by gene dosage imbalance and discuss recent progress using mouse models to uncover their pathogenic mechanisms at molecular, neuronal, and behavioral levels. Finally, we review recent progress and challenges in therapeutic interventions for monogenic ASDs that may guide future research efforts.

2. Smith-Magenis Syndrome versus Potocki-Lupski Syndrome

2.1. Genetics and clinical features

The human chromosome 17 is enriched with protein-coding genes and has a complex rearrangement architecture, predisposing chromosome 17 to non-allelic homologous recombination (NAHR) (Zody et al., 2006). As a result, chromosome 17 is responsible for an array of human CNV disorders including Smith-Magenis Syndrome (SMS, OMIM# 182, 290) (Smith et al., 1986) and Potocki-Lupski Syndrome (PTLS, OMIM#610,883) (Potocki et al., 2000). SMS and PTLS are caused by reciprocal microdeletion and microduplication of the same genomic region on chromosome 17p11.2. They have a similar prevalence (1 in 15,000) with no gender differences (Greenberg et al., 1991; Liu et al., 2011). Intriguingly, SMS and PTLS share several similar clinical manifestations but some disease features have the characteristics of "mirror traits" that are on the opposite ends of the spectrum (Lupski, 2015).

SMS patients show prominent neurological and psychiatric problems including infantile hypotonia, intellectual disability, sleep disturbance, EEG abnormalities and epilepsy, obesity, peripheral neuropathy, and self-injurious and aggressive behaviors (Burns et al., 2010; Goldman et al., 2006; Greenberg et al., 1991; Gropman et al., 2006; Smith et al., 1986). Nearly all SMS patients meet the diagnostic criteria of ASD and show stereotypies, expressive language delays, poor social awareness, and social communication deficits (Table 1) (Gropman et al., 2006; Laje et al., 2010; Oliver et al., 2011). Most SMS cases (70 %) are caused by an NAHR-induced 3.7 Mb interstitial deletion of 17p11.2 between proximal and distal SMS-repeat clusters (Greenberg et al., 1991). The remaining SMS patients either carry *de novo* germline mutations of *Retinoic Acid-Induced 1* (*RAI1*) gene (10 %) or have other *RAI1*-containing deletions (20 %) (Bi et al., 2004b; Girirajan et al., 2005, 2006; Slager et al., 2003). Together, this demonstrates that *RAI1* is the dosage-sensitive gene responsible for SMS. In addition to germline *RAI1* mutations, somatic mosaic 17p11.2 deletion (Goh et al., 2014) and *RAI1* point mutations inherited from mosaic parents (Acquaviva et al., 2017) have also been discovered. Furthermore, CNVs and *de novo* mutations of *RAI1* have been uncovered in idiopathic ASD patients (Satterstrom et al., 2020; van der Zwaag et al., 2009).

The majority (70 %) of PTLS patients carry an NAHR-induced recurrent 17p11.2 microduplication reciprocal to the 3.7 Mb common SMS microdeletion (Chen et al., 1997; Potocki et al., 2007, 2000). The remaining non-recurrent cases (30 %) have breakpoints that map to the

Table 1
Shared and disease-specific clinical features of gene dosage-sensitive ASDs.

	Disease Pairs [OMIM]	Dosage-sensitive genes	Clinical Features			References
			Specific to deletion or duplication	Common to the disease pairs	Common to all	
1	**Smith-Magenis Syndrome [182290]**	*RAI1* deletion	Obesity, poor social awareness, self-injurious and aggressive behavior, poor short-term memory, attention seeker, decreased sensitivity to pain, lethargy in infancy, minor skeletal and craniofacial features	Learning deficits, failure to thrive, anxiety, attention deficits, memory deficits, hyperactive	Infantile hypotonia, developmental delay, speech & language delays, Intellectual disabilities, motor deficits, seizures[a], stereotypies	(Burns et al., 2010; Goldman et al., 2006; Gropman et al., 2006)
	Potocki-Lupski Syndrome [610883]	*RAI1* duplication	Underweight, hypoglycemia, cardiovascular anomalies,sleep disorder breathing and apnea, working memory deficits			(Bissell et al., 2018; Kaplan et al., 2019; Potocki et al., 2007, 1993)
2	**Rett Syndrome [312750]**	*MECP2* deletion	Developmental regression, seizures, ataxia, gait apraxia, hyperventilation in wakefulness, weight loss, mood swings, cardiac abnormalities, scoliosis, breathing disturbance	Poor motor control, anxiety		(Chahrour and Zoghbi, 2007; Han et al., 2012; Young et al., 2007)
	***MECP2* Duplication Syndrome [300260]**	*MECP2* duplication	Progressive spasticity, mild dimorphic facial features, recurrent infection			(Ramocki et al., 2010)
3	**Phelan-McDermid Syndrome [606232]**	*SHANK3* deletion	Decreased perspiration, decreased pain perception, mouthing & chewing non-food items, sleep disturbance	Minor dysmorphic facial features		(Ingiosi et al., 2019; Moessner et al., 2007; Phelan et al., 1993)
	22q13 Duplication Syndrome [615538]	*SHANK3* duplication	Attention deficits hyperactivity disorder, destructive behavior, hyperkinesis, auditory overstimulation, hyperphagia, bipolar disorder			(Han et al., 2013)
4	**Angelman Syndrome [105830]**	*UBE3A* deletion	Sleep disturbance, cerebral palsy, excessive happy behavior, jerky movement, hypopigmented skin	Ataxia, microcephaly		(Cassidy et al., 2000; Hogart et al., 2010; Williams, 2005)
	Dup15q Syndrome [608636]	*UBE3A* duplication	Infantile spasm, abnormal facial features, anxiety, emotional lability, tantrums, hyperactivity			(Hogart et al., 2010; LaSalle et al., 2015; Thomas et al., 1999; Urraca et al., 2013)

[a] Except PTLS.

17p centromere or the pericentromeric regions. Although PTLS patients with *RAI1*-only duplication have not been identified, the smallest genomic overlapping region among PTLS patients has been narrowed down to a 125 kilobase (kb) interval containing only *RAI1* (Zhang et al., 2010). Mounting genetic and clinical evidence support the idea that brain function is exquisitely sensitive to *RAI1* dosage. Similar to SMS, PTLS patients are characterized with infantile hypotonia, failure to thrive, intellectual disability, language impairment, and autistic features (Table 1) (Nakamine et al., 2008; Potocki et al., 2007). Although both disorders are associated with sleep disturbance, most SMS patients show an inversion of melatonin cycle (Boone et al., 2011), while PTLS patients have a milder sleep disturbance (Kaplan et al., 2019). Features like cardiac defects and sleep-disordered breathing are common to PTLS but not SMS (Kaplan et al., 2019; Sanchez-Valle et al., 2011; Yusupov et al., 2011). A stark contrast of SMS and PTLS patients is their body weight. When compared to the general population, PTLS patients have significantly lower body weight and length and show lowered total cholesterol and low-density lipoprotein (LDL) levels (Potocki et al., 2007; Soler--Alfonso et al., 2011). By contrast, the majority of SMS patients show hypercholesterolemia, increased LDL, hyperphagia, and obesity by adolescence (Smith et al., 2002), highlighting an important role for CNVs in body weight homeostasis. Some PTLS patients have milder facial dysmorphia and behavioral problems including atypicality, withdrawal, anxiety, and inattention (Treadwell-Deering et al., 2010). Due to the mild phenotypes, some PTLS cases go undiagnosed until the patient transmitted the allele to their offspring (Magoulas et al., 2014; Yusupov et al., 2011).

2.2. Expression and molecular function of Rai1

The mouse *Rai1* gene was initially cloned based on its induction with retinoic acid during neuronal differentiation of a mouse carcinoma cell line (Imai et al., 1995). Mouse Rai1 protein is widely expressed by many tissues but is particularly enriched in the brain (Fragoso et al., 2015; Imai et al., 1995; Seranski et al., 2001). During development, Rai1 expression is detected in the branchial arch that develops into craniofacial structures at embryonic day 9.5 (E9.5) (Bi et al., 2005; Huang et al., 2016b). In E18.5 cortex, Rai1 is upregulated in the postmitotic neurons, suggesting a role in neuronal differentiation (Huang et al., 2016b). Rai1 mRNA level increases during prenatal development, peaks around 1 week after birth, and persists into adulthood (Huang et al., 2016b). In the adult cortex, 75 % of excitatory neurons, 60 % of inhibitory neurons, and a small number of glial cells express Rai1 (Huang et al., 2016b). While the developmental function of Rai1 has been demonstrated with germline deletion, the function of Rai1 in the adult brain remains unclear. In summary, Rai1 is expressed in many cell types in the brain, with an onset that parallels neuronal differentiation.

Human RAI1 protein contains 1906 residues and is localized in the nucleus, with several regions showing homology to the transcriptional co-activator stromelysin-1 platelet-derived growth factor-responsive element-binding protein/transcription factor 20 (SPBP/TCF20) (Bi et al., 2004a; Rekdal et al., 2000). Human RAI1 and mouse Rai1 share highly similar protein structures (82 % overall sequence identity), both contain nuclear localization signals, a nucleosome binding domain (NBD), and an extended atypical plant homeodomain (ePHD) found in many eukaryotic chromatin regulators (Fig. 1**A**) (Bi et al., 2005, 2004a; Darvekar et al., 2013; Huang et al., 2016b; Slager et al., 2003). *In vitro* studies revealed that overexpressed RAI1 protein associates with nuclear structures with high affinity (Darvekar et al., 2012). Human RAI1 and mouse Rai1 NBDs are highly identical (88 % identity) and can interact with purified HeLa nucleosomes *in vitro* (Darvekar et al., 2013; Huang et al., 2016b). These features suggest that Rai1 may regulate gene expression. Chromatin immunoprecipitation (ChIP)-sequencing and RNA-sequencing experiments show that in the mouse brain, Rai1

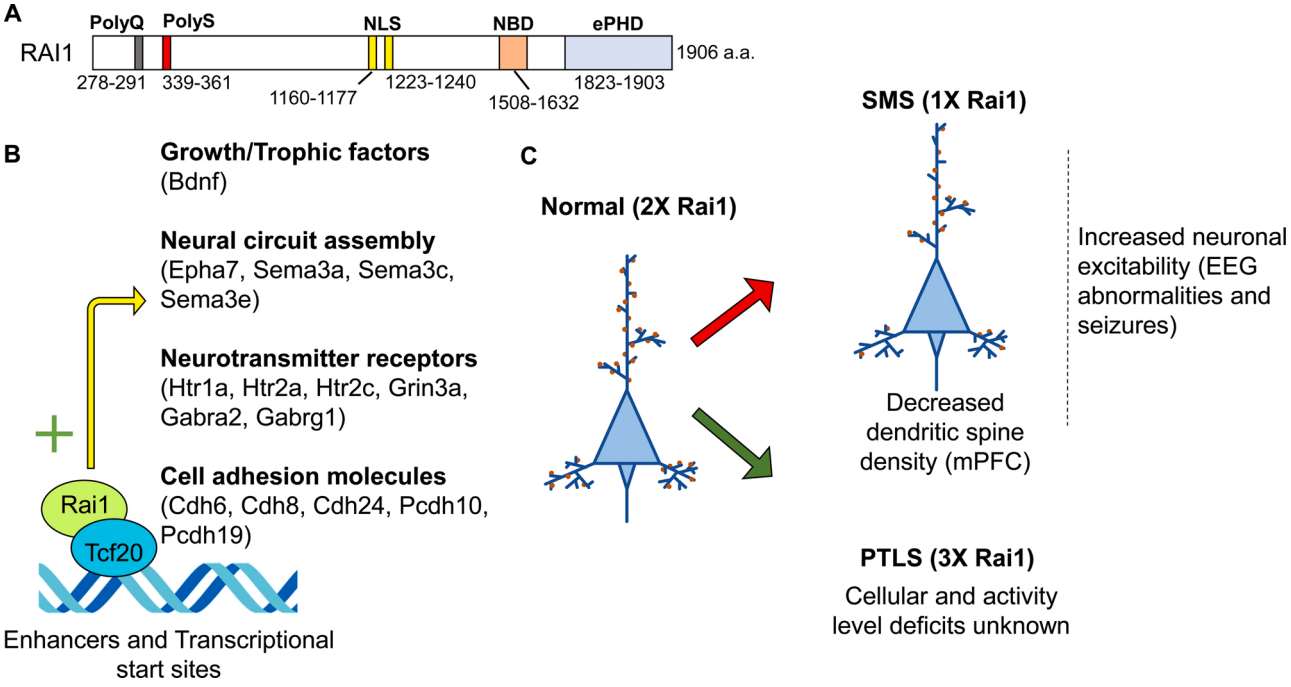

Fig. 1. Molecular and neuronal function of RAI1. **(A)** Functional domains and their locations on the human RAI1 protein. PolyQ: polyglutamine tract, PolyS: polyserine tract, NLS: nuclear localization signal, NBD: nucleosome binding domain, ePHD: extended atypical plant homeodomain. **(B)** A schematic illustrating that Rai1 interacts with Tcf20 and binds to the enhancers and transcriptional start sites to promote gene expression. Tcf20: transcription factor 20, Bdnf: brain-derived neurotrophic factor, Epha7: ephrin type-A receptor 7, Sema3a: semaphorin 3a, Sema3c: semaphorin 3c, Sema3e: semaphorin 3e, Htr1a: 5-hydroxytryptamine receptor 1a, Htr2a: 5-hydroxytryptamine receptor 2a, Htr2c: 5-hydroxytryptamine receptor 2c, Grin3a: glutamate ionotropic receptor NMDA type subunit 3a, Gabra2: gamma-aminobutyric acid type A receptor subunit alpha 2, Gabrg1: gamma-aminobutyric acid type A receptor subunit gamma 1, Cdh6: cadherin-6, Cdh8: cadherin-8, Cdh24: cadherin-24, Pcdh10: protocadherin-10, Pcdh19: protocadherin-19. **(C)** *Rai1* dosage-imbalance alters mPFC spine (indicated in orange) density and increases seizure susceptibility in mouse models of SMS.

functions as a transcription activator that promotes the expression of genes involved in neural circuit assembly, neuronal communication, and neuronal projections (Fig. 1**B**) (Huang et al., 2016b). Interestingly, while Rai1 regulates the same category of genes (neuronal wiring and transmission) in many brain regions including cortex, striatum, and hypothalamus, misregulated genes in different brain regions show minimal overlaps (Huang et al., 2016b). This suggests that the ability of Rai1 to regulate gene expression is cell type-dependent. Bulk tissue RNA-sequencing found that deleting *Rai1* only moderately affects gene expression (Huang et al., 2016b). In the future, single-cell transcriptomic profiling with increased sensitivity will better elucidate Rai1′s mode of action.

2.3. Neuronal and behavioral functions of Rai1

Human chromosome 17 maps entirely to the distal half of mouse chromosome 11 and is the largest human autosome with orthology to a single mouse chromosome (DeBry and Seldin, 1996). This feature prompted the generation of the first SMS (Df(11)17/+) and PTLS (Dp(11)17/+) mouse models by deleting and duplicating a 32–34 centimorgan (cM) region of mouse chromosome 11 syntenic to human 17p.11.2 (Walz et al., 2003). Df(11)17/+ mice are hypoactive and exhibit craniofacial abnormalities, motor dysfunction, seizures, obesity, decreased social dominance-like behavior, abnormal circadian period, and male-specific reduced fertility (Lacaria et al., 2012a; Ricard et al., 2010; Walz et al., 2003, 2004). Dp(11)17/+ mice do not have seizures, craniofacial abnormalities, or reduced fertility (Walz et al., 2003). However, they are hyperactive and underweight, and show increased anxiety, increased social dominance behavior, impaired sociability and social novelty preference, abnormal motor function, and impaired learning and memory (Table 2) (Molina et al., 2008; Ricard et al., 2010; Walz et al., 2004). Dp(11)17/+ and Df(11)17/+ mice show opposing phenotypes in a fluid consumption and licking assay that measures oral sensorimotor functions (Heck et al., 2012). Specifically, Dp(11)17/+ mice show an increased number of visits, inter-visit time, licks per burst and licks per visit, whereas Df(11)17/+ mice exhibit diametrically opposing phenotypes (Heck et al., 2012). These findings underline the importance of reciprocal CNVs in regulating fluid consumption, body weight homeostasis, and social dominance in opposing directions.

Mice carrying *Rai1* null allele (Bi et al., 2005) and *Rai1* transgenic allele ($Rai1^{Tg}$) (Girirajan et al., 2008) were generated to evaluate the behavioral and physiological outcomes of Rai1 under- and over-expression. $Rai1^{+/-}$ mice are viable and fertile, exhibit several SMS-like phenotypes including mild obesity and specific craniofacial and skeletal malformations (Bi et al., 2005, 2007; Yan et al., 2007). $Rai1^{+/-}$ mice also show increased food intake, decreased social dominance behavior, increased repetitive vertical behavior (rearing), and decreased dendritic spine density (Fig. 1**C**) (Burns et al., 2010; Huang et al., 2018; Rao et al., 2017). The vast majority of homozygous $Rai1^{-/-}$ animals die early in embryogenesis, with many of them fail to develop beyond E7.5 and most being resorbed by E11.5. Of the rare $Rai1^{-/-}$ animals born, >90 % die before weaning (Bi et al., 2005). The small number of $Rai1^{-/-}$ mice that survived embryonic and early postnatal lethality show neurobehavioral phenotypes including severe obesity, defective motor skills, impaired learning and memory, and overt seizures and EEG abnormalities (Table 2) (Bi et al., 2007). Interestingly, brain hyperexcitability worsens as *Rai1* level decreases. $Rai1^{+/-}$ mice show frequent epileptiform discharges, with only 2% of them exhibit overt seizure at over 4 months of age (Bi et al., 2005). By contrast, a third of $Rai1^{-/-}$ mice have an overt seizure as early as 3 months of age. How Rai1 controls brain excitability remains unclear but dose-dependent downstream pathways are likely involved.

$Rai1^{Tg}$ mice with 1.5-fold Rai1 overexpression phenocopy several neurobehavioral and physiological features of Dp(11)17/+ mice (Girirajan and Elsea, 2009; Girirajan et al., 2008). This includes growth delay, hyperactivity, increased anxiety, motor dysfunction, and increased social dominance behaviors. Homozygosity of the $Rai1^{Tg}$ allele (4 extra copies of *Rai1*) induces dose-dependent exacerbation of growth defect, hyperactivity, and motor impairment (Girirajan et al., 2008). Together, these data demonstrate that Rai1 level needs to be tightly regulated to maintain proper neurological and physiological functions. Loss and gain of Rai1 are responsible for impaired locomotor activity, social dominance, and body weight homeostasis observed in Df(11)17/+ and Dp(11)17/+ mice (Table 2).

The early lethality in >90 % of the $Rai1^{-/-}$ mice prompted the generation of a loxP-flanked *Rai1* allele ($Rai1^{flox}$) that allows conditional deletion of *Rai1* in restricted cell types (Huang et al., 2016b). Combining $Rai1^{flox}$ and a pan-neural and glial $Nestin^{Cre}$ driver (Luo et al., 2020; Tronche et al., 1999), Huang and colleagues found that brain-specific heterozygous ($Nestin^{Cre}$;$Rai1^{flox/+}$) and homozygous ($Nestin^{Cre}$;$Rai1^{CKO}$) *Rai1* deletion fully recapitulate neurological and physiological phenotypes seen in $Rai1^{+/-}$ and $Rai1^{-/-}$ mice, respectively (Huang et al., 2016b, 2018). Specifically, $Nestin^{Cre}$;$Rai1^{flox/+}$ mice show increased rearing, decreased social dominance, and increased body weight, while $Nestin^{Cre}$;$Rai1^{CKO}$ mice have motor skill impairments, severe obesity, and learning and memory problems. Unlike most $Rai1^{-/-}$ mice that die embryonically, $Nestin^{Cre}$;$Rai1^{CKO}$ mice escape embryonic lethality but show premature postnatal death. Altogether, this demonstrates that SMS-like neurological and physiological features originate from the central nervous system.

Rai1 is widely distributed in all tissues. Therefore, it is possible that (1) each SMS-like phenotype is caused by Rai1 loss in a distinct group of cells; (2) each cell type partially contributes to many phenotypes; or (3) most SMS-like phenotypes are caused by Rai1 loss in one critical group of cells. A cell type screen found that *Rai1* deletion from cortical and subcortical excitatory neurons fully recapitulate motor dysfunction, social interaction deficits, obesity, and learning impairment seen in $Nestin^{Cre}$;$Rai1^{CKO}$ mice. By contrast, mice with *Rai1* deleted only from gamma-aminobutyric acid-expressing (GABAergic) neurons show social and learning impairments (Huang et al., 2016b, 2018). Two groups of excitatory neurons in the hypothalamus, the paraventricular nucleus of hypothalamus (PVH) and the ventromedial nucleus of hypothalamus (VMH), are potentially involved in body weight defects caused by Rai1 loss. Specifically, deleting one or both copies of *Rai1* from the $Sim1^{Cre}$-lineage (including PVH neurons) induce a dose-dependent effect in obesity (Balthasar et al., 2005; Huang et al., 2016b). This is due to hyperphagia but not abnormal energy expenditure. By contrast, deleting one or both *Rai1* alleles from $SF1^{Cre}$-lineage neurons (including VMH neurons) result in a similarly mild bodyweight increase (Dhillon et al., 2006; Huang et al., 2016b). Therefore, $Sim1^{Cre}$- and $SF1^{Cre}$-expressing cells show different sensitivity to *Rai1* dosage. In the context of PTLS, Rai1 overexpression in the CamKII-lineage (including forebrain excitatory and some inhibitory neurons) induces PTLS-like phenotypes (Cao et al., 2014).

2.4. Summary

SMS and PTLS are prime examples of syndromic ASDs caused by reciprocal genomic rearrangements with monogenic roots. The findings in animal models suggest that deleting or duplicating the mouse genomic regions syntenic to SMS and PTLS critical region, or loss or gain of Rai1 alone, induce opposite phenotypes in locomotor activity, social dominance and body weight, but have a similar effect on motor dysfunction and learning impairment. *Rai1* dosage imbalance is also responsible for disease-specific features such as seizures (specific to Rai1 underexpression) and increased anxiety (specific to Rai1 overexpression). Deleting both copies of *Rai1* causes an earlier onset EEG abnormalities and more severe seizures than deleting one allele, while ectopic expression of 2 or 4 extra copies of *Rai1* cause dose-dependent worsening of hyperactivity and motor impairment. Interestingly, body weight homeostasis is sensitive to Rai1 protein abundance: pan-neural homozygous *Rai1* deletion causes a significant weight gain and 4 extra

Table 2
Mouse behavioral features associated with dosage imbalance of syndromic ASD genes.

Diseases [OMIM]	Mouse models	Behavioral phenotypes									References
		Social interaction	Body weight	Motor performance	Learning/ Memory	Seizure susceptibility	Anxiety	Stereotypic behavior	Circadian rhythm	Locomotor behavior	
	Df (11)17/+	ND	↑	↓ (Rotarod, wire hang test)	Normal (Fear conditioning)	↑	↓ (Open field, light-dark test)	ND	↓ (Free-running period)	↓	(Bi et al., 2007; Lacaria et al., 2013; Ricard et al., 2010; Walz et al., 2003, 2004)
Smith-Magenis Syndrome [182290]	*Rai1*$^{-/-}$	Normal (Sociability & social discrimination)	↑ (In brain-specific knockouts[a])	↓ (Pole test, wire hang test)	↓ (Fear conditioning, spatial working memory, Y-maze test)	↑	Normal (Open field, elevated plus maze)	ND	ND	Normal	(Bi et al., 2007; Huang et al., 2016b, 2018)
	Rai1 $^{+/-}$	↓ (Social dominance)	↑	↓ (Wire hang test)	Normal (Fear conditioning)	↑	Normal (Open field, elevated plus maze)	↑ (Rearing)	↓ (Free-running period, increased behavioral hypersensitivity to light)	Normal	(Bi et al., 2007; Huang et al., 2016b, 2018; Lacaria et al., 2013)
Potocki-Lupski Syndrome [610883]	Dp (11)17/+	↑ (Social dominance) ↓ (Sociability & social novelty)	↓	↓ (Rotarod)	↓ (Fear conditioning)	Normal	↑ (Open field, elevated plus maze)	↑ (Rearing, repeated nose pokes)	Normal	↑	(Bi et al., 2007; Lacaria et al., 2012b; Molina et al., 2008; Ricard et al., 2010; Walz et al., 2003, 2006; Walz et al., 2004)
	Rai1^{Tg}	↑ (Social dominance)	↓	↓ (Wire hang test, grip strength)	↓ (Fear conditioning)	Normal	↑ (Open field)	↓ (Rearing)	Asynchronized circadian rhythm	↑	(Girirajan and Elsea, 2009; Girirajan et al., 2008; Mullegama et al., 2017)
Rett Syndrome [312750]	Male *Mecp2*-null (*Mecp2*$^{2lox/y}$, *Mecp2*$^{308/y}$, *Mecp2*$^{-/y}$)	↓ (Partition test, novel partner)	↑	↓ (Wire hang test, rotarod test, nest Build)	↓ (Fear conditioning)	↑	↓ (Open field, elevated plus maze)	↑ (Hindlimb clasping, forelimb stereotypies)	Impaired circadian rhythm	↓	(Chao et al., 2010; Chen et al., 2001; Gemelli et al., 2006; Guy et al., 2001; Li et al., 2015; Moretti et al., 2005; Pelka et al., 2006)
	Female *Mecp2* mosaic	↓ (Three-chamber test)	↑	↓ (Grid walking)	↓ (Fear conditioning, passive avoidance learning)	↑	↓ (Elevated plus maze)	↑ (Hindlimb clasping)	ND	↓	(Colic et al., 2013; Guy et al., 2001; Samaco et al., 2013; Vogel Ciernia et al., 2017)
***MECP2*Duplication Syndrome [300260]**	*Mecp2*^{Tg}	↓ (Familiar partner, novel partner/ object)	↓ (At birth)	↓ (Ataxia)	↑ (Motor & contextual learning)	↑	↑ (Open field, light-dark test, elevated plus maze)	↑ (Forepaw clasping)	ND	↓	(Collins et al., 2004; Samaco et al., 2012)
Phelan-McDermid Syndrome [606232]	*Shank3*$^{(e4-9)}$ *Shank3*$^{(e4-22}$ (exon-specific deletions)	↓ (Social preference)	↑ (at 8 to 12 months)	↓ (Pole test, rotarod)	↓ (Motor learning) ↓ (Morris water maze) Normal (Fear conditioning)	ND	↑ (Open field)	↑ (Self-grooming & repetitive sniffing)	Impaired circadian rhythm[b]	↓	(Ingiosi et al., 2019; Wang et al., 2016, 2011)
		Normal	ND	ND	Normal (Fear conditioning)	↓	Normal (Open field,	↑ (Self-grooming)	ND	Normal	(Yoo et al., 2019b)

(*continued on next page*)

Table 2 (*continued*)

Diseases [OMIM]	Mouse models	Behavioral phenotypes									References
		Social interaction	Body weight	Motor performance	Learning/ Memory	Seizure susceptibility	Anxiety	Stereotypic behavior	Circadian rhythm	Locomotor behavior	
	Shank3^{Q321R} (point mutation)						elevated plus maze) ↑ (Light-dark test)				
	Shank3b$^{-/-}$ (isoform-specific knockout)	↓ (Social interaction)	Normal	Normal (Rotarod)	↓ (Morris water maze, acquisition memory and learning)	↓	↑ (Elevated zero maze, open field, light-dark test)	↑ (self-grooming)	ND	↓	(Dhamne et al., 2017; Peca et al., 2011; Yoo et al., 2019a)
	Shank3a$^{-/-}$ (isoform-specific knockout)	↓ (Social novelty)	ND	Normal (Rotarod)	ND	ND	Normal (Elevated zero maze)	Normal	ND	ND	(Jin et al., 2018; Peca et al., 2011)
22q13 Duplication Syndrome [615538]	*Shank3*^{Tg}	↓ (Social interaction) ↓ (Three- chamber test)	↑	ND	ND	↑ (Spontaneous seizures)	ND	Not present	Impaired circadian rhythm	↑	(Han et al., 2013; Jin et al., 2018)
Angelman Syndrome [105830]	*Ube3a*$^{m-/p+}$ (maternal-specific deletion)	Normal (Sociability) ↓ (Three- chamber test at 12 months)	↑	↓ (Rotarod)	↓ (Spatial learning, Morris water maze, fear conditioning)	↑	↑ (Elevated plus maze)	↑ (Hindlimb clasping)	Impaired circadian rhythm	↓	(Allensworth et al., 2011; Dutta and Crawley, 2019; Huang et al., 2013; Krishnan et al., 2017; Mandel-Brehm et al., 2015; Shi et al., 2015)
Dup15q Syndrome [608636]	*Ube3a*^{1XTg} *Ube3a*^{2XTg}	↓ (Three-chamber test)	ND	Normal	↓ (Contextual fear conditioning)	↑	↑ (Open field, light-dark test, elevated plus maze)	↑ (Self-grooming)	ND	Normal	(Copping et al., 2017; Smith et al., 2011)

↑: Increased; ↓: Decreased; ND: Not Determined.

[a] *Rai1*$^{-/-}$ mice are not obese but deleting both copies of *Rai1* from the brain causes severe obesity. This is potentially due to developmental defects caused by whole-body Rai1 homozygous knockout.

[b] Mice lacking *Shank3* exon 21 show sleep disturbance.

Rai1 alleles induce a dramatic weight loss. By contrast, loss or gain of one copy of *Rai1* induces intermediate phenotypes. Neural circuits involved in fear learning are sensitive to homozygous but not heterozygous *Rai1* loss. These findings, together with the drastically different Rai1 target genes across tissues, suggest a complex interplay between gene dosage and neuronal subtypes in the manifestation of disease features. While Rai1 is ubiquitously expressed, cell type-specific *Rai1* dosage imbalance, especially in cortical and subcortical excitatory neurons, is the main source for disease features in SMS and PTLS mouse models (Table 3). In the future, using cell type- or brain region-specific approaches to dissect molecular and neuronal functions of Rai1 will provide mechanistic insights into how *Rai1* dosage-imbalance drives both opposing and overlapping disease traits.

3. Rett Syndrome versus *MECP2* Duplication Syndrome

3.1. Genetics and clinical features

X-linked gene mutations are an important cause for neurogenetic disorders. A feature of X-linked disorders is the variable clinical symptoms in female patients due to random inactivation of the X chromosome. One such example is Rett Syndrome (RTT, OMIM #312,750), one of the most common causes of monogenic intellectual disability in females (1 in 10,000 girls) (Chahrour and Zoghbi, 2007). More than 95 % of patients diagnosed with typical RTT have loss-of-function missense, nonsense, and frameshift mutations in the *Methyl-CpG Binding Protein 2* (*MECP2*) gene (Amir et al., 1999). Most *MECP2* mutations arise from sporadic mutations in the paternal germline (Trappe et al., 2001). RTT is particularly devastating because patients appear to develop normally for the first 6–18 months of life and achieve appropriate milestones with the exception of deceleration of head growth around 2–4 months of age (Dolce et al., 2013; Lombardi et al., 2015). As age progresses, neurological functions deteriorate quickly. Patients begin to lose purposeful hand use and develop stereotypical hand wringing movements. Previously acquired abilities such as walking, word use, and affinity for social interaction are also lost. Development of respiratory abnormalities like apnea and hyperventilation are followed by mental deterioration and loss of motor coordination. From age 3–10, seizures with different severity appear, and 50–90 % of RTT patients develop epilepsy with refractory seizures (Table 1) (Dolce et al., 2013). Scoliosis, anxiety, and autonomic dysfunction also emerge around this time. In the late stage of RTT pathogenesis, motor function deteriorates. Some patients show Parkinsonian-like features rendering them incapable of walking (Roze et al., 2007). These clinical symptoms are associated with smaller neuronal and dendritic size without signs of neurodegeneration (Armstrong, 2005). In rare cases, hemizygous mutations of *MECP2* in males are inherited from the mother. Depending on the severity of mutations, the symptoms range from moderate intellectual disability, neuropsychiatric symptoms, obesity, epilepsy, early progressive encephalopathy, to lethality in the first year of life (Kankirawatana et al., 2006; Villard et al., 2000). Beyond RTT, *MECP2* mutations are also found in patients with idiopathic ASDs (Carney et al., 2003; Wen et al., 2017).

Intriguingly, loss and gain of *MECP2* result in clinically similar neurological symptoms, confirming that the brain is sensitive to *MECP2* dosage. *MECP2* Duplication Syndrome (MDS, OMIM # 300,260) is a severe progressive neurodevelopmental disorder associated with premature death (Van Esch et al., 2005). The duplication of Xq28 in MDS has been narrowed down to a region containing only *MECP2* and *interleukin-1 receptor-associated kinase 1* (*IRAK1*, involved in innate immunity) (Ramocki et al., 2010). MDS accounts for 1–2 % of X-linked intellectual disability cases (Shimada et al., 2013). Young males carrying *MECP2* duplication show core autistic features similar to idiopathic ASDs (Peters et al., 2013) and a range of RTT-like features including decelerated head growth, failure to thrive, hypotonia, hand stereotypies, seizures, and speech problems (Table 1) (Friez et al., 2006; Lugtenberg et al., 2006). Although less common, female patients carrying Xq28 duplication have been identified (Bijlsma et al., 2012; Grasshoff et al., 2011; Novara et al., 2014). They usually show milder symptoms including moderate cognitive impairment and social and communication problems. Further increase in *MECP2* dosage (triplication) results in symptoms similar to the more severe cases of *MECP2* duplication including macrocephaly, hypotonia, developmental delay, seizures, and regression of neurological functions in late childhood (Tang et al., 2012).

3.2. Expression and molecular function of Mecp2

During embryogenesis, mouse Mecp2 protein level is low and progressively increases during the postnatal neuronal maturation (Balmer et al., 2003; Kishi and Macklis, 2004; Shahbazian et al., 2002). In mice, Mecp2 is widely expressed in all tissues but its expression in neurons is 10-fold higher than in other cell types (Jung et al., 2003; Skene et al., 2010). The expression of Mecp2 in post-mitotic neurons suggests a role in neuronal maturation rather than early cell fate decision. The widespread expression pattern and high abundance also support a global requirement for Mecp2 in multiple cell types (Skene et al., 2010). At the cellular level, Mecp2 protein is concentrated in the heterochromatic foci of the nucleus and has been implicated in organizing chromatin structures such as chromatin compaction (Baker et al., 2013; Linhoff et al., 2015).

Mecp2 was initially identified as a chromatin protein that binds to methylated cytosines in the CpG island via the methyl-CpG-binding domain (MBD) (Fig. 2**A**) (Lewis et al., 1992; Nan et al., 1993). Mecp2 also has a high affinity towards methylated CA nucleotides (mCA) and methylated CAC trinucleotides (Chen et al., 2015; Kinde et al., 2015; Lagger et al., 2017) but not unmethylated CG dinucleotides (Gabel et al., 2015). Interestingly, mCA sites are enriched within the gene bodies of long genes (>100 kb) expressed in post-mitotic neurons and are correlated with transcriptional repression (Gabel et al., 2015; Guo et al., 2014; Sugino et al., 2014). On the genome-wide scale, ChIP-sequencing confirmed that Mecp2 is widely distributed in the genome but enriched within the gene bodies of long genes with high mCA content (Fig. 2**B**) (Boxer et al., 2020; Lagger et al., 2017). Consistent with this finding, both bulk RNA-sequencing and single nucleus-sequencing found that Mecp2 dysfunction is associated with upregulation of highly methylated long genes (Renthal et al., 2018). In addition to gene bodies, Mecp2 also binds to transcriptional start sites of highly methylated long genes to limit gene expression by reducing the rate of RNA polymerase II initiation (Boxer et al., 2020). By contrast, Mecp2 binding is enriched in downregulated genes in *Mecp2*^{Tg} mice (Chahrour et al., 2008). The inverse misregulation of genes in *Mecp2* deletion and duplication models are consistent with a primary pathogenic effect caused by Mecp2′s repressor function. Notably, for subsets of neuronal genes, Mecp2 can function as a transcriptional activator via its interaction with cAMP-responsive element-binding protein 1 (CREB1) (Chahrour et al., 2008) or by recruiting histone deacetylase 3 (HDAC3) to deacetylate the transcription factor forkhead box O3 (FOXO3) and promotes gene expression (Nott et al., 2016). Therefore, Mecp2 has a complex mode of action at the molecular level.

Mecp2 represses gene expression through recruiting corepressors and chromatin remodeling complexes such as Sin3a-histone deacetylase 1/2 (HDAC1/2) complex (Jones et al., 1998; Nan et al., 1997, 1998) and nuclear receptor co-repressor (NCoR)-silencing mediator for retinoic acid and thyroid hormone receptor (SMRT) complex (Fig. 2**B**) (Lyst et al., 2013). Mecp2 recruits Sin3a and HDACs through its C-terminal transcriptional repression domain (TRD) (Nan et al., 1998). *Mecp2* deletion increases histone acetylation in highly methylated long genes, consistent with loss of HDAC activity (Boxer et al., 2020). Mecp2′s ability to repress the expression of long genes relies on its MBD and interaction with the NCoR complex (Boxer et al., 2020). Consistent with the important functions of MBD and TRD, a missense mutation in either domain is sufficient to cause RTT (Yusufzai and Wolffe, 2000). Moreover, mice overexpressing human MeCP2 proteins with either a mutated TRD or MBD domain are healthy and do not show signs of MDS

Table 3
Summary of affected cell types/brain regions and molecular/cellular aberrations in four pairs of monogenic mouse models of syndromic ASDs.

Diseases [OMIM]	Genetic disruption	Cell type-and/or brain region-specific physiological and neurobehavioral phenotypes	Molecular aberrations	Cellular aberrations	References
Smith-Magenis Syndrome [182290]	*Rai1* deletion	Glutamatergic neurons (Subcortical): obesity, learning deficits, impaired social interaction, and motor deficits GABAergic neurons: Learning deficits and impaired social interaction Sim1^{+}: Obesity SF1^{+}: Obesity	↓ Bdnf ↓ Htr2c ↓ Pcdh20 ↓ Sema3a ↓ Pomc ↑ Leptin ↑ Ghrelin ↑ Corticosterone ↑ Mc4r	↓ Spine density (prefrontal cortex neurons)	(Burns et al., 2010; Huang et al., 2016b; Huang et al., 2018)
Potocki-Lupski Syndrome [610883]	*Rai1* duplication	CamkII-lineage forebrain neurons: Underweight, hyperactive, and impaired learning and memory	Not determined	Not determined	(Cao et al., 2014)
Rett Syndrome [312750]	*Mecp2* deletion	Mechanosensory neurons: Anxiety and social & cognitive deficits CamkII lineage forebrain neurons: Hindlimb clasping, impaired motor coordination, increased anxiety, and abnormal social interaction HoxA4^{+} neurons (brain stem & spinal cord): Abnormal breathing Sim1^{+} neurons:Aggression, increased feeding, and altered stress response Glutamatergic neurons: Obesity, tremor, impaired acoustic startled response, and altered anxiety like behavior GABAergic neurons: Repetitive behavior, respiratory dysfunction, progressive motor dysfunction, hypoactivity, social deficits, impaired sensorimotor response, and impaired learning and memory Astrocytes: Respiratory dysfunction, anxiety, and latered locomotion	↑ Histone acetylation of methylated long genes ↑ PcdhB1 ↑ Pcdh7 ↓ Bdnf	↓ Evoked EPSP ↓ mEPSP frequency Normal mIPSPs (somatosensory cortex) ↓ mIPSP amplitude (CA3 pyramidal neurons) ↓ Glutamatergic synapses ↓ Paired pulse ratio Impaired Hippocampal LTP and LTD ↓ Dendritic branch, spine density, and neuronal size	(Armstrong et al., 1995; Asaka et al., 2006; Boxer et al., 2020; Calfa et al., 2015; Chang et al., 2006; Chao et al., 2010; Chao et al., 2007; Chen et al., 2001; Dani et al., 2005; Fukuda et al., 2005; Fyffe et al., 2008; Gemelli et al., 2006; Huang et al., 2016a; Kishi and Macklis, 2004; Lioy et al., 2011; Meng et al., 2016; Miyake et al., 2011; Moretti et al., 2006)
***MECP2* Duplication Syndrome [300260]**	*Mecp2* duplication	Not determined	↑ Crh ↑ Oprm1	↑ Evoked EPSP ↑ mEPSP frequency ↑ Glutamatergic synapses ↑ Paired pulse ratio ↑ Hippocampal LTP ↑ Spine density (young mice) ↑ Apical dendritic arbor overgrowth (pyramidal neurons)	(Chao et al., 2007; Collins et al., 2004; Jiang et al., 2013; Na et al., 2012; Samaco et al., 2012)
Phelan-McDermid Syndrome [606232]	*Shank3* deletion	ACC-specific *Shank3* knockout: ↓ Social interaction D2 dopamine receptor-expressing medium spiny neurons: ↑ Self-grooming Inhibitory neurons(somatosensory cortex): Stimulus hyperreactivity **Glutamatergic neurons (mPFC):** ↑ Direct social interaction, excessive self-grooming	↓ SAPAP3 ↓ Homer-1 ↓ PSD93 ↓ GluA1 & GluA2 (AMPA receptor subunits) ↓ Striatal basal excitatory synaptic transmission ↑ Striatal excitability ↓ Hippocampal LTP	↓ PSD thickness & length ↓ Spine volume ↓ Dendritic spine density ↑ Spine elongation ↓ Dendritic complexity ↑ Striatal mEPSP (early development) ↓ mEPSP (adulthood) ↓ Evoked EPSP amplitude	(Chen et al., 2020; Mei et al., 2016; Peca et al., 2011; Peixoto et al., 2016; Wang et al., 2017a; Wang et al., 2011; Yi et al., 2016; Yoo et al., 2019a)
22q13 Duplication Syndrome [615538]	*Shank3* duplication	Not determined	↑ F-actin cytoskeleton	↑ Number of excitatory synapses ↑ Spine density ↑ mEPSP frequency ↓ Number of inhibitory synapses	(Durand et al., 2012; Han et al., 2013M)
Angelman Syndrome [105830]	*Ube3a* deletion	GABAergic neurons: EEG abnormalities and enhanced seizure susceptibility	↑ p53 level	↓ LTP (hippocampal CA synapses, visual cortex)	(Cao et al., 2013; Egawa et al., 2012; Greer et al., 2010; Jiang et al., 1998;

(*continued on next page*)

Table 3 (*continued*)

Diseases [OMIM]	Genetic disruption	Cell type-and/or brain region-specific physiological and neurobehavioral phenotypes	Molecular aberrations	Cellular aberrations	References
				↓ Cortical synapse maturation ↓ Absent LTD (neocortex) ↓ mEPSP frequency ↓ Dendritic spike density (visual cortex)	Judson et al., 2016; Weeber et al., 2003; Yashiro et al., 2009)
			↓ Bdnf signaling	↓ Number of AMPA receptors (hippocampal neurons)	
			↑ Arc	↑ sEPSP frequency & amplitude ↓ sIPSP frequency & amplitude	
			↓ CaMKII activity	↑ sEPSP/sIPSP ratio (layer 5 pyramidal neurons) ↓ Tonic inhibition of cerebellar granule cells	
Dup15q Syndrome [608636]	*Ube3a duplication*	Glutamatergic neurons (VTA): ↓ Sociability	↓ Arc, ↓ Cbln1	↓ sEPSP frequency & amplitude (layer 2/3 pyramidal neurons) ↑ Paired-pulse ratio	(Krishnan et al., 2017; Smith et al., 2011)

↑: Increased; ↓: Decreased.

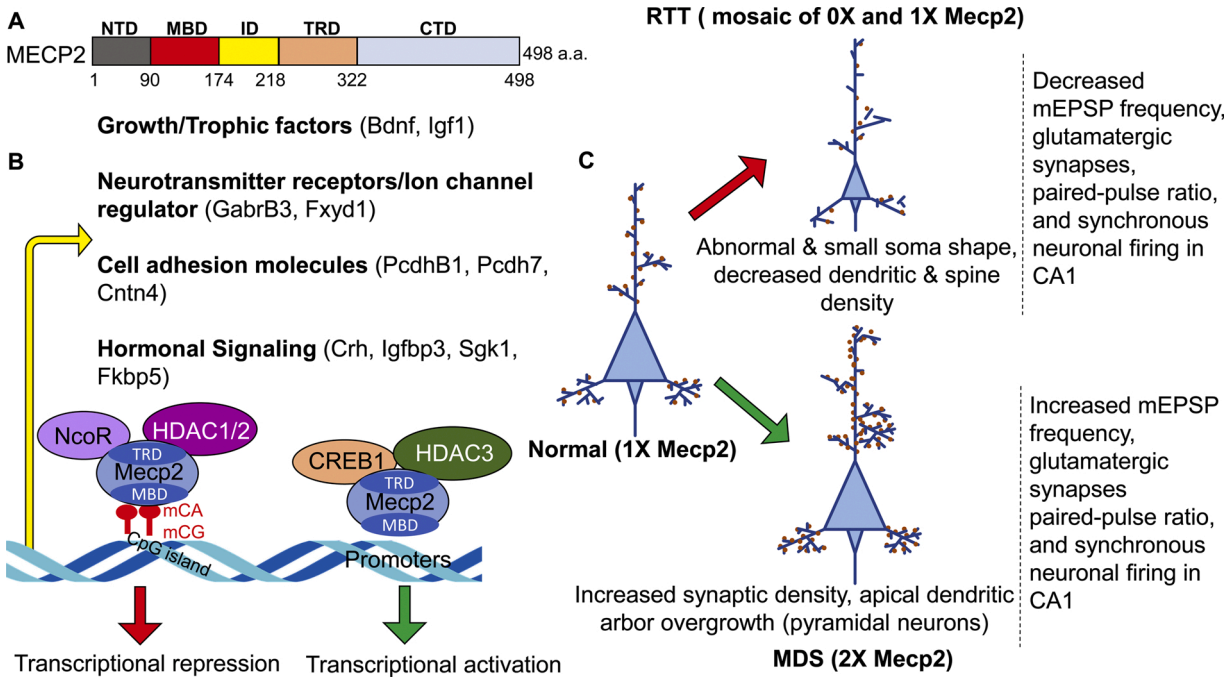

Fig. 2. Molecular and neuronal function of MECP2. **(A)** Functional domains and their locations on the human MECP2 protein. NTD: N-terminal domain, MBD: methyl-CpG-binding domain, ID: intervening domain, TRD: transcriptional repression domain, CTD: C-terminal deletion. **(B)** A schematic illustrating that Mecp2 binds to mCA/mCG to repress gene expression and binds to promoters to activate gene expression. GabrB3: gamma-aminobutyric acid receptor subunit beta-3, Fxyd1: FXYD domain containing ion transport regulator 1, PcdhB1: protocadherin beta 1, Pcdh7: protocadherin-7, Cntn4: contactin 4, Crh: corticotropin-releasing hormone, Igfbp3: insulin-like growth factor binding protein 3, Sgk1: serum/glucocorticoid regulated kinase 1, Fkbp5: FK506 binding protein 5, NCoR: nuclear receptor co-repressor, HDAC1/2: histone deacetylases 1/2, CREB1: cAMP- responsive element-binding protein 1, HDAC3: histone deacetylase 3. **(C)** Mecp2 dosage-imbalance in mice causes opposing cellular and neuronal activity level deficits.

(Heckman et al., 2014). Therefore, both MBD and TRD are required for toxicity in the context of MDS.

3.3. Neuronal and behavioral functions of Mecp2

Shortly after the discovery of the genetic link to RTT, mice lacking *Mecp2* were generated (Chen et al., 2001; Guy et al., 2001). *Mecp2* hemizygous male mice appear normal in early life but become hypoactive and show uncoordinated gait between 3–8 weeks of age. This is associated with reduced brain weight and neuronal size. They soon become obese and show irregular breathing and hindlimb clasping, and 50 % of them die around 10 weeks of age. *Mecp2*-null male mice are more frequently used for pre-clinical research because their phenotypes are more severe and early-onset. Female mice with mosaic *Mecp2* loss

appear normal for the first 4 months of life and eventually develop obesity, hypoactivity, and ataxia. They show a slower regression and their phenotypes are more variable due to random X chromosome inactivation (Table 2).

Brain-specific *Mecp2* deletion in mice recapitulates many RTT-like features (Chen et al., 2001), highlighting a critical role for Mecp2 activity in brain function. Conditional deletions of *Mecp2* from forebrain neurons (Gemelli et al., 2006), brainstem and spinal cord (Huang et al., 2016a), hypothalamic neurons (Fyffe et al., 2008), glutamatergic neurons (Meng et al., 2016), GABAergic neurons (Chao et al., 2010; Ito-Ishida et al., 2015; Ure et al., 2016), and astrocytes (Lioy et al., 2011) induce a portion of neurobehavioral features seen in *Mecp2*-null mice (Table 3). The behavioral deficits of each conditional mutant correspond to the function of the targeted cell types, supporting an emerging theme that Mecp2 performs related neural functions across brain regions. This is distinct from conditional *Rai1* mutant mice showing that not all brain regions require Rai1 for proper neurobehavioral functions (Huang et al., 2016b). Remarkably, mice with GABAergic neuron-specific *Mecp2* deletion recapitulate most features of *Mecp2*-null mice (Chao et al., 2010), consistent with a critical role for GABAergic signaling.

ASD patients and mouse models are characterized with atypical sensory responses including hypersensitivity and reactivity to sensory input (Gogolla et al., 2014; Orefice et al., 2016). Selectively deleting *Mecp2* from mechanosensory neurons causes social and cognitive behavior deficits as well as anxiety-like features (Orefice et al., 2016). By contrast, *Mecp2* loss in primary somatosensory neurons results in modest social behavior deficits without inducing anxiety-like behaviors. This suggests that somatosensory circuits contribute to social dysfunction and anxiety in ASDs.

Mecp2 transgenic mice (*Mecp2*^{Tg}) that mimic MDS have progressive neurobehavioral abnormalities, hypoactivity, forepaw clasping, seizures, and enhanced fear learning and memory (Collins et al., 2004). Selective Mecp2 overexpression in post-mitotic neurons induces growth retardation, ataxia, tremor, excessive grooming, and heightened anxiety (Luikenhuis et al., 2004; Na et al., 2012). Similar to patients with RTT and MDS, loss and gain of Mecp2 in mice result in many overlapping neurobehavioral and physiological phenotypes including reduced lifespan, ataxia, anxiety, and increased seizure susceptibility. By contrast, body weight and fear learning and memory are regulated in opposite directions by *Mecp2* dosage imbalance (Pelka et al., 2006), whereas irregular breathing and tremor are unique to *Mecp2* loss (Table 2).

Alterations in synaptic transmission and plasticity are observed in mice with *Mecp2* deletion and duplication. The magnitude of action potential-evoked excitatory postsynaptic currents (eEPSCs) is decreased in *Mecp2*-null and increased in *Mecp2*^{Tg} neurons when compared to wild-type neurons (Chao et al., 2007). *Mecp2*-null neurons also show decreased miniature EPSC (mEPSC) frequency, whereas *Mecp2*^{Tg} neurons show increased mEPSC frequency (Fig. 2C). Inhibitory neurotransmission is also differentially affected in brain regions; miniature inhibitory postsynaptic currents (mIPSCs) recorded from *Mecp2*-null somatosensory cortex are largely normal (Dani et al., 2005), but hippocampal CA3 pyramidal neurons show a more moderate mIPSC defect (Calfa et al., 2015). Loss and gain of Mecp2 also decrease and increase the number of glutamatergic synapses, respectively (Fig. 2**C**) (Chao et al., 2007). The changes in synapse number normalize over time, suggesting the engagement of a homeostatic mechanism. *Mecp2* loss is also associated with reduced paired-pulse ratio, a form of short-term plasticity reflective of neurotransmitter release probability (Asaka et al., 2006; Moretti et al., 2006). Rapid short-term synaptic depression is also affected upon *Mecp2* deletion (Nelson et al., 2006). On the contrary, *Mecp2* duplication causes increased paired-pulse responses (Collins et al., 2004; Na et al., 2012), supporting the idea that *Mecp2* dosage imbalance bidirectionally controls short term plasticity. Long-term plasticity is also closely correlated with Mecp2 levels. *Mecp2*-null mice show impaired hippocampal long-term potentiation (LTP) and long-term depression (LTD) (Asaka et al., 2006; Moretti et al., 2006), whereas *Mecp2*^{Tg} mice show enhanced hippocampal LTP (Collins et al., 2004). Therefore, loss and gain of Mecp2 regulate synaptic plasticity in opposing directions, consistent with opposing fear learning phenotypes (Collins et al., 2004; Pelka et al., 2006). Defective neuronal plasticity is commonly associated with dendritic morphology defects. RTT patients and *Mecp2*-deficient mice show decreased dendritic branch, spine density, and neuronal size (Armstrong et al., 1995; Chen et al., 2001; Fukuda et al., 2005; Kishi and Macklis, 2004). By contrast, in mouse models of MDS, spine density is higher in young mice (Jiang et al., 2013) but decreases as age progresses, coinciding with the onset of behavioral deficits. Mecp2 overexpression also induces apical dendritic arbor overgrowth of layer 5 pyramidal neurons (Jiang et al., 2013). Altogether, a proper Mecp2 level is crucial for structural dendritic development and synaptic function.

On the circuit level, gain or loss of Mecp2 similarly increases synchronous neuronal firing in CA1 (Lu et al., 2016b). Therefore, *MECP2* disorders may share similar circuit-level dysfunction. This is surprising because *Mecp2*-null neurons show a decreased calcium event rate and amplitude, while *Mecp2*^{Tg}-neurons show an opposite phenotype. While most studies disrupt Mecp2 function in early development, increasing evidence indicates that delayed *Mecp2* loss recapitulates the gene misexpression, neurobehavioral defects (Cheval et al., 2012; McGraw et al., 2011), and reduced dendritic complexity (Du et al., 2016) observed in germline knockouts. For example, Mecp2 activity is critically required after 15 weeks of age. Loss of Mecp2 at this stage (and onward) causes rapid deterioration of neurological function and lethality within days (Cheval et al., 2012; Du et al., 2016). This suggests that Mecp2 function is required for continuous function and stabilization of the mature neural network. These findings have important clinical implications because this implies that treatment for RTT should be maintained throughout life.

3.4. Summary

Mecp2 is an important chromatin protein that regulates many steps of neural development throughout life from neurogenesis to synaptic connections and behaviors. The primary function of Mecp2 is likely to repress gene expression in a NCoR- and DNA methylation-dependent manner. Unlike classical transcription factors that have sequence-specificity, Mecp2 binds globally in the genome through recognizing mCG and mCA dinucleotides. Neuronal genes longer than 100 kb with high mCA content are preferentially upregulated upon *Mecp2* loss. Mecp2 also localizes to transcriptional start sites and represses gene expression by reducing RNA polymerase II initiation. Intriguingly, Mecp2′s repressor function is neuronal subtype-dependent (Sugino et al., 2014) and *Mecp2* mutation-specific (Johnson et al., 2017). Detailed analysis of gene expression kinetics in *Mecp2*-deleted or *Mecp2*-duplicated cells will provide a better understanding of how *Mecp2* dosage imbalance drives gene expression in opposite directions. Patients with *MECP2* deletion and duplication share autistic features, seizures, motor impairments, stereotyped behaviors, and intellectual disability. Paradoxically, halving or doubling *Mecp2* levels causes inverse patterns of gene expression, dendritic morphology, synapse strength and number, and short- and long-term plasticity in mice. Gain and loss of Mecp2 result in neuronal hyper-synchrony, which if generalizable to other brain regions, could be a promising avenue for therapy.

4. Phelan-McDermid Syndrome versus 22q13 Duplication Syndrome

4.1. Genetics and clinical features

In the mammalian brain, the post-synaptic density (PSD) is a specialized protein complex at synaptic junctions that regulates synaptic transmission and plasticity (Ziff, 1997). PSD complex is composed of receptors, scaffolding proteins, signaling molecules, and cytoskeletal

proteins. Its molecular composition shows brain region-specificity (Cheng et al., 2006). Notably, genes encoding synaptic proteins are commonly deleted or duplicated in ASDs (De Rubeis et al., 2014; Zoghbi and Bear, 2012). For instance, Phelan-McDermid Syndrome (PMS, OMIM # 606,232) and 22q13 Duplication Syndrome (also known as *SHANK3* Duplication Syndrome, OMIM # 615,538) are caused by terminal or interstitial deletion (Herman et al., 1988; Watt et al., 1985) and duplication (Durand et al., 2007) of 22q13.3, respectively. The dosage-sensitive gene within 22q13 region responsible for neurological impairments in PMS was identified as *SH3 and multiple ankyrin repeat domains 3* (*SHANK3* gene, also known as ProSAP) (Luciani et al., 2003; Wilson et al., 2003). *SHANK3*, which belongs to the SHANK family, encodes SHANK3, a protein tethered at the PSD of nearly all mammalian excitatory synapses (Naisbitt et al., 1999). *SHANK1* (Sato et al., 2012) and *SHANK2* (Berkel et al., 2010), which encode the SHANK1 and SHANK2 proteins, respectively, are also implicated in ASDs, supporting a general conclusion that SHANK family proteins are crucial for social function.

PMS can be caused by various genetic lesions. While *de novo* deletion of paternal 22q13 accounts for most PMS cases, 20 % of patients carry a balanced rearrangement (Wilson et al., 2003). The sizes of deletion regions in PMS are highly variable (ranging from 0.1 to 10 Mb) because they don't have common breakpoints (Sarasua et al., 2011; Wilson et al., 2003). Missense, frameshift, and splice-site mutations in *SHANK3* cause a monogenic form of ASD that does not fit the PMS profile and accounts for >0.5 % of all ASD cases (Durand et al., 2007; Leblond et al., 2014; Moessner et al., 2007). The mutation frequency of *SHANK3* increases to 2 % in children with intellectual disability (Cooper et al., 2011). Most *SHANK3* point mutations are *de novo* mutations but can also be inherited from parents (Boccuto et al., 2013). Intragenic deletions of *SHANK3* exons 1–9 or exons 1–17 have also been reported (Bonaglia et al., 2011). Therefore, different types of mutations and deletions containing *SHANK3* may explain the wide spectrum of symptomology. Common symptoms include infantile hypotonia, intellectual impairment, global developmental delay, absent to severely delayed speech, minor dysmorphic features, and high prevalence of autistic features (Table 1) (Kolevzon et al., 2014; Soorya et al., 2013). Some PMS individuals also have seizures, cardiac and renal abnormalities, atypical bipolar disorder, increased tolerance to pain, and hearing and visual impairments (Phelan and McDermid, 2012; Phelan et al., 1993; Verhoeven et al., 2012). In summary, consistent with its genetic heterogeneity, the clinical presentations of PMS are also highly variable.

Duplication of 22q13.3 is less common than PMS and is predominantly inherited from parents with balanced rearrangements (Durand et al., 2007; Jafri et al., 2011; Moessner et al., 2007) and occasionally through *de novo* events (Okamoto et al., 2007). The duplications often involve large genomic regions (>0.8 Mb) containing more than 20 genes. However, identification of small 22q13.3 duplications containing only *SHANK3* and *ACR* (encoding Acrosin, a proteinase only expressed in sperm) establishes an important link for *SHANK3* duplication and neurological symptoms (Han et al., 2013). The clinical presentations are also variable, including attention deficit hyperactivity disorder (ADHD), destructive behavior, Asperger syndrome, hyperkinesis, auditory overstimulation, hyperphagia, seizure, learning problems, and bipolar disorder (Durand et al., 2007; Han et al., 2013). Collectively, these findings demonstrate that the proper dosage of *SHANK3* is important for brain function (Table 1).

4.2. Expression and molecular function of Shank3

The mouse *Shank3* gene contains 22 exons and its expression is under complex transcriptional regulation by intragenic promoters and alternatively spliced exons (Maunakea et al., 2010; Wang et al., 2014). *Shank3* expression is also regulated by tissue-specific DNA methylation (Ching et al., 2005). These mechanisms result in an array of mRNA and protein products expressed in a tissue-specific manner. In the mouse brain, Shank3 is widely expressed in the cortex, hippocampus, thalamus, and striatum (Peca et al., 2011). Shank3 protein isoforms have distinct expression patterns. For example, Shank3a and Shank3e are highly expressed in the striatum and are present in other forebrain structures, Shank3b is widely expressed in the brain in low levels, and Shank3c and Shank3d are enriched in the cerebellum (Wang et al., 2014). At the cellular level, Shank3a, Shank3c, and Shank3e are localized in the cytoplasm, and Shank3b is enriched in the nucleus (Wang et al., 2014). This suggests a tissue-, isoform-, and subcellular-specific function. Developmentally, Shank3 level is low during the neonatal stage, but increases in the striatum at the second week of life (Bockers et al., 2001, 2004), coinciding with activity-dependent synaptic maturation. Interestingly, the precise level of Shank3 is regulated by the ubiquitin–proteasome system downstream of synaptic activity (Ehlers, 2003; Kerrisk Campbell and Sheng, 2018). Reducing synaptic activity causes decreased Shank3 ubiquitination and increased Shank3 protein level, whereas increasing synaptic activity promotes ubiquitination and degradation of Shank3. This could affect PSD structure and morphology and potentially serve as a therapeutic entry point for modulating Shank3 abundance.

Shank3 isoforms are composed of unique combinations of different protein domains. Shank3a is the longest isoform, containing five domains including (from N to C terminal): an ankyrin repeat (ANK) domain, an src homology 3 (SH3) domain, a PSD-95/discs large/ZO-1 (PDZ) domain, a proline-rich region containing homer- and cortactin-binding sites (PRO), and a sterile alpha motif (SAM) domain (Fig. 3**A**) (Monteiro and Feng, 2017). Interestingly, each of these domains is responsible for binding specific sets of proteins to regulate synaptic structure and function (Fig. 3B). The ANK domain interacts with PSD protein Sharpin and cytoskeletal protein α-fodrin (Bockers et al., 2001; Lim et al., 2001). The SH3 domain binds to calcium channel $Ca_v1.3$ and glutamate receptor GluR-delta2 (Uemura et al., 2004; Zhang et al., 2005). Shank3-Cav1 interaction regulates calcium currents in a dose-dependent manner (Pym et al., 2017). The SH3 domain also interacts with glutamate receptor-interacting protein 1 (GRIP1) in order to assist trafficking of the α-amino-3--hydroxy-5-methyl-4-isoxazolepropionic acid (AMPA) receptor (Lu and Ziff, 2005; Wyszynski et al., 2002). The PDZ domain is important for Shank3′s interaction with synaptic membrane protein SAPAP1, PSD proteins ProSAP-interacting protein 1 (ProSAPiP1) and ProSAP-interacting protein 2 (ProSAPiP2), and GluR1 subunits of AMPA receptor (Liebau et al., 2009; Naisbitt et al., 1999; Uchino et al., 2006; Wendholt et al., 2006). Shank3-ProSAPiP1 interaction is important for dendritic spine maturation (Reim et al., 2016). The PRO domain binds to PSD proteins Homer1, GTPase Dynamin-2, actin-binding protein Abp1, and Contractin (Hayashi et al., 2009; Naisbitt et al., 1999; Okamoto et al., 2001; Qualmann et al., 2004; Tu et al., 1999). Such extensive protein-interacting network allows Shank3 to functionally couple different synaptic proteins. For example, Shank3-Homer interaction connects the metabotropic receptor (mGluR) with N-methyl-D-aspartate receptor (Tu et al., 1999, 1998). The C-terminal SAM domain mediate self-multimerization and Shank3 synaptic targeting (Baron et al., 2006; Boeckers et al., 2005).

Different combinations of Shank3 protein domains are included in various Shank3 isoforms. For example, Shank3b lacks the PRO domain, Shank3c and Shank3d lack the N-terminal ANK and SH3 domain, and Shank3e and Shank3f lack the ANK, SH3, and PDZ domains (Wang et al., 2014). Importantly, ASD-causing *SHANK3* mutations affect selective isoforms and protein domains. Mutations in exon 4 affect the ANK domain included in the Shank3a and Shank3b isoforms (Boccuto et al., 2013), whereas mutations in exon 21 affect the PRO domain included by all but the Shank3b isoform (Boccuto et al., 2013; Durand et al., 2007; Leblond et al., 2014). Therefore, determining the molecular perturbations caused by distinct *SHANK3* mutations requires detailed knowledge about how each functional domain mediates protein interactions.

Loss of Shank3 leads to significant changes in PSD protein composition such as reduced levels of SAPAP3, Homer-1 and PSD93 (Mei et al., 2016; Peca et al., 2011). The levels of PSD receptors including AMPA

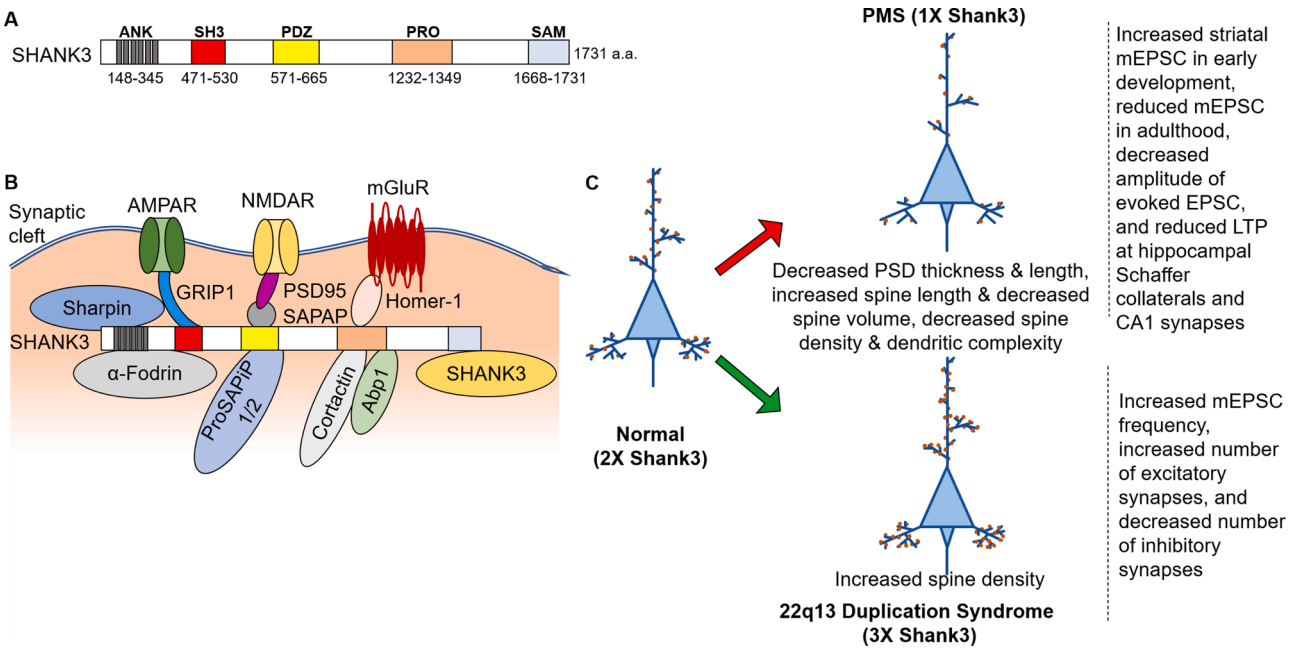

Fig. 3. Molecular and neuronal function of SHANK3. **(A)** Functional domains and their locations on the human SHANK3 protein. ANK: ankyrin repeat domain, SH3: src homology 3 domain, PDZ: PSD-95/discs large/ZO-1 domain, PRO: proline-rich region, SAM: sterile alpha motif domain. **(B)** Examples of Shank3-interacting PSD proteins at synapses. AMPAR: α-amino-3-hydroxy-5-methyl-4-isoxazolepropionic acid receptor, NMDAR: N-methyl-D-aspartate receptor, mGluR: metabotropic glutamate receptor, Sharpin: SHANK associated RH domain interactor, GRIP1: Glutamate receptor-interacting protein 1, ProSAPiP 1/2: PSD proteins ProSAP-interacting protein 1/2, PSD95: postsynaptic density protein 95, SAPAP: synapse-associated protein 90/postsynaptic density-95–associated protein, Abp1:auxin binding protein 1, Homer 1: homer protein homolog 1. **(C)** Dosage-imbalance of *Shank3* in mice results in a shift in the balance between excitation and inhibition by changing the structure and function of dendritic spines.

receptor subunits GluA1 and GluA2 (Wang et al., 2011) and NMDA receptor subunits GluN2A and GluN2B (Peca et al., 2011) are also reduced. The gain of Shank3 (*Shank3*^{Tg}), on the other hand, causes an abnormal increase of F-actin cytoskeleton in the excitatory synapses mediated by actin-related protein 2/actin-related protein 3 (Arp2/3) complex. This leads to decreased localization of actin cytoskeletal proteins Mena and Profilin in the inhibitory synapses and a subsequent reduction of inhibitory synapses in the *Shank3*^{Tg} mice (Han et al., 2013). At the transcriptional level, loss and gain of Shank3 affect the expression of different groups of striatal genes (Lee et al., 2019). This is in contrast to *Mecp2* dosage imbalance, which induces similar sets of target genes to be misregulated in opposite directions (Chahrour et al., 2008). Altogether, gain and loss of Shank3 alter molecular composition in PSD in opposite directions in a brain region- and exon-specific manner (Jiang and Ehlers, 2013; Schmeisser et al., 2012).

4.3. Neuronal and behavioral functions of Shank3

Shank3 is important for dendritic spine size, shape, and synaptic functions. Electron microscopy experiments found decreased PSD thickness and length and decreased spine volume in *Shank3*-deficient mice (Peca et al., 2011). *Shank3* deletion also causes spine elongation and reduced dendritic spine density (Wang et al., 2011), consistent with a role for Shank3 in dendritic spine development and maturation. Dendritic complexity is also reduced upon *Shank3* deletion (Chen et al., 2020). In parallel to structural changes, synaptic transmission is also affected. Loss of Shank3 increases striatal mEPSC in early development (Peixoto et al., 2016) and reduces mEPSC in adulthood (Peca et al., 2011), consistent with a precocious maturation. The amplitude of evoked EPSC is also reduced in mouse and human neurons haploinsufficient for *Shank3* (Yi et al., 2016). Homozygous *Shank3* deletion aggravates the synaptic dysfunction seen in *Shank3* heterozygous mutants (Yi et al., 2016), suggesting that synaptic function is sensitive to Shank3 abundance. While *Shank3* deletion is generally associated with reduced striatal basal excitatory synaptic transmission, striatal excitability is increased, potentially due to increased incoming cortical activity (Peixoto et al., 2016). Shank3 is also involved in synaptic plasticity, as exemplified by reduced LTP at hippocampal Schaffer collaterals and CA1 synapses in *Shank3*-deficient mice (Bozdagi et al., 2010). By contrast, Shank3 overexpression increases the amount of F-actin, results in accelerated spine morphological maturation, and increases the number of excitatory synapses (Durand et al., 2012; Han et al., 2013). Spine density and mEPSC frequency are also increased upon Shank3 overexpression. The number of inhibitory synapses is decreased by a gain of Shank3, resulting in a neural circuit that favors excitation (Han et al., 2013).

Shank3 mutant mice display a dramatic reduction of social interaction in multiple measurements including the three-chamber social arena, reciprocal interaction in an open arena, social sniffing, and ultrasonic vocalizations (Table 2) (Bozdagi et al., 2010; Peca et al., 2011; Wang et al., 2011). Intriguingly, selective deletion of *Shank3* in the anterior cingulate cortex (ACC) reduces AMPA-mediated mEPSC frequency and amplitude and AMPAR-NMDAR ratio (Chen et al., 2020). Behaviorally, ACC-specific *Shank3* knockout is sufficient to cause decreased social interaction. Another characteristic of ASD is repetitive motor behavior (DSM-5, 2013). *Shank3* mutant mice show increased repetitive behaviors like excessive self-grooming (Wang et al., 2011). This is associated with reduced glutamatergic transmission onto the D2 dopamine receptor-expressing medium spiny neurons (MSNs) of the striatum but not D1 MSNs in *Shank3* mutant mice (Wang et al., 2017a). Intriguingly, chemogenetic-mediated enhancement of D2 MSN activity reduces repetitive grooming in *Shank3* mutant mice, supporting the notion that Shank3 regulates the activity balance of striatal pathways. Other behavioral deficits in long-term and remote memory, behavioral inflexibility, and motor function are also observed in *Shank3* mutant mice (Wang et al., 2011). The bodyweight of *Shank3*-deficient mice is also slightly increased at 8–12 months of age (Wang et al., 2011), consistent with mild overgrowth of PMS patients (Phelan, 2008). Similar

to *Mecp2*-deficient mice, *Shank3* mutant mice exhibit altered tactile discrimination and hypersensitivity to gentle touch (Orefice et al., 2016). In addition, stimulus hyperreactivity in *Shank3*-null mice is caused by decreased spontaneous and evoked-activity of inhibitory neurons in the somatosensory cortex, which drives the hyperexcitability of excitatory neurons (Chen et al., 2020). Together, these data demonstrate that Shank3 regulates a wide range of synaptic and neurophysiological functions of many neuronal subtypes.

The spectrum of behavioral deficits is closely linked to Shank3 isoform-specific disruptions. For example, ASD-linked (InsG3680) and schizophrenia-linked (R1117X) *Shank3* mutations encode distinct Shank3 mRNA and protein products (Zhou et al., 2016). Young mice carrying InsG3680 but not R1117X mutation exhibit reduced striatal field population spikes and increased compensatory mEPSC amplitude. In adults, *Shank3* mutant mice carrying either mutation also show defective striatal synaptic transmission. However, only R1117X mutation but not InsG3680 is associated with profound cortical synaptic defects. Both mutant models exhibit similar motor learning and coordination deficits, anxiety-like behaviors, reduced response to pre-pulse inhibition, and social interaction deficits. Interestingly, InsG3680 mutant but not R1117X mutant mice show skin lesions associated with excessive grooming and compulsive behaviors. Another autism-linked *Shank3* S685I mutation diminishes Shank3-Abl (a subunit of WAVE regulatory complex) interaction and causes defective actin nucleation (Wang et al., 2019b). Loss of Shank3-Abl interaction reduces spine density and mEPSC frequency, increases sniffing and allogrooming behavior, and decreases ultrasonic vocalization. This supports the notion that different *Shank3* mutations drive neurological deficits through diverse mechanisms at distinct developmental stages.

Shank3^{Tg} mice overexpressing Shank3 by 1.5-fold show increased locomotor activity and hyperactivity, which is aggravated by acute injection of amphetamine (Han et al., 2013). This is consistent with a mania-bipolar disorder-like feature (Shaltiel et al., 2008). Unlike *Shank3*-deficient mice, *Shank3*^{Tg} mice do not exhibit repetitive behavior, but display decreased social interaction, reduced ultrasonic vocalization, elevated acoustic startle response with reduced prepulse inhibition, abnormal circadian rhythms, hyperphagia, and spontaneous seizures (Table 2). Hyperexcitability discharges, increased excitatory synapses, and decreased inhibitory synapses in the *Shank3*^{Tg} brains indicate an unbalanced excitation and inhibition (Fig. 3C). Interestingly, while normal basal transmissions remain intact in the Schaffer collateral-CA1 synapses of *Shank3*^{Tg} mice, the frequency of $GABA_A$ receptor-mediated mIPSC is reduced. Taken together, *Shank3* duplication in mice induces hyperkinetic phenotypes that resemble mania and show neuronal hyperexcitability.

4.4. Summary

Shank3 is an important scaffolding protein localized in the distal area of PSD that interacts directly or indirectly with multiple PSD proteins including glutamate receptors, adaptor and scaffolding proteins, and cytoskeletal and signaling molecules. *Shank3* dosage imbalance is detrimental to the structure and function of dendritic spines, causing a shift in the balance between excitation and inhibition. Loss of Shank3 reduces synaptic proteins and impairs glutamatergic transmission in excitatory synapses, whereas gain of Shank3 disrupts inhibitory synapses and neurotransmission, driving hyperexcitability. *Shank3*-deficient mice are hyposocial, show repetitive grooming behavior, memory deficits, and motor dysfunction. *Shank3*^{Tg} mice are also hyposocial and show hyperactivity, mania-like features, and seizures. Therefore, *Shank3* dosage imbalance causes social dysfunction and several disease-specific features. Symptoms associated with *SHANK3* mutations are highly variable because each affected protein domain has specific sets of interacting partners. Adding to the complexity, each SHANK3 isoform contains different protein-interacting domains and is localized to distinct subcellular compartments and brain regions. Therefore, *SHANK3* mutations could result in both distinct and shared defects at the molecular, synaptic, circuit, and behavioral levels (see Table 2 for examples of how different *Shank3* mutations affect mouse behavior). It remains to be determined if different *SHANK3* point mutations affect similar or distinct downstream synaptic pathways across the brain. Together, PMS and 22q13 duplication syndrome highlight the functional maturation of synapses in many brain regions including social circuits that are sensitive to *SHANK3* dosage. Understanding pathogenic pathways associated with each *SHANK3* mutation in disease-relevant brain regions is an important first step towards developing targeted therapies.

5. Angelman Syndrome versus Dup15q Syndrome

5.1. Genetics and clinical features

Genomic imprinting is an epigenetic mechanism that regulates monoallelic expression of about 100–200 genes required for proper development (Monk et al., 2019). During gametogenesis, methyl groups are covalently added onto the GC rich DNA regions called imprinting regions in a parental-origin-specific fashion (Monk et al., 2019). Defects in imprinting are responsible for several human disorders. An example is Angelman Syndrome (AS, OMOM #105,830), a severe neurodevelopmental disorder affecting approximately 1 in 15,000 individuals. The genomic locus of AS is localized on the long arm of chromosome 15 between bands q11 and q13 (15q11-q13) containing ~40 genes (Magenis et al., 1987). Remarkably, AS only occurs when maternal chromosome 15 is deleted (Knoll et al., 1989), whereas deleting paternal 15q11-q13 causes Prader-Willi Syndrome (PWS, OMIM # 176,270) (Butler and Palmer, 1983), an entirely different disorder characterized by hyperphagia and obesity. Interestingly, some AS patients carry two copies of paternal chromosome 15 (Malcolm et al., 1991), and some PWS patients carry two maternal chromosomes 15 (Nicholls et al., 1989), suggesting that these loci are subjected to genomic imprinting.

It was later found that paternal imprinting of a dosage-sensitive gene within 15q11-q13, *Ubiquitin protein ligase E3A* (*UBE3A*), is responsible for AS (Albrecht et al., 1997; Kishino et al., 1997; Matsuura et al., 1997; Rougeulle et al., 1997). Unlike most imprinted genes, the promoter of *UBE3A* is completely unmethylated in both parental chromosomes. However, *UBE3A* expression from the paternal allele is suppressed by a non-coding antisense transcript *SNHG14* (also known as UBE3A-ATS) (Meng et al., 2012; Rougeulle et al., 1997; Runte et al., 2001) localized within an imprinting center called small nuclear ribonucleoprotein-associated protein N (SNRPN) region (Buiting et al., 1995; Sutcliffe et al., 1994). In humans and mice, *UBE3A* is only imprinted in neurons (Albrecht et al., 1997; Vu and Hoffman, 1997). Therefore, in the neurons of normal individuals, *SNHG14* transcript expression is initiated by the paternal promoter of SNRPN and extends into the *UBE3A* genomic region. This potentially causes RNA polymerase II proteins that transcribe *SNHG14* and *UBE3A* in opposite directions to collide and interfere with paternal *UBE3A* expression (Meng et al., 2013). As a result, normal individuals only express *UBE3A* from the maternal chromosome. In non-neuronal tissues, *SNHG14* mRNA does not extend to *UBE3A* (Runte et al., 2004), allowing *UBE3A* to be expressed from both parental chromosomes. AS patients do not express maternal *UBE3A* due to maternal 15q11-q13 deletions containing *UBE3A* (75 %) or point mutations in *UBE3A* (20 %) (Kishino et al., 1997; Lossie et al., 2001; Matsuura et al., 1997). Less common causes of AS include paternal uniparental disomy (2 %) and imprinting defect (3 %). AS patients with large deletions show more severe symptoms compared to other genotypes, suggesting that other genes within 15q11–q13 modify disease severity.

AS was first observed in three patients described as “Puppet Children” that exhibited microcephaly, seizures, diminished cognitive skills, and motor anomalies such as ataxia, hypotonia, and hyperreflexia

(Buiting et al., 2016; Hart, 2008). Psychomotor delay typically develops at 6 months of age, and seizures become evident at 1–3 years of age and persist into adulthood (Larson et al., 2015). 80 % of AS patients show notched δ and rhythmic θ activity, as well as epileptiform EEG discharges (Thibert et al., 2013), highlighting a critical role for *UBE3A* in brain excitability. Microcephaly is often present after 3 years of age and accompanies delayed myelination without gross brain structural abnormalities (Harting et al., 2009; Jay et al., 1991). AS was later described as "Happy Puppet" syndrome because of their distinct characteristics including happy grimacing, frequent smiling, and bouts of excessive laughter initiated by social interaction (Bower and Jeavons, 1967). AS children are also exploratory and inquisitive. Other common features of AS include feeding difficulties, abnormal sleep-wake cycles, and little or no expressive speech (Table 1). As age progresses, AS patients show a gradually diminished physical activity, muscle rigidity, and tremulous movements.

During oogenesis, isodicentric triplication (80 %) and interstitial duplication (20 %) of maternal 15q11-q13 containing *UBE3A* result in Dup15q Syndrome (OMIM # 608,636) (Cook et al., 1997; Repetto et al., 1998), a common cytogenetic anomaly in ASD individuals (1 in 5000 live births) (Kirov et al., 2014). Symptoms associated with maternal isodicentric triplication are usually more severe than those associated with interstitial duplication (Dennis et al., 2006), consistent with dosage-sensitivity of the 15q11-q13 region. For example, ASDs are more common in individuals with triplication (Hogart et al., 2010). Dup15q individuals share many characteristics with AS including hypotonia and motor delays, intellectual disability, developmental delay, language impairment, and ASDs (Table 1) (Hogart et al., 2010). Similar to AS, seizures are hard to control and common (>60 %) in Dup15q patients, which often begin as infantile spasms and are associated with a learning disability (Conant et al., 2014; Urraca et al., 2013). At teenage and young adult age, some Dup15q individuals develop sudden unexpected death in epilepsy (SUDEP) (Devinsky, 2011; Wegiel et al., 2012). Although patients have gait problems (Bundey et al., 1994), they can walk independently after two or three years (Al Ageeli et al., 2014; Dennis et al., 2006). This is in contrast to some AS patients that eventually become wheelchair-bound. Interestingly, paternally-derived duplication can be transmitted from unaffected mothers because they retain a relatively normal neurological function (Browne et al., 1997; Roberts et al., 2002). The discovery of a small maternally-inherited 129 kb duplication containing only *UBE3A* in a Dup15q patient suggests an important role for *UBE3A* in Dup15q pathogenesis (Noor et al., 2015).

5.2. Expression and molecular function of Ube3a

The human *UBE3A* gene comprises 16 exons that span 120 kb. *UBE3A* encodes an 875 amino acids (a.a.) E3 ubiquitin ligase called E6AP, characterized by a C-terminal homologous to E6-associated protein carboxyl-terminus (HECT) domain (Fig. 4**A**) (Huibregtse et al., 1993; Lemak et al., 2011). Many AS-related mutations are localized within this HECT domain and around the catalytic active site within the HECT domain (Cooper et al., 2004; Nawaz et al., 1999). E6AP belongs to the ubiquitin-proteasome system that transfers ubiquitin to mark proteins for subsequent proteasomal degradation (Hershko and Ciechanover, 1992). E6AP is named after its interaction with the E6 protein encoded by human papillomavirus 16, and this interaction mediates the degradation of the p53 tumor suppressor protein (Huibregtse et al., 1991; Scheffner et al., 1993). Interestingly, AS patients and *Ube3a*-deficient mice show increased p53 level in the absence of E6 viral protein (Jiang et al., 1998). In addition to p53, E6AP ubiquitinates a wide array of substrates including guanine nucleotide exchange factors ECT2 and ephexin-5, circadian rhythm-related transcription factor brain and muscle ARNT-like 1 (BMAL1), cyclin-dependent kinase inhibitor p27, calcium-activated potassium channels SK2 and voltage-dependent big potassium (BK) channels, GABA transporter GAT1, and E6AP itself (Egawa et al., 2012; Gossan et al., 2014; Margolis et al., 2010; Mishra et al., 2009; Nuber et al., 1998; Reiter et al., 2006; Shi et al., 2015; Sun et al., 2019, 2015).

E6AP regulates various aspects of neural development and function through ligase-substrate interaction. For example, E6AP-mediated

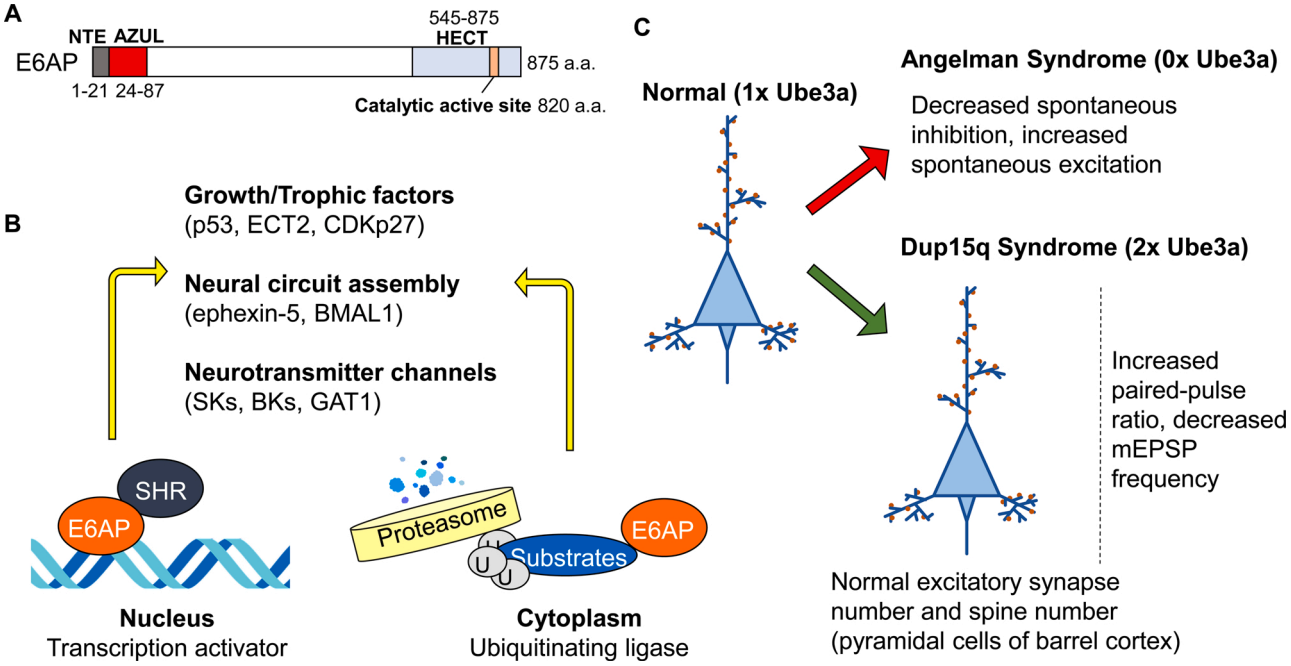

Fig. 4. Molecular and neuronal function of E6AP, encoded by *UBE3A*. **(A)** Functional domains and their locations on E6AP protein. NTE: N terminal extension, AZUL: amino-terminal zinc binding domain, HECT: homologous to the E6AP carboxyl terminus. **(B)** Examples of E6AP transcriptional and ubiquitination targets that are involved in hormonal and neuronal signalings. ECT2: epithelial cell transforming 2, CDKp27: cyclin-dependent kinase inhibitor 27, BMAL1: brain and muscle ARNT-like 1, SKs: Calcium-activated potassium channels, BKs: big potassium channels, GAT1: GABA transporter 1, SHR: steroid hormone receptor. **(C)** Dosage-imbalance of Ube3a in mice causes several opposing cellular and neural activity-level deficits.

ephexin-5 degradation relieves a developmental brake and promotes ephrin B receptor-mediated excitatory synapse development (Margolis et al., 2010). E6AP also regulates neuronal excitability by directly ubiquitinating SK and BK channels (Sun et al., 2019, 2015). The importance of E6AP's ligase activity in pathogenesis is further demonstrated by an ASD-associated mutation that disrupts a phosphorylation site at residue 485 (Yi et al., 2015). Normally, the E3 ligase activity of E6AP is suppressed by protein kinase A (PKA)-mediated phosphorylation. This point mutation disinhibits E6AP activity and promotes substrate turnover and excessive dendritic spine development. Apart from its E3 ligase activity, E6AP can also function as a transcriptional coactivator for the nuclear hormone receptor superfamily (Fig. 4**B**) (Ramamoorthy and Nawaz, 2008).

During postnatal development, neurons downregulate paternal E6AP as they mature, and turn on maternal E6AP expression (Judson et al., 2014; Sato and Stryker, 2010). In AS mice, neurons likely develop normally until paternal E6AP expression diminishes around P7. This suggests that AS symptoms arise from neuronal dysfunction during the early postnatal period. Brain regions that express maternal E6AP and are potentially responsible for AS pathogenesis include cortex, hippocampus, hypothalamus, olfactory bulb, striatum, thalamus, and midbrain (Yashiro et al., 2009). Both excitatory and inhibitory neurons express E6AP from the maternal allele (Gustin et al., 2010), whereas glial cells including astrocytes and oligodendrocytes biallelically express E6AP (Judson et al., 2014).

Strikingly, as neurons mature, E6AP shifts from cytoplasm and synaptic compartments to the nucleus (Dindot et al., 2008; Judson et al., 2014), consistent with its involvement in transcriptional regulation (Ramamoorthy and Nawaz, 2008). The cytoplasmic and nuclear E6AP proteins are two different isoforms generated by alternative splicing. In the mouse brain, the cytoplasmic long isoform and nuclear short isoform are only differentiated by a 21 residues N-terminal extension (Avagliano Trezza et al., 2019; Miao et al., 2013). The nuclear E6AP isoform is four times more abundant than cytoplasmic isoform, suggesting an important nuclear function. E6AP is targeted to the nucleus by proteasome 26S subunit, non-ATPase 4 (PSMD4) through the amino-terminal Zn-finger of Ube3a ligase (AZUL) domain of E6AP (Avagliano Trezza et al., 2019). Mice lacking the nuclear but not cytoplasmic isoform exhibit AS-like synaptic and behavioral phenotypes, whereas mice lacking the cytoplasmic isoform appear normal. This is consistent with a crucial role of the E6AP nuclear isoform in brain function.

5.3. Neuronal and behavioral functions of Ube3a

Mice carrying a 1.6 Mb deletion including *Ube3a* show impaired learning and surprisingly, increased neonatal ultrasonic vocalization (Jiang et al., 2010). A more targeted deletion of maternal *Ube3a* in mice drives AS-like features including hypoactivity, reduced exploratory range, motor dysfunction, defects in contextual and reversal learning, anxiety-like behavior, disturbances in circadian clock and light/dark entrainment, audiogenic seizure, and abnormal hippocampal EEGs (Table 2) (Allensworth et al., 2011; Godavarthi et al., 2012; Heck et al., 2008; Huang et al., 2013; Jiang et al., 1998; Miura et al., 2002; Shi et al., 2015). AS-like mice also show reduced capacity for marble burying, nest building, and increased immobility in a forced swim test (Silva-Santos et al., 2015; Sonzogni et al., 2018). Notably, the learning impairment phenotypes are mild and variable (Born et al., 2017), whereas accelerating rotating rod (rotarod) is the most reproducible and robust motor test (Silva-Santos et al., 2015). These behavioral deficits are not observed in mice with postnatal *Ube3a* deletion (Sonzogni et al., 2019), confirming that Ube3a expression is critical for early brain development. The most consistent AS-like behavioral features, including rotarod test, marble burying, nest building, open field, and forced swim test, have been verified in six independent *Ube3a* mutant lines (Sonzogni et al., 2018). This standardized test battery should be useful for pre-clinical drug trials for AS.

Mice carrying a maternally-inherited genomic duplication syntenic to 15q11-q13 region show a significantly slower acoustic startle response while retaining normal social function and grooming behavior (Nakatani et al., 2009). Soon after, mice carrying single *Ube3a* transgene ($Ube3a^{1XTg}$) and double ($Ube3a^{2XTg}$) transgenes were generated to model Dup15q patients with interstitial duplication and isodicentric triplication, respectively (Smith et al., 2011). $Ube3a^{1XTg}$ mice display limited alterations in social behavior impairment and ultrasonic vocalizations. By contrast, $Ube3a^{2XTg}$ mice show a more severe social defect, vocalization defect, and increased repetitive behavior, consistent with the dosage-sensitivity of *Ube3a* (Table 2). Interestingly, Ube3a overexpression and the subsequent downregulation of cerebellin 1 precursor (Cbln1) in the midbrain ventral tegmental area (VTA) is associated with decreased sociability in mice (Krishnan et al., 2017). Restoring Cbln1 in VTA glutamatergic neurons is sufficient to rescue defective social interaction.

Loss of Ube3a affects the balance between excitatory and inhibitory synaptic transmissions in many brain regions. In the visual cortex, panneural loss of maternal Ube3a causes a 50 % reduction in mIPSC frequency onto layer 2/3 pyramidal neurons and a 28 % decrease in mEPSC frequency (Wallace et al., 2012). Therefore, reduction of inhibitory input outweighs the loss of excitation, consistent with cortical hyperexcitability and seizures in AS mice. A follow-up study of selective deletion of *Ube3a* from either GABAergic or glutamatergic neurons found that deleting maternal *Ube3a* in GABAergic inhibitory neurons is responsible for EEG abnormalities and enhanced seizure susceptibility (Judson et al., 2016). Paradoxically, GABAergic Ube3a loss does not recapitulate inhibitory transmission defects seen in whole-brain knockouts but is associated with presynaptic accumulations of clathrin-coated vesicles. By contrast, loss of Ube3a from the glutamatergic neurons impairs inhibitory transmission onto layer 2/3 pyramidal neurons without eliciting seizures. Therefore, the mechanism underlying circuit hyperexcitability in AS remains to be elucidated. In layer 5 of the prefrontal cortex (PFC), maternal *Ube3a* deletion results in a decreased spontaneous inhibitory transmission and increased spontaneous excitatory transmission (Fig. 4**C**) (Rotaru et al., 2018). This is potentially due to a decreased sodium channel level that decreases the excitability of fast-spiking interneurons. Maternal deletion of *Ube3a* also decreases tonic inhibition of cerebellar granule cells through degradation of GAT1 (Egawa et al., 2012). The hippocampal CA1 pyramidal cells are also more hyperexcitable upon Ube3a loss (Kaphzan et al., 2011), potentially due to altered passive and active membrane properties, increased Na^+/K^+-ATPase levels, and increased axon initial segment length. Although Ube3a loss is generally associated with increased neuronal excitability, in layer 2/3 of visual cortex, loss of maternal Ube3a reduces mEPSC frequency and dendritic spine density (Yashiro et al., 2009). In addition to basal synaptic transmission, maternally-expressed E6AP also participates in experience-driven spine maintenance (Kim et al., 2016), cortical plasticity (Yashiro et al., 2009), and LTP (Jiang et al., 1998), consistent with cognitive defects in AS. Despite a general observation of increased excitability in AS mice, decreased spine density and morphology are observed in the cerebellum, hippocampus, and cortex (Dindot et al., 2008; Kim et al., 2016; Miao et al., 2013). This likely represents a compensatory homeostatic mechanism.

$Ube3a^{2XTg}$ mice display decreased spontaneous and mEPSC amplitude and frequency in layer 2/3 pyramidal neurons of barrel cortex without defects in spontaneous or miniature inhibitory transmissions (Fig. 4**C**) (Smith et al., 2011), consistent with both pre- and postsynaptic excitatory neurotransmission defects. Interestingly, $Ube3a^{2XTg}$ mice show normal excitatory synapse number and spine structures (Smith et al., 2011) but are associated with an increased paired-pulse ratio. This indicates that Ube3a overexpression decreases the release probability of glutamate synapses, resulting in reduced mEPSC frequency. Altogether, the glutamatergic synaptic defects observed in AS and $Ube3a^{2XTg}$ mice cannot be simply predicted by inverting the defects. *Ube3a* dosage

imbalance decreases mEPSC frequency but has different effects on spine density, suggesting distinct neuronal mechanisms.

5.4. Summary

UBE3A dosage imbalance is an important contributor for AS and Dp15q syndrome. The protein product E6AP regulates multiple pathways important for dendritic spine development and the balance of excitatory and inhibitory synaptic transmission. While brain hyperexcitability is associated with maternal loss of Ube3a in cortical GABAergic neurons, the cell types responsible for each AS- and Dup15q-like neurological phenotypes are not known. In addition, the mechanism by which E6AP regulates gene expression and proteasomal activity is not completely understood. The neuronal and behavioral deficits caused by Ube3a loss could be explained by the function of downstream substrates in specific cell types. For example, E6AP interacts with GAT1, SK2, ephexin5, and sodium channels to regulate neuronal excitability and synaptic transmission or structure. The main challenge is the identification of *bona fide* substrates of E6AP because ligase-substrate interaction is intrinsically weak. Incorporating new technologies such as global protein stability profiling (Emanuele et al., 2011; Yen and Elledge, 2008) or orthogonal ubiquitin transfer (Wang et al., 2017b) will help uncover new substrates of E6AP and expand therapeutic options. Quantitative proteomic methods will also help elucidate molecular level pathogenesis underlying gain and loss of Ube3a.

6. Dosage-sensitive syndromic ASDs: converging and diverging features

The overlapping and distinct neurological and physiological features arising from deleting or duplicating the same genes suggest that neural pathways mediating cognition and social behavior are sensitive to the proper level of *RAI1*, *MECP2*, *SHANK3*, and *UBE3A*. Consistent with this observation, the mPFC neurons of *Rai1*$^{+/-}$ mice show decreased spine density (Huang et al., 2018). The same brain region shows increased neuronal excitability upon *Shank3* deletion (Yoo et al., 2019a) and is differently innervated by the ventral hippocampus in RTT mice (Phillips et al., 2019). The ACC region also plays a prominent role in social interaction deficits in *Shank3* mutant mice (Guo et al., 2019). In the subcortical brain regions, Ube3a overexpression in VTA glutamatergic neurons synergizes with seizures to drive social interaction deficits (Krishnan et al., 2017). Studying the neural circuit mechanism underlying social cognition should provide valuable insights into the potential brain regions and cell types mediating social dysfunction in ASDs.

At the molecular level, mounting evidence in mouse models found that these dosage-sensitive proteins regulate the expression of growth and trophic factors, ion channels, neurotransmitter receptors, and cell adhesion molecules. These molecules in turn control circuit assembly, synaptic transmission, neuronal excitability, and neuronal morphology during development (Fig. 5). In some cases, dosage-sensitive proteins regulate a similar set of molecules (see Tables 2 and Table 3 for summary). For example, deleting *Ube3a*, *Mecp2*, or *Rai1* in mice leads to reduced brain-derived trophic factor (Bdnf) signaling (Burns et al., 2010; Cao et al., 2013; Chang et al., 2006). While the involvement of

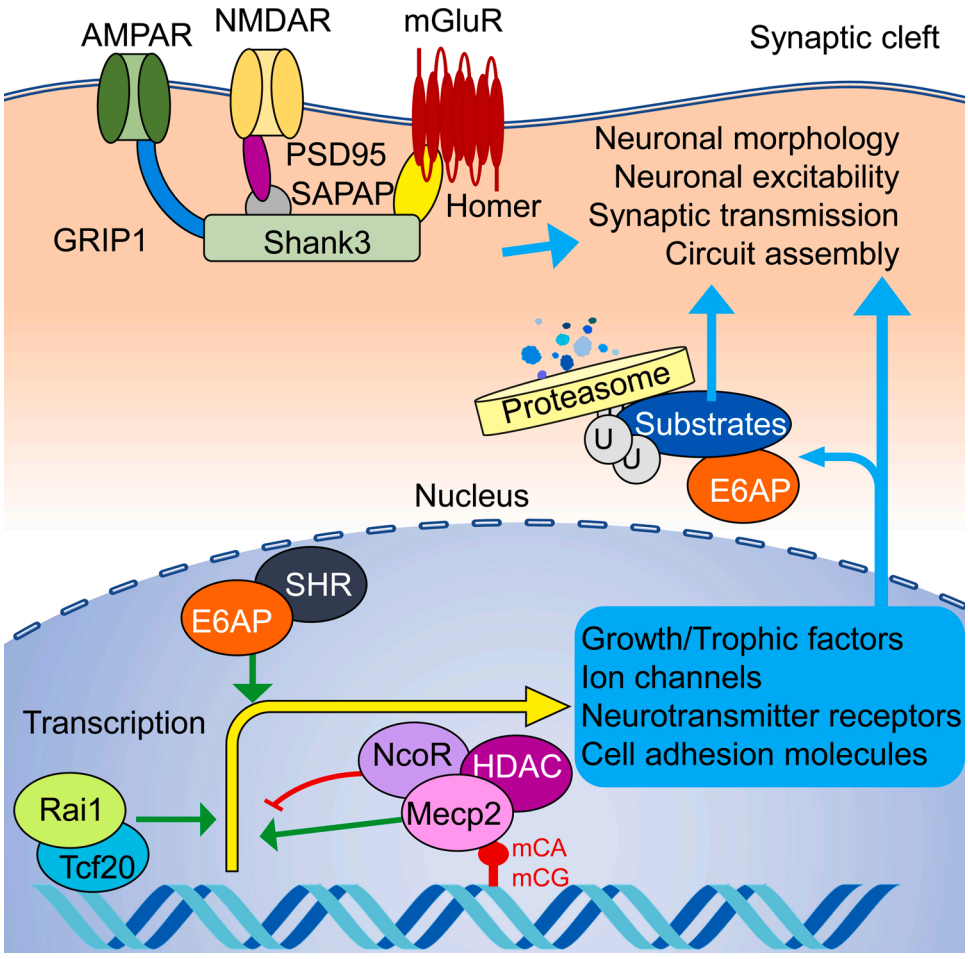

Fig. 5. Molecular pathways regulated by dosage-sensitive syndromic ASD genes. In the nucleus, transcriptional activators (i.e. Rai1 and Mecp2, by binding to promoters and enhancers) and repressors (i.e. Mecp2, by binding to mCA and mCG) associate with interacting partners and regulate the expression of neurotrophic factors, growth factors, ion channels, neurotransmitter receptors, and cell adhesion molecules. E6AP can either regulate protein homeostasis through its E3 ligase activity or regulate gene expression by interacting with steroid hormone receptors (SHR). Shank3 is localized in the post-synaptic densities and directly regulates synaptic structure and function through multiple interacting proteins. In ASDs, these pathways alter neuronal morphology, excitability, synaptic transmission, and circuit assembly, causing network and behavioral deficits.

Bdnf in ASD core symptoms remains unclear, abnormal Bdnf signaling may be responsible for some cognitive and physiological deficits observed in mouse models and human patients of syndromic ASDs (Han, 2016; Skogstrand et al., 2019).

While using mouse to study ASD, one should be aware of the potential limitations of the models. Monogenic ASD models exhibit excellent construct validity. However, their face validity and predictive validity need to be critically evaluated. For instance, core features of ASDs (social dysfunction and repetitive behaviors) displayed by genetic mouse models are quite distinct from human ASD patients. Another limitation of mouse models (including but not limited to ASD) is that disease-like features are sensitive to genetic background, limiting the generalizability of disease-relevant traits (Molenhuis et al., 2018; Sittig et al., 2016). Validating behavioral readouts in multiple strains or using F1 hybrids should minimize the confounding effect (Molenhuis et al., 2018). Finally, it is important to recognize that mouse models while useful, only recapitulate selective aspects of a disorder instead of the full spectrum of the symptomatology. For instance, unlike SMS patients, *Rai1*$^{+/-}$ mice do not show decreased sensitivity to pain (Greenberg et al., 1996; Huang et al., 2016b).

Despite sharing several ASD core features, the eight neurodevelopmental disorders discussed here exhibit disease-specific features resulting from the unique biological properties of each dosage-sensitive protein. This is exemplified by inversed melatonin secretion cycle in SMS (Boone et al., 2011), late childhood regression and irregular breathing in RTT (Chahrour and Zoghbi, 2007), and the overly happy and excitable demeanor in AS (Bower and Jeavons, 1967). This suggests that ASDs are likely many different forms of neurodevelopmental disorders that fall under the general diagnosis term due to the lack of characteristic brain pathology and reliable biomarkers. As a result, diagnosis and classification of ASDs rely on behavioral observations, which is subjective and prone to diagnostic bias (Loomes et al., 2017; Randall et al., 2018). Advances in neurogenetics will help uncover novel genetic causes of ASDs to standardize disease categorization and tailor personalized therapies.

7. Recent progress in treating dosage-sensitive ASDs in mouse models

A key question in ASD is whether the symptoms are caused by early and irreversible defects during brain development or by disruption of potentially reversible defects in adult neural function. On the one hand, ASDs are early-onset and are often diagnosed around toddler age (DSM-5, 2013). ASD-risk genes are expressed during early brain development and may arise from disruption of time-sensitive developmental milestones including neuronal proliferation, migration, differentiation, and activity-dependent circuit refinement (Marin, 2016; Satterstrom et al., 2020). On the other hand, some ASD-risk genes have a continuous function throughout life. For example, adult deletion of *Mecp2* induces many RTT-like features (McGraw et al., 2011). CNV-related ASDs present a unique challenge because precise normalization of gene dosage to endogenous level requires careful calibration. Here, we present recent progress that uncovers remarkable plasticity of the brain, which allows functional rescues of selective features in animal models of monogenic syndromic ASDs. The strategies include directly targeting the endogenous mRNA and protein abundance and repairing downstream molecular changes. Another option is bypassing molecular deficits caused by dosage imbalance and directly treating the neural circuit level deficits. Whatever the therapeutic strategy might be, ASDs may require life-long therapy. Therefore, drug safety is an important consideration currently evaluated by several clinical trials. A major challenge in conducting clinical trials in affected children is the limited number of patients rendering the trails statistically underpowered (Berry-Kravis et al., 2018). Developing precision medicine that directly and specifically targets disease-causing mutations should be beneficial.

7.1. Genetic rescues

Reactivation and deletion of ASD-causing genes in animal models provide important proof-of-principle evidence for the reversibility of each disease feature and pinpoint the most effective therapeutic windows. These experiments often require genetically-engineered mice in which temporal window and cell type-specificity are achieved through Cre-LoxP-mediated recombination. Correcting disease symptoms using clinically applicable methods like adeno-associated virus (AAVs)-mediated gene therapy also shows great promise but not without limitations such as transduction efficiency and control of expression levels.

7.1.1. Genetic reactivation and silencing

7.1.1.1. Temporal window- and Cell type-specific rescues. A landmark study using gene re-expression strategy found that global genetic normalization of *Mecp2* in symptomatic RTT mice reverses overall health, motor deficits, and breathing phenotypes (Guy et al., 2007). Interestingly, the treatment is only beneficial when Mecp2 level is gradually restored because abrupt *Mecp2* activation induces neurological symptoms and lethality (Guy et al., 2007). This highlights the importance of tailoring the course of treatment according to protein function. Similarly, in an MDS mouse model, genetic normalization restores the abnormal transcriptome, hypoactivity, anxiety-like behavior, motor abnormalities, and social deficits in symptomatic mice (Sztainberg et al., 2015). This suggests that the temporal window for treatment may extend well beyond the early developmental stage.

Studies in other ASD models support the notion that the near-complete rescues seen in symptomatic *Mecp2* deletion and duplication models are likely an exception rather than a general rule. For example, genetic normalization of *Rai1* at adult stage does not improve the social dysfunction or repetitive rearing phenotypes in *Rai1* haploinsufficient mice (Huang et al., 2018). Similarly, delayed normalization of *Rai1* dosage in a mouse model of PTLS found that Rai1 level during early development is critical for ameliorating PTLS-like phenotypes (Cao et al., 2014). Adult restoration of Ube3a to endogenous level does not have any measurable impact on behavioral outputs (Silva-Santos et al., 2015). Adult reintroduction of *Shank3* only selectively rescues the repetitive grooming and social deficits but does not improve anxiety and motor coordination phenotypes (Mei et al., 2016). However, the anxiety and motor phenotype of *Shank3* mutant mice can be rescued by reintroducing *Shank3* at weaning age (P21), highlighting the value of an early intervention. Indeed, correcting *Rai1* level at weaning age also ameliorates abnormal social interaction and partially repairs the transcriptomic defects (Huang et al., 2018). *Ube3a* reactivation at weaning age rescues the motor deficits and epilepsy but not anxiety and repetitive behaviors (Gu et al., 2019; Silva-Santos et al., 2015). In comparison to behavioral defects, cellular and synaptic phenotypes are more easily corrected by delayed genetic reactivation. For instance, synaptic properties including LTP deficits as well as dendritic spine phenotypes are rescued by post-symptomatic normalization of *Mecp2* (Guy et al., 2007; Sztainberg et al., 2015), *Shank3* (Mei et al., 2016), and *Ube3a* (Rotaru et al., 2018; Silva-Santos et al., 2015). While not always associated with behavioral rescues, these findings nevertheless demonstrate the remarkable plasticity of the brain circuit. The window of plasticity for behavioral improvement in ASDs closes earlier than the window for synaptic rescues, arguing for earlier diagnosis and intervention. The duration and age of treatment will substantially affect the extent to which neural functions are restored.

While temporal studies demonstrate disease reversibility, brain region- and cell type-specific genetic rescues evaluate the therapeutic potential of targeting selective populations in the brain. This is best demonstrated by a series of studies in RTT models. Reactivating *Mecp2* in cortical and subcortical glutamatergic neurons rescues hypoactivity of the cortical pyramidal neurons (Meng et al., 2016). In *Mecp2*-null

male mice, restoring *Mecp2* in glutamatergic neurons prevents the development of obesity, anxiety, tremor, acoustic startle response, and premature death but not seizures, ataxia, and repetitive behaviors. *Mecp2* heterozygous female mice benefit more than *Mecp2*-null males. For example, ataxia is normalized in females but not males (Meng et al., 2016). Restoring *Mecp2* expression in GABAergic neurons of male mice normalizes body weight, extends lifespan, and improves motor function, repetitive behavior, apraxia, and social phenotypes (Ure et al., 2016). This is consistent with a major role in GABAergic signaling in RTT pathogenesis (Chao et al., 2010). Compared to male mice, *Mecp2* heterozygous female mice show a smaller improvement, suggesting that somatic mosaic *Mecp2* expression causes neural defects that cannot be repaired by the presence of wild-type GABAergic neurons (Ure et al., 2016). Brain-region specific Mecp2 restoration found that selective respiratory phenotypes and lifespan of *Mecp2*-null mice can be improved by using a $HoxA4^{Cre}$ line that targets hindbrain neurons caudal to the fourth ventricle (Huang et al., 2016a, 2012). In addition to neurons, wild-type astrocytes alone are sufficient to increase lifespan and prevent locomotor defects, anxiety, and respiratory abnormalities in an otherwise *Mecp2*-null brain (Lioy et al., 2011). The astrocyte-specific rescue also restores neuronal soma size and dendritic complexity phenotype associated with Mecp2 loss (Lioy et al., 2011), consistent with a role for Mecp2 in glial-neuronal signaling (Ballas et al., 2009). By contrast, genetic restoration of *Mecp2* in microglia does not prevent neurological decline and early lethality in *Mecp2*-null mice (Wang et al., 2015). In addition to understanding the neurobiology of ASD-causing genes, these findings directly inform clinical practice including arguing against transplanting wild-type bone marrow as a treatment for RTT (Wang et al., 2015).

7.1.1.2. AAV- and CRISPR-mediated gene therapy. AAV has recently become a popular therapeutic platform for gene delivery. AAV variants including AAV9 can target neurons and astrocytes in the brain (Foust et al., 2009). Gene replacement therapy using AAV9 that restores Mecp2 level in 10–25 % of the brain cells improves the general health, motor coordination, seizures, and survival of male and female RTT mouse models (Garg et al., 2013). Memory and synaptic deficits associated with maternal Ube3a loss are also rescued by AAV-mediated Ube3a expression (Daily et al., 2011). A limiting factor for AAV-mediated gene replacement lies in its DNA packaging capacity. The commonly used self-complementary AAVs can accommodate up to 2.4 kb of DNA (Hastie and Samulski, 2015). By contrast, most genes involved in ASDs tend to be exceptionally long (mean ~217.3 kb, compared to the mean of cortical neurons ~59.3 kb) (King et al., 2013). Therefore, AAV-mediated gene replacement has only been achieved with smaller genes such as *Mecp2* (cDNA <500 bp), *Ube3a* (cDNA ~2.5 kb), and *Fmr1* (causal gene for Fragile X syndrome, cDNA < 600 bp) (Gholizadeh et al., 2014; Zeier et al., 2009). Identifying functional domains could hold the key to resolving this issue. For example, a recent study demonstrates that AAV-mediated expression of truncated Mecp2 containing only the MBD and NCoR-SMRT interaction domain reduces symptom severity and increases lifespan in *Mecp2*-null mice (Tillotson et al., 2017).

Because ASD genes are expressed by most cells in the brain, another limiting factor of AAV therapy is achieving brain-wide targeting with local injections. The recent discovery that intravenous injection of a modified AAV in mice could cross blood-brain barriers to efficiently transduce glial cells and neurons in multiple brain regions demonstrates the feasibility of treating ASDs using viral vectors (Deverman et al., 2016). A promising future direction is combining brain-wide AAV transduction with the newly emerging gene-editing approaches such as clustered regularly interspaced short palindromic repeats (CRISPR) technology (Heidenreich and Zhang, 2016). The CRISPR technology can repair point mutations and promote or silence gene expression through non-homologous end-joining (NHEJ) or homology-directed repair (HDR). These properties make CRISPR uniquely suited to correct dosage-imbalance in genetic disorders. For example, CRISPR-mediated activation (CRISPRa) has been used to target *Sim1* promoters and enhancers and rescue the obesity phenotype associated with *Sim1* haploinsufficiency in mice (Matharu et al., 2019). In human neurons induced from patients with fragile X syndrome (FXS), fragile X mental retardation 1 (FMR1) expression has been restored by CRISPR-mediated DNA methylation editing that switches the silenced FMR1 promoter into an active chromatin state (Liu et al., 2018). In addition, CRISPR-Gold (a non-viral Cas9 protein delivery vehicle)-mediated targeting of mGluR5 rescues the exaggerated repetitive behaviors in a mouse model of FXS (Lee et al., 2018). CRISPRa has also been used in a mutation-independent approach to promote the expression of a functionally-compensatory disease-modifier protein to treat muscular dystrophy (Kemaladewi et al., 2019). One of the advantages of the CRISPR technology is that it can overcome the DNA packaging limit inherent to AAV gene replacement strategy. However, off-target effects remain a major concern and investigating the mitigating strategies is warranted. Altogether, AAV- and CRISPR-mediated gene therapy are promising strategies to treat ASDs associated with dosage-imbalance.

7.1.2. Harnessing the functional allele

While temporal window- and cell type-specific genetic reactivation and silencing establish the reversibility of each disorder, to have an immediate clinical impact, pharmacological therapies need to be developed. Targeting the over- and under-expressed allele is a direct way to treat CNV-related ASDs. For disorders associated with X chromosomal inactivation and imprinting such as RTT and AS, allele unsilencing is another strategy to regain endogenous expression. Therapies designed to harness the remaining functional allele using antisense therapy and protein stability modifiers also achieved different levels of success.

7.1.2.1. Epigenetic level therapy: unsilencing the intact allele. In AS, the maternal *UBE3A* allele is active in the majority of neurons, whereas the paternal allele is intact but epigenetically silenced (except in certain populations such as suprachiasmatic nucleus) (Albrecht et al., 1997; Jones et al., 2016; Rougeulle et al., 1997; Vu and Hoffman, 1997). Similarly, ~50 % of cells in female RTT patients carry a wild-type but silenced copy of *MECP2* on the inactive X chromosome. This raises the possibility that *UBE3A* and *MECP2* expression can be increased by activating the epigenetically-silenced wild-type allele. To search for compounds that could activate the silent paternal copy of *Ube3a*, a high-throughput drug screen was designed using mouse cortical neurons carrying paternally inherited *Ube3a-YFP* allele (Huang et al., 2011). The screen found that irinotecan and topotecan (clinically used topoisomerase type I inhibitors) inhibit the expression of *Ube3a* antisense transcript, resulting in a concomitant upregulation of paternal *Ube3a-YFP* in a dose- and time-dependent manner (Huang et al., 2011). Infusing topotecan into the mouse brain can unsilence paternal *Ube3a* expression. However, topotecan induces downregulation of other paternally expressed genes and is quickly metabolized and removed from the brain within 5 hours (except subsets of spinal cord neurons). The value of prescribing cancer drugs to AS patients is also unclear. However, this study beautifully demonstrates that unsilencing paternal *Ube3a* is a viable strategy to treat AS.

While X chromosome inactivation has been extensively studied, the mechanism of X chromosome reactivation is less understood (Pasque and Plath, 2015). Therefore, reactivating *Mecp2* depends on high-throughput screens using ~60,000 small hairpin RNAs (Sripathy et al., 2017) or ~367,000 small molecules (Lessing et al., 2016). Intriguingly, intracerebroventricular injection of pharmacological inhibitors in phosphatidylinositol-3-kinase (PI3K) and bone morphogenetic protein (BMP) pathways reactivate the silenced *Mecp2* allele in adult mice (Przanowski et al., 2018). A major distinction between AS and RTT is that in AS, all neurons carry a silenced *UBE3A* allele whereas

female RTT patients have 50 % of wild-type cells and the other 50 % are mutant cells carrying an inactive *MECP2* allele. Therefore, reactivating X chromosome in female RTT patients could normalize *MECP2* dosage in mutant cells but have the unwanted side effect of *MECP2* duplication in wild-type cells. Targeting the mutant but not wild-type cells is an unsolved issue in the field.

7.1.2.2. mRNA level therapy: Antisense oligonucleotides (ASOs). Therapeutic ASOs complementary to sense strand of mRNA have been recently used to treat genetically-defined disorders such as spinal muscular atrophy (Mercuri et al., 2018) and Duchenne muscular dystrophy (Cirak et al., 2011). ASOs regulate target mRNA level by altering splicing or recruiting RNase H to cleave the ASO:RNA duplex, resulting in subsequent RNA degradation by exonucleases (Scoles et al., 2019). ASOs are well-tolerated during intracerebroventricular delivery and have a broad tissue distribution and long duration of action. In addition, because the concentration and duration of ASOs can be precisely regulated, it is a promising tool to target ASDs associated with gene dosage imbalance. In disorders associated with underexpression of ASD genes such as AS, ASOs have been used to target the antisense transcript *SNHG14* that normally silences the functional paternal *Ube3a* allele (Meng et al., 2015). This method is advantageous over topotecan-mediated *Ube3a* unsilencing (Huang et al., 2011) because ASOs directly target *SNHG14* while leaving the expression of other paternally expressed genes intact. Remarkably, a single injection of ASOs in 2–4 months old AS-like mice unmutes the paternal *Ube3a* for at least 4 months, restores hippocampal LTP, and abolishes fear learning defects (Meng et al., 2015). However, motor deficits, repetitive behaviors, and anxiety phenotypes are not rescued, consistent with previous findings that adult Ube3a restoration has limited impact on selective behavioral phenotypes (Silva-Santos et al., 2015). In ASDs associated with gene duplication such as MDS, continuous intracerebral delivery of ASOs in 2-month-old *Mecp2*-duplication mice for 6–7 weeks normalizes motor learning defect. After 10–11 weeks of ASO treatment, hypoactivity, abnormal anxiety-like, and social behaviors are reversed (Sztainberg et al., 2015). Abnormal hippocampal transcriptome and epileptiform EEG patterns are also improved. Consistent with the continuous requirement for Mecp2 in the adult brain (McGraw et al., 2011), disease features re-emerge 10 weeks after the cessation of ASO treatment. Together, ASOs show great promise in pre-clinical mouse models of CNV-related ASDs. Future studies should focus on careful screening of the ASO sequence to avoid off-target effects, as well as identifying critical therapeutic windows and optimizing the delivery route, frequency, and dose.

7.1.2.3. Protein level therapy: modulate protein stability by kinase modifiers. A straightforward strategy to treat ASDs associated with dosage-sensitive genes is to target the root of the disorders: protein abundance. The precise protein levels of many ASD genes are tightly regulated by post-translational modifications such as phosphorylation (Lombardi et al., 2017; Wang et al., 2019a). Kinase and phosphatase are excellent points of intervention because they are readily targeted by small molecule inhibitors (Noble et al., 2004). Fine-tuning protein levels using pharmacology is also advantageous and a potentially safer option in comparison to gene replacement therapy because if protein level is not carefully regulated, we could fix one disease by causing another. The Zoghbi group at Baylor College of Medicine has pioneered a kinome-wide, small interfering RNA (siRNA)-mediated modifier screen platform to modulate protein stability and treat neurodegenerative disorders (Lasagna-Reeves et al., 2016; Park et al., 2013) as well as ASDs associated with *Mecp2* and *Shank3* dosage imbalance (Lombardi et al., 2017; Wang et al., 2019a). To monitor MECP2 protein level, they engineered a human cell line stably expressing *Discosoma sp.* red fluorescent protein (DsRed)-internal ribosomal entry site (IRES)–human MECP2–enhanced green fluorescent protein (EGFP). This clever design ensures that two fluorophores are encoded in equimolar amounts. Therefore, MECP2-EGFP versus DsRed ratio will provide a direct readout for the relative abundance of MECP2 while controlling for fluctuations in transcription. Using this reporter cell line, siRNAs targeting human kinases and phosphatases were transfected, and the alterations in the EGFP-DsRed ratio were measured using fluorescence-activated cell sorting. With carefully controlled secondary screen and follow up studies, this method identifies *in vivo* stabilizers of MeCP2 including homeodomain-interacting protein kinase 2 (HIPK2) and protein phosphatase 2A (PP2A) (Lombardi et al., 2017). Intriguingly, pharmacological inhibition of PP2A reduces brain Mecp2 level and rescues motor abnormalities in a mouse model of MDS (Lombardi et al., 2017). Using a similar method, they identified a destabilizer of SHANK3 protein called extracellular signal-regulated kinases 2 (ERK2) that promotes SHANK3 ubiquitination and degradation (Wang et al., 2019a).

A kinase downstream of Shank3, cdc2-like kinase 2 (CLK2), was also identified as a therapeutic target for PMS (Bidinosti et al., 2016). Specifically, *Shank3* deletion increases CLK2 level. Inhibiting CLK2 rescues synaptic deficits in neurons derived from *Shank3*-deficient mice and PMS patients and restores normal sociability in *Shank3*-deficient mice. In a separate study, reducing the inhibitory phosphorylation on CamKII downstream of E6AP also ameliorates hippocampal learning and plasticity defects, seizure propensity and motor function in a mouse model of AS (van Woerden et al., 2007). Altogether, kinases that regulate protein abundance or downstream of dosage-sensitive genes are excellent therapeutic targets and provide readily-druggable targets.

7.2. Mechanism-based therapies

While directly restoring the expression level of dosage-sensitive genes is a straightforward strategy, the proper expression level is a concern because if it is not carefully calibrated, too much or too little protein could drive pathogenesis. Alternatively, correcting the abnormal neuronal signaling pathways or circuit level phenotypes caused by dosage imbalance could avoid the potential toxicity associated with improper protein levels. Moreover, neuronal signaling pathways and ion channels are readily targeted by existing drugs which can be readily repurposed. Of note, because ASDs are different neurodevelopmental disorders that share selective clinical manifestations, a one-drug-fits-all strategy may not exist. Instead, mechanism-based therapies should be specifically developed for each ASD subtype.

7.2.1. Targeting downstream neuronal signaling pathways

ASD-risk genes are overrepresented by chromatin proteins, transcription factors, and synaptic molecules (De Rubeis et al., 2014). While these molecules have a wide range of downstream targets, misregulation of neurotrophic and growth factors signaling pathways are commonly observed in ASDs (Skogstrand et al., 2019). Chromatin factors like Mecp2 and Rai1 regulate genes involved in neuronal signaling and circuit assembly, including *Bdnf* (Burns et al., 2010; Chen et al., 2003; Huang et al., 2016b). Furthermore, ASD patients show abnormal circulating BDNF protein level (Skogstrand et al., 2019). Bdnf signaling plays an important role in neural circuit development and function, such as LTP (Park and Poo, 2013). Overexpressing Bdnf in *Mecp2* mutant mice extends their lifespan, improves locomotor function, and rescues the lower spontaneous activity of cortical neurons (Chang et al., 2006). Administering fingolimod, a blood–brain barrier-penetrant sphingosine-1 phosphate analog, increases Bdnf level, improves motor deficits, and extends the lifespan of *Mecp2*-null male mice (Deogracias et al., 2012). A clinical trial aimed at assessing the safety and efficacy of fingolimod therapy in RTT patients has been conducted (clinical trial number: NCT02061137, results pending). Another group of modulators of Bdnf expression and release are AMPA receptor modulators (known as ampakines) (Jourdi et al., 2009). Ampakine treatment restores irregular breathing frequency and minute volume in *Mecp2*-null mice (Ogier et al., 2007). In a mouse model of AS, ampakine also corrects the defective actin polymerization, LTP, and

learning associated with Ube3a loss (Baudry et al., 2012).

Insulin-like growth factor-1 (IGF-1) is another attractive candidate for therapy because it crosses the blood-brain barrier (Pristera et al., 2019) and is a Mecp2 direct target (Itoh et al., 2007). IGF-1 regulates the maturation of excitatory synapses through PIK3-AKT-PSD95 pathway, which is misregulated in *Mecp2*-deficient mice (Castro et al., 2014; Tropea et al., 2009). Treatment with full-length IGF-1 (Castro et al., 2014) or an active tripeptide fragment (Tropea et al., 2009) extends the lifespan and alleviates the breathing irregularities in *Mecp2*-mutant mice. Similarly, in *Shank3*-deficient mice, daily IGF-1 injections for 2 weeks improve LTP defect, AMPA signaling, and motor deficits (Bozdagi et al., 2013). Importantly, induced pluripotent stem cells generated from PMS patients also respond to IGF-1 treatment (Shcheglovitov et al., 2013). Although recombinant human IGF-1 protein is well-tolerated by RTT patients (Khwaja et al., 2014), it has a limited therapeutic effect on neurobehavioral symptoms or clinical apnea in RTT girls (O'Leary et al., 2018). However, a breakdown product of IGF-1 (Trofinetide, NNZ-2566) recently shows excellent safety and tolerability in RTT patients in a phase 2 clinical trial (Glaze et al., 2019). Intriguingly, IGF-1 analog significantly improves clinical symptoms based on the Rett Syndrome Behavior Questionnaire and prompted an ongoing phase 3 clinical trial (NCT02715115). In addition to treating RTT, a clinical trial using IGF-1 to treat PMS was recently granted by the US Food and Drug Administration (FDA). Importantly, it should be noted that Bdnf and IGF-1 treatment in *Mecp2* and *Shank3* mutant mice only improve comorbidities but not the core features of ASD. Nevertheless, these studies reinforce the importance of studying the neurobiological function of ASD genes in animal models. Because gene replacement therapy could cause a deleterious effect if the proper dosage is not tightly regulated, targeting neuronal signaling is potentially safer because only one of many downstream pathways is modulated. While most studies currently focus on syndromes associated with gene deletion, the success could inspire future research study to target pathways regulated in opposite directions in duplication syndromes.

7.2.2. *Correcting neuronal activity level abnormalities*

The abnormal neuronal activity caused by imbalanced excitatory and inhibitory synaptic transmission is a common feature of ASD and has been long hypothesized to underlie comorbidities including epilepsy and cognitive dysfunction (Rubenstein and Merzenich, 2003). Evidence supporting primary deficits in loss of inhibition (Chao et al., 2010), overexcitation (Han et al., 2013), and overcompensation caused by defective homeostasis mechanism (Antoine et al., 2019) have been observed. Importantly, how gene dosage imbalance affects neuronal excitability depends on cell types and brain regions. For example, loss of Mecp2 causes increased activity in the nucleus of the solitary tract (Kron et al., 2012) and decreased activity in layer V pyramidal cells within the somatosensory cortex (Dani et al., 2005). Therefore, to correct circuit-level abnormalities, targeting specific brain region is potentially more effective than simply increasing or decreasing neurotransmission in the whole brain. A consistent finding in mouse models of RTT is impaired fear learning (Chao et al., 2010; Moretti et al., 2006). In freely moving RTT-like mice, deep brain stimulation in hippocampal dentate gyrus improves contextual and spatial learning deficits (Hao et al., 2015). Forniceal deep brain stimulation rescues hippocampal memory through normalizing expression of ~25 % of the genes involved in synaptic function, cell survival, and neurogenesis in *Mecp2* -null mice (Pohodich et al., 2018). Optogenetic activation of PFC also partially or fully reverses social interaction deficits in mouse models of SMS and PMS (Chen et al., 2020; Huang et al., 2018). Together, circuit-level intervention such as deep brain stimulation has the potential to rescue activity- and molecular-level deficits and should be explored to treat other ASD models associated with learning impairment. Additional brain regions responsible for other symptoms such as motor coordination are also potential sites for deep brain stimulation.

At the molecular level, neuronal activity is regulated by ion channels, synaptic proteins, and neurotransmitter receptors. These neuronal membrane proteins are common downstream targets of ASD genes (Huang et al., 2016b; Sugino et al., 2014). Neurotransmission receptors are an attractive candidate of intervention because they are druggable targets. RTT patients and *Mecp2*-deficient mice show defects in biogenic amine levels (Zoghbi et al., 1985) and abnormal NMDA signaling (Mierau et al., 2016). Interestingly, ketamine (an NMDA antagonist) administration improves RTT-like behavioral phenotypes and extends the lifespan of *Mecp2*-null mice (Kron et al., 2012; Patrizi et al., 2016). The safety of ketamine is being evaluated by clinical trial (NCT03633058).

The involvement of ion channel dysfunction is perhaps best demonstrated by AS. Many protein substrates of E6AP are ion channels, including a synaptic small-conductance potassium channel SK2 (Sun et al., 2015). Loss of Ube3a in mice induces an increased postsynaptic SK2 level and impairs hippocampal LTP. Treatment with apamin, an SK channel blocker found in bee venom, improves learning and memory performance in an AS mouse model. Another E6AP substrate is the calcium- and BK channels (Sun et al., 2019). *UBE3A*-null human neurons show increased BK channel current. Paxilline (a BK channel blocker) administration normalizes neuronal hyperexcitability in both human and mouse neurons. It also corrects the EEG abnormalities and ameliorates seizure susceptibility in *Ube3a*-deficient mice.

Decreased GABAergic neurotransmission is a hallmark of several monogenic ASDs. E6AP directly controls the degradation of GABA transporter 1 (GAT1) (Egawa et al., 2012). Decreased E6AP induces GAT1 overexpression and the subsequent decrease in extrasynaptic GABA concentration. Treating *Ube3a*-deficient mice with a $GABA_A$-receptor agonist rescues cerebellar Purkinje cell firing *in vitro* and improves motor performance *in vivo*. Enhancing inhibition using clonazepam also rescues abnormal network firing in cultured cortical neurons lacking *Shank3* (Lu et al., 2016a). Neuronal and behavioral hyperexcitability detected in $Shank3^{Tg}$ mice can also be rescued using valproate that increases GABAergic neurotransmission and inhibits sodium and calcium channels (Han et al., 2013). Altogether, neuronal membrane proteins such as neurotransmitter receptors and ion channels remain an important class of targets for ASD therapy. In fact, around 90 % of the new drugs treating central nervous system disorders approved by FDA target neuronal membrane proteins (Ghosh et al., 2013). In the future, quantitative proteomic technologies including proximity labeling (Han et al., 2018) and reverse-phase proteomic array (Creighton and Huang, 2015) could be harnessed to precisely capture defects in neural signaling and membrane protein caused by gene dosage imbalance and uncover converging targets that could improve activity level defects in syndromic and potentially idiopathic ASDs.

8. Conclusions and future prospects

Dosage-sensitive genes regulate many aspects of human behavior and physiology including social interaction, physical activity level, energy balance, synaptic plasticity, learning and memory, and brain excitability. They participate in many biological processes including transcriptional regulation, synaptic structure and function, as well as protein homeostasis (De Rubeis et al., 2014; Glessner et al., 2009). This is consistent with findings in yeast that regulatory and structural proteins are highly dosage-sensitive (Papp et al., 2003). Because the molecular interaction of regulatory and structural proteins often demands precise stoichiometry (Toro et al., 2010), fluctuations in the abundance of a single component could disorganize the entire protein complex. This is exemplified by point mutations in *SHANK3* that disrupt interaction with many protein partners. Studying the function of monogenic ASD genes in animal models has provided many new insights into the neurobiology of gene dosage-sensitivity. First of all, regardless of the molecular perturbation, disruption of synaptic homeostasis is a recurring theme in ASD pathogenesis (Zoghbi and Bear, 2012). We also learned that neurons residing in nearby brain regions may show distinct

gene dosage-sensitivity, as demonstrated by heterozygous and homozygous loss of Rai1 in PVH and VMH neurons (Huang et al., 2016b). Studying Mecp2 led to the discovery of the mechanism underlying repression of neuronal long genes marked by mCA (Boxer et al., 2020). Point mutations in one gene, Shank3, differentially impact protein isoforms containing different protein domains. Each Shank3 mutation is associated with a spectrum of neurobehavioral phenotypes, highlighting the complexity of excitatory synapses throughout the brain (Monteiro and Feng, 2017). In AS, studies in animal models also elucidated the imprinting mechanism regulating parent-of-origin-specific *Ube3a* allele expression (Albrecht et al., 1997). While most studies have focused on loss-of-function phenotypes in mice, gain-of-function studies have fueled the discovery of corresponding human duplication syndromes in some cases (Collins et al., 2004; Han et al., 2013).

Interestingly, gain and loss of the same gene do not always result in quantitative, diametric neuronal and behavioral traits. This is because imbalanced protein levels do not always linearly translate into opposing changes in gene expression, protein interaction, synaptic function, or neuronal activity (Crespi, 2013). They could also trigger different downstream compensatory pathways. Despite the fact that most ASD genes are expressed throughout the brain, mouse studies have shown that the activity of each gene product is required in different temporal windows and brain regions. For example, while Rai1 is critical for Vglut2^{+} excitatory neurons but may be dispensable for astrocytes (Huang et al., 2016b), loss of Mecp2 in most cell types affects their normal functions (Lyst and Bird, 2015). Future studies focusing on a critical brain region or a cell type mediating opposing phenotypes could decipher the molecular and neural mechanisms underlying diametrically altered disease features. A similar logic can also be applied to study how dosage imbalance causes the same phenotype.

A key to dissecting the mechanism underlying dosage-sensitive ASDs is the quantitative and high-throughput molecular and neuroscience technologies. At the neuronal activity level, we lack understanding of how gene dosage imbalance impacts neuronal activity across the brain during certain brain or behavioral states (such as during social interaction). To tackle this question, whole-brain clearing and imaging methods (i.e. iDISCO^{+}) can be combined with immunostaining of immediate-early proteins (i.e. Fos) to identify differentially activated brain regions in mutant mice displaying opposing behaviors (Greenberg and Ziff, 1984; Renier et al., 2016). At the neuronal connectivity level, we still lack understanding of how dosage-sensitive genes affect brain connectivity across brain regions. Cell type-specific viral tracing tools can be combined with whole-brain clearing and imaging to systematically quantify connections and determine alterations in an input-output relationship (Luo et al., 2018; Miyamichi et al., 2013; Weissbourd et al., 2014). Large volume neuronal activity recording with high spatiotemporal resolution such as using Neuropixel probes (Jun et al., 2017) or cortex-wide calcium imaging (Allen et al., 2017) could uncover abnormalities in neuronal activities in awake genetic mutant mice in an unprecedented scale and precision. Because the functions of many dosage-sensitive genes are cell type- and brain region-specific, site-specific and non-invasive neuromodulation holds great promise to target ASD features associated with specific brain regions (Wang et al., 2018). Quantitative proteomic methods like reverse-phase proteomic array can be used to map abnormal protein signaling network caused by CNVs (Creighton and Huang, 2015). Proximity labeling coupled with quantitative mass-spectrometry will facilitate identification of novel protein interactors of ASD gene products and uncover faulty interactions (Han et al., 2018). Furthermore, CRISPR and ASOs could treat ASDs by normalizing the abundance of mRNA or protein (Heidenreich and Zhang, 2016). Finally, the regulatory mechanism for the expression of dosage-sensitive genes remains an understudied subject and should provide therapeutic insights. In conclusion, studying the neurobiology of monogenic ASDs in animal models will help identify molecular and neural pathways critical for brain functions that may one day lead to developing a targeted and effective therapy for each subclass of ASDs.

Funding

We acknowledge the support of the Natural Sciences and Engineering Research Council of Canada (NSERC), the SMS Research Foundation (SMSRF), and the Research Institute of McGill University Health Centre (RI-MUHC) for WHH. SJ is supported by the RI-MUHC PhD Studentship.

Declaration of Competing Interest

None.

Acknowledgements

We thank the support from NSERC, RI-MUHC, and SMSRF.

References

Acquaviva, F., Sana, M.E., Della Monica, M., Pinelli, M., Postorivo, D., Fontana, P., Falco, M.T., Nardone, A.M., Lonardo, F., Iascone, M., Scarano, G., 2017. First evidence of Smith-Magenis syndrome in mother and daughter due to a novel RAI mutation. Am. J. Med. Genet. A 173, 231–238.

Al Ageeli, E., Drunat, S., Delanoe, C., Perrin, L., Baumann, C., Capri, Y., Fabre-Teste, J., Aboura, A., Dupont, C., Auvin, S., El Khattabi, L., Chantereau, D., Moncla, A., Tabet, A.C., Verloes, A., 2014. Duplication of the 15q11-q13 region: clinical and genetic study of 30 new cases. Eur. J. Med. Genet. 57, 5–14.

Albrecht, U., Sutcliffe, J.S., Cattanach, B.M., Beechey, C.V., Armstrong, D., Eichele, G., Beaudet, A.L., 1997. Imprinted expression of the murine Angelman syndrome gene, Ube3a, in hippocampal and Purkinje neurons. Nat. Genet. 17, 75–78.

Allen, W.E., Kauvar, I.V., Chen, M.Z., Richman, E.B., Yang, S.J., Chan, K., Gradinaru, V., Deverman, B.E., Luo, L., Deisseroth, K., 2017. Global representations of goal-directed behavior in distinct cell types of mouse neocortex. Neuron 94 (891-907), e896.

Allensworth, M., Saha, A., Reiter, L.T., Heck, D.H., 2011. Normal social seeking behavior, hypoactivity and reduced exploratory range in a mouse model of Angelman syndrome. BMC Genet. 12, 7.

Amir, R.E., Van den Veyver, I.B., Wan, M., Tran, C.Q., Francke, U., Zoghbi, H.Y., 1999. Rett syndrome is caused by mutations in X-linked MECP2, encoding methyl-CpG-binding protein 2. Nat. Genet. 23, 185–188.

Antoine, M.W., Langberg, T., Schnepel, P., Feldman, D.E., 2019. Increased excitation-inhibition ratio stabilizes synapse and circuit excitability in four autism mouse models. Neuron 101, 648-661.e644.

Armstrong, D.D., 2005. Neuropathology of rett syndrome. J. Child Neurol. 20, 747–753.

Armstrong, D., Dunn, J.K., Antalffy, B., Trivedi, R., 1995. Selective dendritic alterations in the cortex of Rett syndrome. J. Neuropathol. Exp. Neurol. 54, 195–201.

Asaka, Y., Jugloff, D.G., Zhang, L., Eubanks, J.H., Fitzsimonds, R.M., 2006. Hippocampal synaptic plasticity is impaired in the Mecp2-null mouse model of Rett syndrome. Neurobiol. Dis. 21, 217–227.

Avagliano Trezza, R., Sonzogni, M., Bossuyt, S.N.V., Zampeta, F.I., Punt, A.M., van den Berg, M., Rotaru, D.C., Koene, L.M.C., Munshi, S.T., Stedehouder, J., Kros, J.M., Williams, M., Heussler, H., de Vrij, F.M.S., Mientjes, E.J., van Woerden, G.M., Kushner, S.A., Distel, B., Elgersma, Y., 2019. Loss of nuclear UBE3A causes electrophysiological and behavioral deficits in mice and is associated with Angelman syndrome. Nat. Neurosci. 22, 1235–1247.

Baker, S.A., Chen, L., Wilkins, A.D., Yu, P., Lichtarge, O., Zoghbi, H.Y., 2013. An AT-hook domain in MeCP2 determines the clinical course of Rett syndrome and related disorders. Cell 152, 984–996.

Ballas, N., Lioy, D.T., Grunseich, C., Mandel, G., 2009. Non-cell autonomous influence of MeCP2-deficient glia on neuronal dendritic morphology. Nat. Neurosci. 12, 311–317.

Balmer, D., Goldstine, J., Rao, Y.M., LaSalle, J.M., 2003. Elevated methyl-CpG-binding protein 2 expression is acquired during postnatal human brain development and is correlated with alternative polyadenylation. J. Mol. Med. 81, 61–68.

Balthasar, N., Dalgaard, L.T., Lee, C.E., Yu, J., Funahashi, H., Williams, T., Ferreira, M., Tang, V., McGovern, R.A., Kenny, C.D., Christiansen, L.M., Edelstein, E., Choi, B., Boss, O., Aschkenasi, C., Zhang, C.Y., Mountjoy, K., Kishi, T., Elmquist, J.K., Lowell, B.B., 2005. Divergence of melanocortin pathways in the control of food intake and energy expenditure. Cell 123, 493–505.

Baron, M.K., Boeckers, T.M., Vaida, B., Faham, S., Gingery, M., Sawaya, M.R., Salyer, D., Gundelfinger, E.D., Bowie, J.U., 2006. An architectural framework that may lie at the core of the postsynaptic density. Science 311, 531–535.

Baudry, M., Kramar, E., Xu, X., Zadran, H., Moreno, S., Lynch, G., Gall, C., Bi, X., 2012. Ampakines promote spine actin polymerization, long-term potentiation, and learning in a mouse model of Angelman syndrome. Neurobiol. Dis. 47, 210–215.

Berkel, S., Marshall, C.R., Weiss, B., Howe, J., Roeth, R., Moog, U., Endris, V., Roberts, W., Szatmari, P., Pinto, D., Bonin, M., Riess, A., Engels, H., Sprengel, R., Scherer, S.W., Rappold, G.A., 2010. Mutations in the SHANK2 synaptic scaffolding gene in autism spectrum disorder and mental retardation. Nat. Genet. 42, 489–491.

Berry-Kravis, E.M., Lindemann, L., Jonch, A.E., Apostol, G., Bear, M.F., Carpenter, R.L., Crawley, J.N., Curie, A., Des Portes, V., Hossain, F., Gasparini, F., Gomez-Mancilla, B., Hessl, D., Loth, E., Scharf, S.H., Wang, P.P., Von Raison, F., Hagerman, R., Spooren, W., Jacquemont, S., 2018. Drug development for

neurodevelopmental disorders: lessons learned from fragile X syndrome. Nat. Rev. Drug Discov. 17, 280–299.
Bi, W., Saifi, G.M., Shaw, C.J., Walz, K., Fonseca, P., Wilson, M., Potocki, L., Lupski, J.R., 2004a. Mutations of RAI1, a PHD-containing protein, in nondeletion patients with Smith-Magenis syndrome. Hum. Genet. 115, 515–524.
Bi, W., Saifi, G.M., Shaw, C.J., Walz, K., Fonseca, P., Wilson, M., Potocki, L., Lupski, J.R., 2004b. Mutations of RAI1, a PHD-containing protein, in nondeletion patients with Smith-Magenis syndrome. Hum. Genet. 115, 515-524-524.
Bi, W., Ohyama, T., Nakamura, H., Yan, J., Visvanathan, J., Justice, M.J., Lupski, J.R., 2005. Inactivation of Rai1 in mice recapitulates phenotypes observed in chromosome engineered mouse models for Smith-Magenis syndrome. Hum. Mol. Genet. 14, 983–995.
Bi, W., Yan, J., Shi, X., Yuva-Paylor, L.A., Antalffy, B.A., Goldman, A., Yoo, J.W., Noebels, J.L., Armstrong, D.L., Paylor, R., Lupski, J.R., 2007. Rai1 deficiency in mice causes learning impairment and motor dysfunction, whereas Rai1 heterozygous mice display minimal behavioral phenotypes. Hum. Mol. Genet. 16, 1802–1813.
Bidinosti, M., Botta, P., Kruttner, S., Proenca, C.C., Stoehr, N., Bernhard, M., Fruh, I., Mueller, M., Bonenfant, D., Voshol, H., Carbone, W., Neal, S.J., McTighe, S.M., Roma, G., Dolmetsch, R.E., Porter, J.A., Caroni, P., Bouwmeester, T., Luthi, A., Galimberti, I., 2016. CLK2 inhibition ameliorates autistic features associated with SHANK3 deficiency. Science 351, 1199–1203.
Bijlsma, E.K., Collins, A., Papa, F.T., Tejada, M.I., Wheeler, P., Peeters, E.A., Gijsbers, A. C., van de Kamp, J.M., Kriek, M., Losekoot, M., Broekma, A.J., Crolla, J.A., Pollazzon, M., Mucciolo, M., Katzaki, E., Disciglio, V., Ferreri, M.I., Marozza, A., Mencarelli, M.A., Castagnini, C., Dosa, L., Ariani, F., Mari, F., Canitano, R., Hayek, G., Botella, M.P., Gener, B., Minguez, M., Renieri, A., Ruivenkamp, C.A., 2012. Xq28 duplications including MECP2 in five females: expanding the phenotype to severe mental retardation. Eur. J. Med. Genet. 55, 404–413.
Bissell, S., Wilde, L., Richards, C., Moss, J., Oliver, C., 2018. The behavioural phenotype of Potocki-Lupski syndrome: a cross-syndrome comparison. J. Neurodev. Disord. 10, 2.
Boccuto, L., Lauri, M., Sarasua, S.M., Skinner, C.D., Buccella, D., Dwivedi, A., Orteschi, D., Collins, J.S., Zollino, M., Visconti, P., Dupont, B., Tiziano, D., Schroer, R.J., Neri, G., Stevenson, R.E., Gurrieri, F., Schwartz, C.E., 2013. Prevalence of SHANK3 variants in patients with different subtypes of autism spectrum disorders. Eur. J. Hum. Genet. 21, 310–316.
Bockers, T.M., Mameza, M.G., Kreutz, M.R., Bockmann, J., Weise, C., Buck, F., Richter, D., Gundelfinger, E.D., Kreienkamp, H.J., 2001. Synaptic scaffolding proteins in rat brain. Ankyrin repeats of the multidomain Shank protein family interact with the cytoskeletal protein alpha-fodrin. J. Biol. Chem. 276, 40104–40112.
Bockers, T.M., Segger-Junius, M., Iglauer, P., Bockmann, J., Gundelfinger, E.D., Kreutz, M.R., Richter, D., Kindler, S., Kreienkamp, H.J., 2004. Differential expression and dendritic transcript localization of Shank family members: identification of a dendritic targeting element in the 3' untranslated region of Shank1 mRNA. Mol. Cell. Neurosci. 26, 182–190.
Boeckers, T.M., Liedtke, T., Spilker, C., Dresbach, T., Bockmann, J., Kreutz, M.R., Gundelfinger, E.D., 2005. C-terminal synaptic targeting elements for postsynaptic density proteins ProSAP1/Shank2 and ProSAP2/Shank3. J. Neurochem. 92, 519–524.
Bonaglia, M.C., Giorda, R., Beri, S., De Agostini, C., Novara, F., Fichera, M., Grillo, L., Galesi, O., Vetro, A., Ciccone, R., Bonati, M.T., Giglio, S., Guerrini, R., Osimani, S., Marelli, S., Zucca, C., Grasso, R., Borgatti, R., Mani, E., Motta, C., Molteni, M., Romano, C., Greco, D., Reitano, S., Baroncini, A., Lapi, E., Cecconi, A., Arrigo, G., Patricelli, M.G., Pantaleoni, C., D'Arrigo, S., Riva, D., Sciacca, F., Dalla Bernardina, B., Zoccante, L., Darra, F., Termine, C., Maserati, E., Bigoni, S., Priolo, E., Bottani, A., Gimelli, S., Bena, F., Brusco, A., di Gregorio, E., Bagnasco, I., Giussani, U., Nitsch, L., Politi, P., Martinez-Frias, M.L., Martinez-Fernandez, M.L., Martinez Guardia, N., Bremer, A., Anderlid, B.M., Zuffardi, O., 2011. Molecular mechanisms generating and stabilizing terminal 22q13 deletions in 44 subjects with Phelan/McDermid syndrome. PLoS Genet. 7, e1002173.
Boone, P.M., Reiter, R.J., Glaze, D.G., Tan, D.X., Lupski, J.R., Potocki, L., 2011. Abnormal circadian rhythm of melatonin in Smith-Magenis syndrome patients with RAI1 point mutations. Am. J. Med. Genet. A 155A, 2024–2027.
Born, H.A., Dao, A.T., Levine, A.T., Lee, W.L., Mehta, N.M., Mehra, S., Weeber, E.J., Anderson, A.E., 2017. Strain-dependence of the Angelman Syndrome phenotypes in Ube3a maternal deficiency mice. Sci. Rep. 7, 8451.
Bower, B.D., Jeavons, P.M., 1967. The "happy puppet" syndrome. Arch. Dis. Child. 42, 298–302.
Boxer, L.D., Renthal, W., Greben, A.W., Whitwam, T., Silberfeld, A., Stroud, H., Li, E., Yang, M.G., Kinde, B., Griffith, E.C., Bonev, B., Greenberg, M.E., 2020. MeCP2 represses the rate of transcriptional initiation of highly methylated long genes. Mol. Cell 77 (294-309), e299.
Bozdagi, O., Sakurai, T., Papapetrou, D., Wang, X., Dickstein, D.L., Takahashi, N., Kajiwara, Y., Yang, M., Katz, A.M., Scattoni, M.L., Harris, M.J., Saxena, R., Silverman, J.L., Crawley, J.N., Zhou, Q., Hof, P.R., Buxbaum, J.D., 2010. Haploinsufficiency of the autism-associated Shank3 gene leads to deficits in synaptic function, social interaction, and social communication. Mol. Autism 1, 15.
Bozdagi, O., Tavassoli, T., Buxbaum, J.D., 2013. Insulin-like growth factor-1 rescues synaptic and motor deficits in a mouse model of autism and developmental delay. Mol. Autism 4, 9.
Browne, C.E., Dennis, N.R., Maher, E., Long, F.L., Nicholson, J.C., Sillibourne, J., Barber, J.C., 1997. Inherited interstitial duplications of proximal 15q: genotype-phenotype correlations. Am. J. Hum. Genet. 61, 1342–1352.
Buiting, K., Saitoh, S., Gross, S., Dittrich, B., Schwartz, S., Nicholls, R.D., Horsthemke, B., 1995. Inherited microdeletions in the Angelman and Prader-Willi syndromes define an imprinting centre on human chromosome 15. Nat. Genet. 9, 395–400.
Buiting, K., Williams, C., Horsthemke, B., 2016. Angelman syndrome - insights into a rare neurogenetic disorder. Nat. Rev. Neurol. 12, 584–593.
Bundey, S., Hardy, C., Vickers, S., Kilpatrick, M.W., Corbett, J.A., 1994. Duplication of the 15q11-13 region in a patient with autism, epilepsy and ataxia. Dev. Med. Child Neurol. 36, 736–742.
Burns, B., Schmidt, K., Williams, S.R., Kim, S., Girirajan, S., Elsea, S.H., 2010. Rai1 haploinsufficiency causes reduced Bdnf expression resulting in hyperphagia, obesity and altered fat distribution in mice and humans with no evidence of metabolic syndrome. Hum. Mol. Genet. 19, 4026–4042.
Butler, M.G., Palmer, C.G., 1983. Parental origin of chromosome 15 deletion in Prader-Willi syndrome. Lancet 1, 1285–1286.
Calfa, G., Li, W., Rutherford, J.M., Pozzo-Miller, L., 2015. Excitation/inhibition imbalance and impaired synaptic inhibition in hippocampal area CA3 of Mecp2 knockout mice. Hippocampus 25, 159–168.
Cao, C., Rioult-Pedotti, M.S., Migani, P., Yu, C.J., Tiwari, R., Parang, K., Spaller, M.R., Goebel, D.J., Marshall, J., 2013. Impairment of TrkB-PSD-95 signaling in Angelman syndrome. PLoS Biol. 11, e1001478.
Cao, L., Molina, J., Abad, C., Carmona-Mora, P., Cárdenas Oyarzo, A., Young, J.I., Walz, K., 2014. Correct developmental expression level of Rai1 in forebrain neurons is required for control of body weight, activity levels and learning and memory. Hum. Mol. Genet. 23, 1771–1782.
Carney, R.M., Wolpert, C.M., Ravan, S.A., Shahbazian, M., Ashley-Koch, A., Cuccaro, M. L., Vance, J.M., Pericak-Vance, M.A., 2003. Identification of MeCP2 mutations in a series of females with autistic disorder. Pediatr. Neurol. 28, 205–211.
Carvalho, C.M., Lupski, J.R., 2016. Mechanisms underlying structural variant formation in genomic disorders. Nat. Rev. Genet. 17, 224–238.
Cassidy, S.B., Dykens, E., Williams, C.A., 2000. Prader-Willi and Angelman syndromes: sister imprinted disorders. Am. J. Med. Genet. 97, 136–146.
Castro, J., Garcia, R.I., Kwok, S., Banerjee, A., Petravicz, J., Woodson, J., Mellios, N., Tropea, D., Sur, M., 2014. Functional recovery with recombinant human IGF1 treatment in a mouse model of Rett Syndrome. Proc Natl Acad Sci U S A 111, 9941–9946.
Chahrour, M., Jung, S.Y., Shaw, C., Zhou, X., Wong, S.T., Qin, J., Zoghbi, H.Y., 2008. MeCP2, a key contributor to neurological disease, activates and represses transcription. Science 320, 1224–1229.
Chahrour, M., Zoghbi, H.Y., 2007. The story of Rett syndrome: from clinic to neurobiology. Neuron 56, 422–437.
Chang, Q., Khare, G., Dani, V., Nelson, S., Jaenisch, R., 2006. The disease progression of Mecp2 mutant mice is affected by the level of BDNF expression. Neuron 49, 341–348.
Chao, H.T., Zoghbi, H.Y., Rosenmund, C., 2007. MeCP2 controls excitatory synaptic strength by regulating glutamatergic synapse number. Neuron 56, 58–65.
Chao, H.T., Chen, H., Samaco, R.C., Xue, M., Chahrour, M., Yoo, J., Neul, J.L., Gong, S., Lu, H.C., Heintz, N., Ekker, M., Rubenstein, J.L., Noebels, J.L., Rosenmund, C., Zoghbi, H.Y., 2010. Dysfunction in GABA signalling mediates autism-like stereotypies and Rett syndrome phenotypes. Nature 468, 263–269.
Chen, K.S., Manian, P., Koeuth, T., Potocki, L., Zhao, Q., Chinault, A.C., Lee, C.C., Lupski, J.R., 1997. Homologous recombination of a flanking repeat gene cluster is a mechanism for a common contiguous gene deletion syndrome. Nat. Genet. 17, 154–163.
Chen, R.Z., Akbarian, S., Tudor, M., Jaenisch, R., 2001. Deficiency of methyl-CpG binding protein-2 in CNS neurons results in a Rett-like phenotype in mice. Nat. Genet. 27, 327–331.
Chen, W.G., Chang, Q., Lin, Y., Meissner, A., West, A.E., Griffith, E.C., Jaenisch, R., Greenberg, M.E., 2003. Derepression of BDNF transcription involves calcium-dependent phosphorylation of MeCP2. Science 302, 885–889.
Chen, L., Chen, K., Lavery, L.A., Baker, S.A., Shaw, C.A., Li, W., Zoghbi, H.Y., 2015. MeCP2 binds to non-CG methylated DNA as neurons mature, influencing transcription and the timing of onset for Rett syndrome. Proc Natl Acad Sci U S A 112, 5509–5514.
Chen, Q., Deister, C.A., Gao, X., Guo, B., Lynn-Jones, T., Chen, N., Wells, M.F., Liu, R., Goard, M.J., Dimidschstein, J., Feng, S., Shi, Y., Liao, W., Lu, Z., Fishell, G., Moore, C.I., Feng, G., 2020. Dysfunction of cortical GABAergic neurons leads to sensory hyper-reactivity in a Shank3 mouse model of ASD. Nat. Neurosci.
Cheng, D., Hoogenraad, C.C., Rush, J., Ramm, E., Schlager, M.A., Duong, D.M., Xu, P., Wijayawardana, S.R., Hanfelt, J., Nakagawa, T., Sheng, M., Peng, J., 2006. Relative and absolute quantification of postsynaptic density proteome isolated from rat forebrain and cerebellum. Mol. Cell Proteomics 5, 1158–1170.
Cheval, H., Guy, J., Merusi, C., De Sousa, D., Selfridge, J., Bird, A., 2012. Postnatal inactivation reveals enhanced requirement for MeCP2 at distinct age windows. Hum. Mol. Genet. 21, 3806–3814.
Ching, T.T., Maunakea, A.K., Jun, P., Hong, C., Zardo, G., Pinkel, D., Albertson, D.G., Fridlyand, J., Mao, J.H., Shchors, K., Weiss, W.A., Costello, J.F., 2005. Epigenome analyses using BAC microarrays identify evolutionary conservation of tissue-specific methylation of SHANK3. Nat. Genet. 37, 645–651.
Cirak, S., Arechavala-Gomeza, V., Guglieri, M., Feng, L., Torelli, S., Anthony, K., Abbs, S., Garralda, M.E., Bourke, J., Wells, D.J., Dickson, G., Wood, M.J., Wilton, S.D., Straub, V., Kole, R., Shrewsbury, S.B., Sewry, C., Morgan, J.E., Bushby, K., Muntoni, F., 2011. Exon skipping and dystrophin restoration in patients with Duchenne muscular dystrophy after systemic phosphorodiamidate morpholino oligomer treatment: an open-label, phase 2, dose-escalation study. Lancet 378, 595–605.
Colic, S., Wither, R.G., Zhang, L., Eubanks, J.H., Bardakjian, B.L., 2013. Characterization of seizure-like events recorded in vivo in a mouse model of Rett syndrome. Neural Netw. 46, 109–115.
Collins, A.L., Levenson, J.M., Vilaythong, A.P., Richman, R., Armstrong, D.L., Noebels, J. L., David Sweatt, J., Zoghbi, H.Y., 2004. Mild overexpression of MeCP2 causes a progressive neurological disorder in mice. Hum. Mol. Genet. 13, 2679–2689.

Conant, K.D., Finucane, B., Cleary, N., Martin, A., Muss, C., Delany, M., Murphy, E.K., Rabe, O., Luchsinger, K., Spence, S.J., Schanen, C., Devinsky, O., Cook, E.H., LaSalle, J., Reiter, L.T., Thibert, R.L., 2014. A survey of seizures and current treatments in 15q duplication syndrome. Epilepsia 55, 396–402.
Cook Jr, E.H., Lindgren, V., Leventhal, B.L., Courchesne, R., Lincoln, A., Shulman, C., Lord, C., Courchesne, E., 1997. Autism or atypical autism in maternally but not paternally derived proximal 15q duplication. Am. J. Hum. Genet. 60, 928–934.
Cooper, E.M., Hudson, A.W., Amos, J., Wagstaff, J., Howley, P.M., 2004. Biochemical analysis of Angelman syndrome-associated mutations in the E3 ubiquitin ligase E6-associated protein. J. Biol. Chem. 279, 41208–41217.
Cooper, G.M., Coe, B.P., Girirajan, S., Rosenfeld, J.A., Vu, T.H., Baker, C., Williams, C., Stalker, H., Hamid, R., Hannig, V., Abdel-Hamid, H., Bader, P., McCracken, E., Niyazov, D., Leppig, K., Thiese, H., Hummel, M., Alexander, N., Gorski, J., Kussmann, J., Shashi, V., Johnson, K., Rehder, C., Ballif, B.C., Shaffer, L.G., Eichler, E.E., 2011. A copy number variation morbidity map of developmental delay. Nat. Genet. 43, 838–846.
Copping, N.A., Christian, S.G.B., Ritter, D.J., Islam, M.S., Buscher, N., Zolkowska, D., Pride, M.C., Berg, E.L., LaSalle, J.M., Ellegood, J., Lerch, J.P., Reiter, L.T., Silverman, J.L., Dindot, S.V., 2017. Neuronal overexpression of Ube3a isoform 2 causes behavioral impairments and neuroanatomical pathology relevant to 15q11.2-q13.3 duplication syndrome. Hum. Mol. Genet. 26, 3995–4010.
Creighton, C.J., Huang, S., 2015. Reverse phase protein arrays in signaling pathways: a data integration perspective. Drug Des. Devel. Ther. 9, 3519–3527.
Crespi, B., 2013. Diametric gene-dosage effects as windows into neurogenetic architecture. Curr. Opin. Neurobiol. 23, 143–151.
Daily, J.L., Nash, K., Jinwal, U., Golde, T., Rogers, J., Peters, M.M., Burdine, R.D., Dickey, C., Banko, J.L., Weeber, E.J., 2011. Adeno-associated virus-mediated rescue of the cognitive defects in a mouse model for Angelman syndrome. PLoS One 6, e27221.
Dani, V.S., Chang, Q., Maffei, A., Turrigiano, G.G., Jaenisch, R., Nelson, S.B., 2005. Reduced cortical activity due to a shift in the balance between excitation and inhibition in a mouse model of Rett syndrome. Proc Natl Acad Sci U S A 102, 12560–12565.
Darvekar, S., Johnsen, S.S., Eriksen, A.B., Johansen, T., Sjøttem, E., 2012. Identification of two independent nucleosome-binding domains in the transcriptional co-activator SPBP. Biochem. J. 442, 65–75.
Darvekar, S., Rekdal, C., Johansen, T., Sjøttem, E., 2013. A phylogenetic study of SPBP and RAI1: evolutionary conservation of chromatin binding modules. PLoS One 8, e78907.
de la Torre-Ubieta, L., Won, H., Stein, J.L., Geschwind, D.H., 2016d. Advancing the understanding of autism disease mechanisms through genetics. Nat. Med. 22, 345–361.
De Rubeis, S., He, X., Goldberg, A.P., Poultney, C.S., Samocha, K., Cicek, A.E., Kou, Y., Liu, L., Fromer, M., Walker, S., Singh, T., Klei, L., Kosmicki, J., Shih-Chen, F., Aleksic, B., Biscaldi, M., Bolton, P.F., Brownfeld, J.M., Cai, J., Campbell, N.G., Carracedo, A., Chahrour, M.H., Chiocchetti, A.G., Coon, H., Crawford, E.L., Curran, S.R., Dawson, G., Duketis, E., Fernandez, B.A., Gallagher, L., Geller, E., Guter, S.J., Hill, R.S., Ionita-Laza, J., Jimenz Gonzalez, P., Kilpinen, H., Klauck, S.M., Kolevzon, A., Lee, I., Lei, I., Lei, J., Lehtimäki, T., Lin, C.F., Ma'ayan, A., Marshall, C. R., McInnes, A.L., Neale, B., Owen, M.J., Ozaki, N., Parellada, M., Parr, J.R., Purcell, S., Puura, K., Rajagopalan, D., Rehnström, K., Reichenberg, A., Sabo, A., Sachse, M., Sanders, S.J., Schafer, C., Schulte-Rüther, M., Skuse, D., Stevens, C., Szatmari, P., Tammimies, K., Valladares, O., Voran, A., Li-San, W., Weiss, L.A., Willsey, A.J., Yu, T.W., Yuen, R.K., Cook, E.H., Freitag, C.M., Gill, M., Hultman, C. M., Lehner, T., Palotie, A., Schellenberg, G.D., Sklar, P., State, M.W., Sutcliffe, J.S., Walsh, C.A., Scherer, S.W., Zwick, M.E., Barett, J.C., Cutler, D.J., Roeder, K., Devlin, B., Daly, M.J., Buxbaum, J.D., Study, D., Autism, H.M.Cf., Consortium, U.K, 2014. Synaptic, transcriptional and chromatin genes disrupted in autism. Nature 515, 209–215.
DeBry, R.W., Seldin, M.F., 1996. Human/mouse homology relationships. Genomics 33, 337–351.
Dennis, N.R., Veltman, M.W., Thompson, R., Craig, E., Bolton, P.F., Thomas, N.S., 2006. Clinical findings in 33 subjects with large supernumerary marker(15) chromosomes and 3 subjects with triplication of 15q11-q13. Am. J. Med. Genet. A 140, 434–441.
Deogracias, R., Yazdani, M., Dekkers, M.P., Guy, J., Ionescu, M.C., Vogt, K.E., Barde, Y. A., 2012. Fingolimod, a sphingosine-1 phosphate receptor modulator, increases BDNF levels and improves symptoms of a mouse model of Rett syndrome. Proc Natl Acad Sci U S A 109, 14230–14235.
Deverman, B.E., Pravdo, P.L., Simpson, B.P., Kumar, S.R., Chan, K.Y., Banerjee, A., Wu, W.L., Yang, B., Huber, N., Pasca, S.P., Gradinaru, V., 2016. Cre-dependent selection yields AAV variants for widespread gene transfer to the adult brain. Nat. Biotechnol. 34, 204–209.
Devinsky, O., 2011. Sudden, unexpected death in epilepsy. N. Engl. J. Med. 365, 1801–1811.
Dhamne, S.C., Silverman, J.L., Super, C.E., Lammers, S.H.T., Hameed, M.Q., Modi, M.E., Copping, N.A., Pride, M.C., Smith, D.G., Rotenberg, A., Crawley, J.N., Sahin, M., 2017. Replicable in vivo physiological and behavioral phenotypes of the Shank3B null mutant mouse model of autism. Mol. Autism 8, 26.
Dhillon, H., Zigman, J.M., Ye, C., Lee, C.E., McGovern, R.A., Tang, V., Kenny, C.D., Christiansen, L.M., White, R.D., Edelstein, E.A., Coppari, R., Balthasar, N., Cowley, M.A., Chua Jr, S., Elmquist, J.K., Lowell, B.B., 2006. Leptin directly activates SF1 neurons in the VMH, and this action by leptin is required for normal body-weight homeostasis. Neuron 49, 191–203.
Dindot, S.V., Antalffy, B.A., Bhattacharjee, M.B., Beaudet, A.L., 2008. The Angelman syndrome ubiquitin ligase localizes to the synapse and nucleus, and maternal deficiency results in abnormal dendritic spine morphology. Hum. Mol. Genet. 17, 111–118.
Dolce, A., Ben-Zeev, B., Naidu, S., Kossoff, E.H., 2013. Rett syndrome and epilepsy: an update for child neurologists. Pediatr. Neurol. 48, 337–345.
DSM-5, A.P.A., 2013. Diagnostic and Statistical Manual of Mental Disorders, dsm–5, 5th ed. DSM-5.
Du, F., Nguyen, M.V., Karten, A., Felice, C.A., Mandel, G., Ballas, N., 2016. Acute and crucial requirement for MeCP2 function upon transition from early to late adult stages of brain maturation. Hum. Mol. Genet. 25, 1690–1702.
Durand, C.M., Betancur, C., Boeckers, T.M., Bockmann, J., Chaste, P., Fauchereau, F., Nygren, G., Rastam, M., Gillberg, I.C., Anckarsater, H., Sponheim, E., Goubran-Botros, H., Delorme, R., Chabane, N., Mouren-Simeoni, M.C., de Mas, P., Bieth, E., Roge, B., Heron, D., Burglen, L., Gillberg, C., Leboyer, M., Bourgeron, T., 2007. Mutations in the gene encoding the synaptic scaffolding protein SHANK3 are associated with autism spectrum disorders. Nat. Genet. 39, 25–27.
Durand, C.M., Perroy, J., Loll, F., Perrais, D., Fagni, L., Bourgeron, T., Montcouquiol, M., Sans, N., 2012. SHANK3 mutations identified in autism lead to modification of dendritic spine morphology via an actin-dependent mechanism. Mol. Psychiatry 17, 71–84.
Dutta, R., Crawley, J.N., 2019. Behavioral evaluation of angelman syndrome mice at older ages. Neuroscience.
Egawa, K., Kitagawa, K., Inoue, K., Takayama, M., Takayama, C., Saitoh, S., Kishino, T., Kitagawa, M., Fukuda, A., 2012. Decreased tonic inhibition in cerebellar granule cells causes motor dysfunction in a mouse model of Angelman syndrome. Sci. Transl. Med. 4, 163ra157.
Ehlers, M.D., 2003. Activity level controls postsynaptic composition and signaling via the ubiquitin-proteasome system. Nat. Neurosci. 6, 231–242.
Emanuele, M.J., Elia, A.E., Xu, Q., Thoma, C.R., Izhar, L., Leng, Y., Guo, A., Chen, Y.N., Rush, J., Hsu, P.W., Yen, H.C., Elledge, S.J., 2011. Global identification of modular cullin-RING ligase substrates. Cell 147, 459–474.
Folstein, S., Rutter, M., 1977. Infantile autism: a genetic study of 21 twin pairs. J. Child Psychol. Psychiatry 18, 297–321.
Foust, K.D., Nurre, E., Montgomery, C.L., Hernandez, A., Chan, C.M., Kaspar, B.K., 2009. Intravascular AAV9 preferentially targets neonatal neurons and adult astrocytes. Nat. Biotechnol. 27, 59–65.
Fragoso, Y.D., Stoney, P.N., Shearer, K.D., Sementilli, A., Nanescu, S.E., Sementilli, P., McCaffery, P., 2015. Expression in the human brain of retinoic acid induced 1, a protein associated with neurobehavioural disorders. Brain Struct. Funct. 220, 1195–1203.
Friez, M.J., Jones, J.R., Clarkson, K., Lubs, H., Abuelo, D., Bier, J.A., Pai, S., Simensen, R., Williams, C., Giampietro, P.F., Schwartz, C.E., Stevenson, R.E., 2006. Recurrent infections, hypotonia, and mental retardation caused by duplication of MECP2 and adjacent region in Xq28. Pediatrics 118, e1687–1695.
Fukuda, T., Itoh, M., Ichikawa, T., Washiyama, K., Goto, Y., 2005. Delayed maturation of neuronal architecture and synaptogenesis in cerebral cortex of Mecp2-deficient mice. J. Neuropathol. Exp. Neurol. 64, 537–544.
Fyffe, S.L., Neul, J.L., Samaco, R.C., Chao, H.T., Ben-Shachar, S., Moretti, P., McGill, B.E., Goulding, E.H., Sullivan, E., Tecott, L.H., Zoghbi, H.Y., 2008. Deletion of Mecp2 in Sim1-expressing neurons reveals a critical role for MeCP2 in feeding behavior, aggression, and the response to stress. Neuron 59, 947–958.
Gabel, H.W., Kinde, B., Stroud, H., Gilbert, C.S., Harmin, D.A., Kastan, N.R., Hemberg, M., Ebert, D.H., Greenberg, M.E., 2015. Disruption of DNA-methylation-dependent long gene repression in Rett syndrome. Nature 522, 89–93.
Garg, S.K., Lioy, D.T., Cheval, H., McGann, J.C., Bissonnette, J.M., Murtha, M.J., Foust, K.D., Kaspar, B.K., Bird, A., Mandel, G., 2013. Systemic delivery of MeCP2 rescues behavioral and cellular deficits in female mouse models of Rett syndrome. J. Neurosci. 33, 13612–13620.
Gaugler, T., Klei, L., Sanders, S.J., Bodea, C.A., Goldberg, A.P., Lee, A.B., Mahajan, M., Manaa, D., Pawitan, Y., Reichert, J., Ripke, S., Sandin, S., Sklar, P., Svantesson, O., Reichenberg, A., Hultman, C.M., Devlin, B., Roeder, K., Buxbaum, J.D., 2014. Most genetic risk for autism resides with common variation. Nat. Genet. 46, 881–885.
Gemelli, T., Berton, O., Nelson, E.D., Perrotti, L.I., Jaenisch, R., Monteggia, L.M., 2006. Postnatal loss of methyl-CpG binding protein 2 in the forebrain is sufficient to mediate behavioral aspects of Rett syndrome in mice. Biol. Psychiatry 59, 468–476.
Gholizadeh, S., Arsenault, J., Xuan, I.C., Pacey, L.K., Hampson, D.R., 2014. Reduced phenotypic severity following adeno-associated virus-mediated Fmr1 gene delivery in fragile X mice. Neuropsychopharmacology 39, 3100–3111.
Ghosh, A., Michalon, A., Lindemann, L., Fontoura, P., Santarelli, L., 2013. Drug discovery for autism spectrum disorder: challenges and opportunities. Nat. Rev. Drug Discov. 12, 777–790.
Gilman, S.R., Iossifov, I., Levy, D., Ronemus, M., Wigler, M., Vitkup, D., 2011. Rare de novo variants associated with autism implicate a large functional network of genes involved in formation and function of synapses. Neuron 70, 898–907.
Girirajan, S., Elsea, S.H., 2009. Abnormal maternal behavior, altered sociability, and impaired serotonin metabolism in Rai1-transgenic mice. Mamm. Genome 20, 247–255.
Girirajan, S., Elsas, L.J., Devriendt, K., Elsea, S.H., 2005. RAI1 variations in Smith-Magenis syndrome patients without 17p11.2 deletions. J. Med. Genet. 42, 820–828.
Girirajan, S., Vlangos, C.N., Szomju, B.B., Edelman, E., Trevors, C.D., Dupuis, L., Nezarati, M., Bunyan, D.J., Elsea, S.H., 2006. Genotype-phenotype correlation in Smith-Magenis syndrome: evidence that multiple genes in 17p11.2 contribute to the clinical spectrum. Genet. Med. 8, 417–427.
Girirajan, S., Patel, N., Slager, R.E., Tokarz, M.E., Bucan, M., Wiley, J.L., Elsea, S.H., 2008. How much is too much? Phenotypic consequences of Rai1 overexpression in mice. Eur. J. Hum. Genet. 16, 941–954.
Glaze, D.G., Neul, J.L., Kaufmann, W.E., Berry-Kravis, E., Condon, S., Stoms, G., Oosterholt, S., Della Pasqua, O., Glass, L., Jones, N.E., Percy, A.K., Rett 002 Study, G, 2019. Double-blind, randomized, placebo-controlled study of trofinetide in pediatric Rett syndrome. Neurology 92, e1912–e1925.

Glessner, J.T., Wang, K., Cai, G., Korvatska, O., Kim, C.E., Wood, S., Zhang, H., Estes, A., Brune, C.W., Bradfield, J.P., Imielinski, M., Frackelton, E.C., Reichert, J., Crawford, E.L., Munson, J., Sleiman, P.M., Chiavacci, R., Annaiah, K., Thomas, K., Hou, C., Glaberson, W., Flory, J., Otieno, F., Garris, M., Soorya, L., Klei, L., Piven, J., Meyer, K.J., Anagnostou, E., Sakurai, T., Game, R.M., Rudd, D.S., Zurawiecki, D., McDougle, C.J., Davis, L.K., Miller, J., Posey, D.J., Michaels, S., Kolevzon, A., Silverman, J.M., Bernier, R., Levy, S.E., Schultz, R.T., Dawson, G., Owley, T., McMahon, W.M., Wassink, T.H., Sweeney, J.A., Nurnberger, J.I., Coon, H., Sutcliffe, J.S., Minshew, N.J., Grant, S.F., Bucan, M., Cook, E.H., Buxbaum, J.D., Devlin, B., Schellenberg, G.D., Hakonarson, H., 2009. Autism genome-wide copy number variation reveals ubiquitin and neuronal genes. Nature 459, 569–573.

Godavarthi, S.K., Dey, P., Maheshwari, M., Jana, N.R., 2012. Defective glucocorticoid hormone receptor signaling leads to increased stress and anxiety in a mouse model of Angelman syndrome. Hum. Mol. Genet. 21, 1824–1834.

Gogolla, N., Takesian, A.E., Feng, G., Fagiolini, M., Hensch, T.K., 2014. Sensory integration in mouse insular cortex reflects GABA circuit maturation. Neuron 83, 894–905.

Goh, E.S., Banwell, B., Stavropoulos, D.J., Shago, M., Yoon, G., 2014. Mosaic microdeletion of 17p11.2-p12 and duplication of 17q22-q24 in a girl with Smith-Magenis phenotype and peripheral neuropathy. Am. J. Med. Genet. A 164A, 748–752.

Goldman, A.M., Potocki, L., Walz, K., Lynch, J.K., Glaze, D.G., Lupski, J.R., Noebels, J.L., 2006. Epilepsy and chromosomal rearrangements in Smith-Magenis Syndrome [del (17)(p11.2p11.2)]. J. Child Neurol. 21, 93–98.

Gossan, N.C., Zhang, F., Guo, B., Jin, D., Yoshitane, H., Yao, A., Glossop, N., Zhang, Y.Q., Fukada, Y., Meng, Q.J., 2014. The E3 ubiquitin ligase UBE3A is an integral component of the molecular circadian clock through regulating the BMAL1 transcription factor. Nucleic Acids Res. 42, 5765–5775.

Grasshoff, U., Bonin, M., Goehring, I., Ekici, A., Dufke, A., Cremer, K., Wagner, N., Rossier, E., Jauch, A., Walter, M., Bauer, C., Bauer, P., Horber, K., Beck-Woedl, S., Wieczorek, D., 2011. De novo MECP2 duplication in two females with random X-inactivation and moderate mental retardation. Eur. J. Hum. Genet. 19, 507–512.

Greenberg, F., Guzzetta, V., Montes de Oca-Luna, R., Magenis, R.E., Smith, A.C., Richter, S.F., Kondo, I., Dobyns, W.B., Patel, P.I., Lupski, J.R., 1991. Molecular analysis of the Smith-Magenis syndrome: a possible contiguous-gene syndrome associated with del(17)(p11.2). Am. J. Hum. Genet. 49, 1207–1218.

Greenberg, F., Lewis, R.A., Potocki, L., Glaze, D., Parke, J., Killian, J., Murphy, M.A., Williamson, D., Brown, F., Dutton, R., McCluggage, C., Friedman, E., Sulek, M., Lupski, J.R., 1996. Multi-disciplinary clinical study of Smith-Magenis syndrome (deletion 17p11.2). Am. J. Med. Genet. 62, 247–254.

Greenberg, M.E., Ziff, E.B., 1984. Stimulation of 3T3 cells induces transcription of the c-fos proto-oncogene. Nature 311, 433–438.

Greer, P.L., Hanayama, R., Bloodgood, B.L., Mardinly, A.R., Lipton, D.M., Flavell, S.W., Kim, T.K., Griffith, E.C., Waldon, Z., Maehr, R., Ploegh, H.L., Chowdhury, S., Worley, P.F., Steen, J., Greenberg, M.E., 2010. The Angelman Syndrome protein Ube3A regulates synapse development by ubiquitinating arc. Cell 140, 704–716.

Gropman, A.L., Duncan, W.C., Smith, A.C., 2006. Neurologic and developmental features of the Smith-Magenis syndrome (del 17p11.2). Pediatr. Neurol. 34, 337–350.

Gu, B., Carstens, K.E., Judson, M.C., Dalton, K.A., Rougie, M., Clark, E.P., Dudek, S.M., Philpot, B.D., 2019. Ube3a reinstatement mitigates epileptogenesis in Angelman syndrome model mice. J. Clin. Invest. 129, 163–168.

Guo, J.U., Su, Y., Shin, J.H., Shin, J., Li, H., Xie, B., Zhong, C., Hu, S., Le, T., Fan, G., Zhu, H., Chang, Q., Gao, Y., Ming, G.L., Song, H., 2014. Distribution, recognition and regulation of non-CpG methylation in the adult mammalian brain. Nat. Neurosci. 17, 215–222.

Guo, B., Chen, J., Chen, Q., Ren, K., Feng, D., Mao, H., Yao, H., Yang, J., Liu, H., Liu, Y., Jia, F., Qi, C., Lynn-Jones, T., Hu, H., Fu, Z., Feng, G., Wang, W., Wu, S., 2019. Anterior cingulate cortex dysfunction underlies social deficits in Shank3 mutant mice. Nat. Neurosci. 22, 1223–1234.

Gustin, R.M., Bichell, T.J., Bubser, M., Daily, J., Filonova, I., Mrelashvili, D., Deutch, A. Y., Colbran, R.J., Weeber, E.J., Haas, K.F., 2010. Tissue-specific variation of Ube3a protein expression in rodents and in a mouse model of Angelman syndrome. Neurobiol. Dis. 39, 283–291.

Guy, J., Hendrich, B., Holmes, M., Martin, J.E., Bird, A., 2001. A mouse Mecp2-null mutation causes neurological symptoms that mimic Rett syndrome. Nat. Genet. 27, 322–326.

Guy, J., Gan, J., Selfridge, J., Cobb, S., Bird, A., 2007. Reversal of neurological defects in a mouse model of Rett syndrome. Science 315, 1143–1147.

Han, J.C., 2016. Rare syndromes and common variants of the brain-derived neurotrophic factor gene in human obesity. Prog. Mol. Biol. Transl. Sci. 140, 75–95.

Han, Z.A., Jeon, H.R., Kim, S.W., Park, J.Y., Chung, H.J., 2012. Clinical characteristics of children with rett syndrome. Ann. Rehabil. Med. 36, 334–339.

Han, K., Holder Jr, J.L., Schaaf, C.P., Lu, H., Chen, H., Kang, H., Tang, J., Wu, Z., Hao, S., Cheung, S.W., Yu, P., Sun, H., Breman, A.M., Patel, A., Lu, H.C., Zoghbi, H.Y., 2013. SHANK3 overexpression causes manic-like behaviour with unique pharmacogenetic properties. Nature 503, 72–77.

Han, S., Li, J., Ting, A.Y., 2018. Proximity labeling: spatially resolved proteomic mapping for neurobiology. Curr. Opin. Neurobiol. 50, 17–23.

Hao, S., Tang, B., Wu, Z., Ure, K., Sun, Y., Tao, H., Gao, Y., Patel, A.J., Curry, D.J., Samaco, R.C., Zoghbi, H.Y., Tang, J., 2015. Forniceal deep brain stimulation rescues hippocampal memory in Rett syndrome mice. Nature 526, 430–434.

Hart, H., 2008. 'Puppet' children. A report on three cases (1965). Dev. Med. Child Neurol. 50, 564.

Harting, I., Seitz, A., Rating, D., Sartor, K., Zschocke, J., Janssen, B., Ebinger, F., Wolf, N. I., 2009. Abnormal myelination in Angelman syndrome. Eur. J. Paediatr. Neurol. 13, 271–276.

Hastie, E., Samulski, R.J., 2015. Recombinant adeno-associated virus vectors in the treatment of rare diseases. Expert Opin. Orphan Drugs 3, 675–689.

Hayashi, M.K., Tang, C., Verpelli, C., Narayanan, R., Stearns, M.H., Xu, R.M., Li, H., Sala, C., Hayashi, Y., 2009. The postsynaptic density proteins Homer and Shank form a polymeric network structure. Cell 137, 159–171.

Heck, D.H., Zhao, Y., Roy, S., LeDoux, M.S., Reiter, L.T., 2008. Analysis of cerebellar function in Ube3a-deficient mice reveals novel genotype-specific behaviors. Hum. Mol. Genet. 17, 2181–2189.

Heck, D.H., Gu, W., Cao, Y., Qi, S., Lacaria, M., Lupski, J.R., 2012. Opposing phenotypes in mice with Smith-Magenis deletion and Potocki-Lupski duplication syndromes suggest gene dosage effects on fluid consumption behavior. Am. J. Med. Genet. A 158A, 2807–2814.

Heckman, L.D., Chahrour, M.H., Zoghbi, H.Y., 2014. Rett-causing mutations reveal two domains critical for MeCP2 function and for toxicity in MECP2 duplication syndrome mice. Elife 3.

Heidenreich, M., Zhang, F., 2016. Applications of CRISPR-Cas systems in neuroscience. Nat. Rev. Neurosci. 17, 36–44.

Herman, G.E., Greenberg, F., Ledbetter, D.H., 1988. Multiple congenital anomaly/mental retardation (MCA/MR) syndrome with Goldenhar complex due to a terminal del (22q). Am. J. Med. Genet. 29, 909–915.

Hershko, A., Ciechanover, A., 1992. The ubiquitin system for protein degradation. Annu. Rev. Biochem. 61, 761–807.

Hogart, A., Wu, D., LaSalle, J.M., Schanen, N.C., 2010. The comorbidity of autism with the genomic disorders of chromosome 15q11.2-q13. Neurobiol. Dis. 38, 181–191.

Huang, H.S., Allen, J.A., Mabb, A.M., King, I.F., Miriyala, J., Taylor-Blake, B., Sciaky, N., Dutton Jr, J.W., Lee, H.M., Chen, X., Jin, J., Bridges, A.S., Zylka, M.J., Roth, B.L., Philpot, B.D., 2011. Topoisomerase inhibitors unsilence the dormant allele of Ube3a in neurons. Nature 481, 185–189.

Huang, W.H., Tupal, S., Huang, T.W., Ward, C.S., Neul, J.L., Klisch, T.J., Gray, P.A., Zoghbi, H.Y., 2012. Atoh1 governs the migration of postmitotic neurons that shape respiratory effectiveness at birth and chemoresponsiveness in adulthood. Neuron 75, 799–809.

Huang, H.S., Burns, A.J., Nonneman, R.J., Baker, L.K., Riddick, N.V., Nikolova, V.D., Riday, T.T., Yashiro, K., Philpot, B.D., Moy, S.S., 2013. Behavioral deficits in an Angelman syndrome model: effects of genetic background and age. Behav. Brain Res. 243, 79–90.

Huang, T.W., Kochukov, M.Y., Ward, C.S., Merritt, J., Thomas, K., Nguyen, T., Arenkiel, B.R., Neul, J.L., 2016a. Progressive changes in a distributed neural circuit underlie breathing abnormalities in mice lacking MeCP2. J. Neurosci. 36, 5572–5586.

Huang, W.H., Guenthner, C.J., Xu, J., Nguyen, T., Schwarz, L.A., Wilkinson, A.W., Gozani, O., Chang, H.Y., Shamloo, M., Luo, L., 2016b. Molecular and neural functions of Rai1, the causal gene for smith-magenis syndrome. Neuron 92, 392–406.

Huang, W.H., Wang, D.C., Allen, W.E., Klope, M., Hu, H., Shamloo, M., Luo, L., 2018. Early adolescent Rai1 reactivation reverses transcriptional and social interaction deficits in a mouse model of Smith-Magenis syndrome. Proc Natl Acad Sci U S A.

Huibregtse, J.M., Scheffner, M., Howley, P.M., 1991. A cellular protein mediates association of p53 with the E6 oncoprotein of human papillomavirus types 16 or 18. EMBO J. 10, 4129–4135.

Huibregtse, J.M., Scheffner, M., Howley, P.M., 1993. Cloning and expression of the cDNA for E6-AP, a protein that mediates the interaction of the human papillomavirus E6 oncoprotein with p53. Mol. Cell. Biol. 13, 775–784.

Imai, Y., Suzuki, Y., Matsui, T., Tohyama, M., Wanaka, A., Takagi, T., 1995. Cloning of a retinoic acid-induced gene, GT1, in the embryonal carcinoma cell line P19: neuron-specific expression in the mouse brain. Brain Res. Mol. Brain Res. 31, 1–9.

Ingiosi, A.M., Schoch, H., Wintler, T., Singletary, K.G., Righelli, D., Roser, L.G., Medina, E., Risso, D., Frank, M.G., Peixoto, L., 2019. Shank3 modulates sleep and expression of circadian transcription factors. Elife 8.

Itoh, M., Ide, S., Takashima, S., Kudo, S., Nomura, Y., Segawa, M., Kubota, T., Mori, H., Tanaka, S., Horie, H., Tanabe, Y., Goto, Y., 2007. Methyl CpG-binding protein 2 (a mutation of which causes Rett syndrome) directly regulates insulin-like growth factor binding protein 3 in mouse and human brains. J. Neuropathol. Exp. Neurol. 66, 117–123.

Ito-Ishida, A., Ure, K., Chen, H., Swann, J.W., Zoghbi, H.Y., 2015. Loss of MeCP2 in parvalbumin-and somatostatin-expressing neurons in mice leads to distinct rett syndrome-like phenotypes. Neuron 88, 651–658.

Jafri, F., Fink, J., Higgins, R.R., Tervo, R., 2011. 22q13.32 deletion and duplication and inversion in the same family: a rare occurrence. ISRN Pediatr. 2011, 829825.

Jay, V., Becker, L.E., Chan, F.W., Perry Sr, T.L., 1991. Puppet-like syndrome of Angelman: a pathologic and neurochemical study. Neurology 41, 416–422.

Jiang, Y.H., Ehlers, M.D., 2013. Modeling autism by SHANK gene mutations in mice. Neuron 78, 8–27.

Jiang, Y.H., Armstrong, D., Albrecht, U., Atkins, C.M., Noebels, J.L., Eichele, G., Sweatt, J.D., Beaudet, A.L., 1998. Mutation of the Angelman ubiquitin ligase in mice causes increased cytoplasmic p53 and deficits of contextual learning and long-term potentiation. Neuron 21, 799–811.

Jiang, Y.H., Pan, Y., Zhu, L., Landa, L., Yoo, J., Spencer, C., Lorenzo, I., Brilliant, M., Noebels, J., Beaudet, A.L., 2010. Altered ultrasonic vocalization and impaired learning and memory in Angelman syndrome mouse model with a large maternal deletion from Ube3a to Gabrb3. PLoS One 5, e12278.

Jiang, M., Ash, R.T., Baker, S.A., Suter, B., Ferguson, A., Park, J., Rudy, J., Torsky, S.P., Chao, H.T., Zoghbi, H.Y., Smirnakis, S.M., 2013. Dendritic arborization and spine dynamics are abnormal in the mouse model of MECP2 duplication syndrome. J. Neurosci. 33, 19518–19533.

Jin, C., Zhang, Y., Kim, S., Kim, Y., Lee, Y., Han, K., 2018. Spontaneous seizure and partial lethality of juvenile Shank3-overexpressing mice in C57BL/6 J background. Mol. Brain 11, 57.
Johnson, B.S., Zhao, Y.T., Fasolino, M., Lamonica, J.M., Kim, Y.J., Georgakilas, G., Wood, K.H., Bu, D., Cui, Y., Goffin, D., Vahedi, G., Kim, T.H., Zhou, Z., 2017. Biotin tagging of MeCP2 in mice reveals contextual insights into the Rett syndrome transcriptome. Nat. Med. 23, 1203–1214.
Jones, P.L., Veenstra, G.J., Wade, P.A., Vermaak, D., Kass, S.U., Landsberger, N., Strouboulis, J., Wolffe, A.P., 1998. Methylated DNA and MeCP2 recruit histone deacetylase to repress transcription. Nat. Genet. 19, 187–191.
Jones, K.A., Han, J.E., DeBruyne, J.P., Philpot, B.D., 2016. Persistent neuronal Ube3a expression in the suprachiasmatic nucleus of Angelman syndrome model mice. Sci. Rep. 6, 28238.
Jorde, L.B., Hasstedt, S.J., Ritvo, E.R., Mason-Brothers, A., Freeman, B.J., Pingree, C., McMahon, W.M., Petersen, B., Jenson, W.R., Mo, A., 1991. Complex segregation analysis of autism. Am. J. Hum. Genet. 49, 932–938.
Jourdi, H., Hsu, Y.T., Zhou, M., Qin, Q., Bi, X., Baudry, M., 2009. Positive AMPA receptor modulation rapidly stimulates BDNF release and increases dendritic mRNA translation. J. Neurosci. 29, 8688–8697.
Judson, M.C., Sosa-Pagan, J.O., Del Cid, W.A., Han, J.E., Philpot, B.D., 2014. Allelic specificity of Ube3a expression in the mouse brain during postnatal development. J. Comp. Neurol. 522, 1874–1896.
Judson, M.C., Wallace, M.L., Sidorov, M.S., Burette, A.C., Gu, B., van Woerden, G.M., King, I.F., Han, J.E., Zylka, M.J., Elgersma, Y., Weinberg, R.J., Philpot, B.D., 2016. GABAergic neuron-specific loss of Ube3a causes angelman syndrome-like EEG abnormalities and enhances seizure susceptibility. Neuron 90, 56–69.
Jun, J.J., Steinmetz, N.A., Siegle, J.H., Denman, D.J., Bauza, M., Barbarits, B., Lee, A.K., Anastassiou, C.A., Andrei, A., Aydin, C., Barbic, M., Blanche, T.J., Bonin, V., Couto, J., Dutta, B., Gratiy, S.L., Gutnisky, D.A., Hausser, M., Karsh, B., Ledochowitsch, P., Lopez, C.M., Mitelut, C., Musa, S., Okun, M., Pachitariu, M., Putzeys, J., Rich, P.D., Rossant, C., Sun, W.L., Svoboda, K., Carandini, M., Harris, K. D., Koch, C., O'Keefe, J., Harris, T.D., 2017. Fully integrated silicon probes for high-density recording of neural activity. Nature 551, 232–236.
Jung, B.P., Jugloff, D.G., Zhang, G., Logan, R., Brown, S., Eubanks, J.H., 2003. The expression of methyl CpG binding factor MeCP2 correlates with cellular differentiation in the developing rat brain and in cultured cells. J. Neurobiol. 55, 86–96.
Kankirawatana, P., Leonard, H., Ellaway, C., Scurlock, J., Mansour, A., Makris, C.M., Dure, L.St., Friez, M., Lane, J., Kiraly-Borri, C., Fabian, V., Davis, M., Jackson, J., Christodoulou, J., Kaufmann, W.E., Ravine, D., Percy, A.K., 2006. Early progressive encephalopathy in boys and MECP2 mutations. Neurology 67, 164–166.
Kaphzan, H., Buffington, S.A., Jung, J.I., Rasband, M.N., Klann, E., 2011. Alterations in intrinsic membrane properties and the axon initial segment in a mouse model of Angelman syndrome. J. Neurosci. 31, 17637–17648.
Kaplan, K., McCool, C., Lupski, J.R., Glaze, D., Potocki, L., 2019. Objective measures of sleep disturbances in children with Potocki-Lupski syndrome. Am. J. Med. Genet. A 179, 1982–1986.
Kemaladewi, D.U., Bassi, P.S., Erwood, S., Al-Basha, D., Gawlik, K.I., Lindsay, K., Hyatt, E., Kember, R., Place, K.M., Marks, R.M., Durbeej, M., Prescott, S.A., Ivakine, E.A., Cohn, R.D., 2019. A mutation-independent approach for muscular dystrophy via upregulation of a modifier gene. Nature 572, 125–130.
Kerrisk Campbell, M., Sheng, M., 2018. USP8 deubiquitinates SHANK3 to control synapse density and SHANK3 activity-dependent protein levels. J. Neurosci. 38, 5289–5301.
Khwaja, O.S., Ho, E., Barnes, K.V., O'Leary, H.M., Pereira, L.M., Finkelstein, Y., Nelson 3rd, C.A., Vogel-Farley, V., DeGregorio, G., Holm, I.A., Khatwa, U., Kapur, K., Alexander, M.E., Finnegan, D.M., Cantwell, N.G., Walco, A.C., Rappaport, L., Gregas, M., Fichorova, R.N., Shannon, M.W., Sur, M., Kaufmann, W.E., 2014. Safety, pharmacokinetics, and preliminary assessment of efficacy of mecasermin (recombinant human IGF-1) for the treatment of Rett syndrome. Proc Natl Acad Sci U S A 111, 4596–4601.
Kim, H., Kunz, P.A., Mooney, R., Philpot, B.D., Smith, S.L., 2016. Maternal loss of Ube3a impairs experience-driven dendritic spine maintenance in the developing visual cortex. J. Neurosci. 36, 4888–4894.
Kinde, B., Gabel, H.W., Gilbert, C.S., Griffith, E.C., Greenberg, M.E., 2015. Reading the unique DNA methylation landscape of the brain: Non-CpG methylation, hydroxymethylation, and MeCP2. Proc Natl Acad Sci U S A 112, 6800–6806.
King, I.F., Yandava, C.N., Mabb, A.M., Hsiao, J.S., Huang, H.S., Pearson, B.L., Calabrese, J.M., Starmer, J., Parker, J.S., Magnuson, T., Chamberlain, S.J., Philpot, B.D., Zylka, M.J., 2013. Topoisomerases facilitate transcription of long genes linked to autism. Nature 501, 58–62.
Kirov, G., Rees, E., Walters, J.T., Escott-Price, V., Georgieva, L., Richards, A.L., Chambert, K.D., Davies, G., Legge, S.E., Moran, J.L., McCarroll, S.A., O'Donovan, M. C., Owen, M.J., 2014. The penetrance of copy number variations for schizophrenia and developmental delay. Biol. Psychiatry 75, 378–385.
Kishi, N., Macklis, J.D., 2004. MECP2 is progressively expressed in post-migratory neurons and is involved in neuronal maturation rather than cell fate decisions. Mol. Cell. Neurosci. 27, 306–321.
Kishino, T., Lalande, M., Wagstaff, J., 1997. UBE3A/E6-AP mutations cause Angelman syndrome. Nat. Genet. 15, 70–73.
Knoll, J.H., Nicholls, R.D., Magenis, R.E., Graham Jr, J.M., Lalande, M., Latt, S.A., 1989. Angelman and Prader-Willi syndromes share a common chromosome 15 deletion but differ in parental origin of the deletion. Am. J. Med. Genet. 32, 285–290.
Kolevzon, A., Angarita, B., Bush, L., Wang, A.T., Frank, Y., Yang, A., Rapaport, R., Saland, J., Srivastava, S., Farrell, C., Edelmann, L.J., Buxbaum, J.D., 2014. Phelan-McDermid syndrome: a review of the literature and practice parameters for medical assessment and monitoring. J. Neurodev. Disord. 6, 39.
Krishnan, V., Stoppel, D.C., Nong, Y., Johnson, M.A., Nadler, M.J., Ozkaynak, E., Teng, B. L., Nagakura, I., Mohammad, F., Silva, M.A., Peterson, S., Cruz, T.J., Kasper, E.M., Arnaout, R., Anderson, M.P., 2017. Autism gene Ube3a and seizures impair sociability by repressing VTA Cbln1. Nature 543, 507–512.
Kron, M., Howell, C.J., Adams, I.T., Ransbottom, M., Christian, D., Ogier, M., Katz, D.M., 2012. Brain activity mapping in Mecp2 mutant mice reveals functional deficits in forebrain circuits, including key nodes in the default mode network, that are reversed with ketamine treatment. J. Neurosci. 32, 13860–13872.
Lacaria, M., Saha, P., Potocki, L., Bi, W., Yan, J., Girirajan, S., Burns, B., Elsea, S., Walz, K., Chan, L., Lupski, J.R., Gu, W., 2012a. A duplication CNV that conveys traits reciprocal to metabolic syndrome and protects against diet-induced obesity in mice and men. PLoS Genet. 8, e1002713.
Lacaria, M., Spencer, C., Gu, W., Paylor, R., Lupski, J.R., 2012b. Enriched rearing improves behavioral responses of an animal model for CNV-based autistic-like traits. Hum. Mol. Genet. 21, 3083–3096.
Lacaria, M., Gu, W., Lupski, J.R., 2013. Circadian abnormalities in mouse models of Smith-Magenis syndrome: evidence for involvement of RAI1. Am. J. Med. Genet. A 161A, 1561–1568.
Lagger, S., Connelly, J.C., Schweikert, G., Webb, S., Selfridge, J., Ramsahoye, B.H., Yu, M., He, C., Sanguinetti, G., Sowers, L.C., Walkinshaw, M.D., Bird, A., 2017. MeCP2 recognizes cytosine methylated tri-nucleotide and di-nucleotide sequences to tune transcription in the mammalian brain. PLoS Genet. 13, e1006793.
Laje, G., Morse, R., Richter, W., Ball, J., Pao, M., Smith, A.C., 2010. Autism spectrum features in Smith-Magenis syndrome. Am. J. Med. Genet. C Semin. Med. Genet. 154C, 456–462.
Larson, A.M., Shinnick, J.E., Shaaya, E.A., Thiele, E.A., Thibert, R.L., 2015. Angelman syndrome in adulthood. Am. J. Med. Genet. A 167A, 331–344.
Lasagna-Reeves, C.A., de Haro, M., Hao, S., Park, J., Rousseaux, M.W., Al-Ramahi, I., Jafar-Nejad, P., Vilanova-Velez, L., See, L., De Maio, A., Nitschke, L., Wu, Z., Troncoso, J.C., Westbrook, T.F., Tang, J., Botas, J., Zoghbi, H.Y., 2016. Reduction of Nuak1 decreases tau and reverses phenotypes in a tauopathy mouse model. Neuron 92, 407–418.
LaSalle, J.M., Reiter, L.T., Chamberlain, S.J., 2015. Epigenetic regulation of UBE3A and roles in human neurodevelopmental disorders. Epigenomics 7, 1213–1228.
Leblond, C.S., Nava, C., Polge, A., Gauthier, J., Huguet, G., Lumbroso, S., Giuliano, F., Stordeur, C., Depienne, C., Mouzat, K., Pinto, D., Howe, J., Lemiere, N., Durand, C. M., Guibert, J., Ey, E., Toro, R., Peyre, H., Mathieu, A., Amsellem, F., Rastam, M., Gillberg, I.C., Rappold, G.A., Holt, R., Monaco, A.P., Maestrini, E., Galan, P., Heron, D., Jacquette, A., Afenjar, A., Rastetter, A., Brice, A., Devillard, F., Assouline, B., Laffargue, F., Lespinasse, J., Chiesa, J., Rivier, F., Bonneau, D., Regnault, B., Zelenika, D., Delepine, M., Lathrop, M., Sanlaville, D., Schluth-Bolard, C., Edery, P., Perrin, L., Tabet, A.C., Schmeisser, M.J., Boeckers, T.M., Coleman, M., Sato, D., Szatmari, P., Scherer, S.W., Rouleau, G.A., Betancur, C., Leboyer, M., Gillberg, C., Delorme, R., Bourgeron, T., 2014. Meta-analysis of SHANK Mutations in Autism Spectrum disorders: a gradient of severity in cognitive impairments. PLoS Genet. 10, e1004580.
Lee, B., Lee, K., Panda, S., Gonzales-Rojas, R., Chong, A., Bugay, V., Park, H.M., Brenner, R., Murthy, N., Lee, H.Y., 2018. Nanoparticle delivery of CRISPR into the brain rescues a mouse model of fragile X syndrome from exaggerated repetitive behaviours. Nat. Biomed. Eng. 2, 497–507.
Lee, Y., Kang, H., Jin, C., Zhang, Y., Kim, Y., Han, K., 2019. Transcriptome analyses suggest minimal effects of Shank3 dosage on directional gene expression changes in the mouse striatum. Anim Cells Syst (Seoul) 23, 270–274.
Lemak, A., Yee, A., Bezsonova, I., Dhe-Paganon, S., Arrowsmith, C.H., 2011. Zn-binding AZUL domain of human ubiquitin protein ligase Ube3A. J. Biomol. NMR 51, 185–190.
Lessing, D., Dial, T.O., Wei, C., Payer, B., Carrette, L.L., Kesner, B., Szanto, A., Jadhav, A., Maloney, D.J., Simeonov, A., Theriault, J., Hasaka, T., Bedalov, A., Bartolomei, M.S., Lee, J.T., 2016. A high-throughput small molecule screen identifies synergism between DNA methylation and Aurora kinase pathways for X reactivation. Proc Natl Acad Sci U S A 113, 14366–14371.
Levy, D., Ronemus, M., Yamrom, B., Lee, Y.H., Leotta, A., Kendall, J., Marks, S., Lakshmi, B., Pai, D., Ye, K., Buja, A., Krieger, A., Yoon, S., Troge, J., Rodgers, L., Iossifov, I., Wigler, M., 2011. Rare de novo and transmitted copy-number variation in autistic spectrum disorders. Neuron 70, 886–897.
Lewis, J.D., Meehan, R.R., Henzel, W.J., Maurer-Fogy, I., Jeppesen, P., Klein, F., Bird, A., 1992. Purification, sequence, and cellular localization of a novel chromosomal protein that binds to methylated DNA. Cell 69, 905–914.
Li, Q., Loh, D.H., Kudo, T., Truong, D., Derakhshesh, M., Kaswan, Z.M., Ghiani, C.A., Tsoa, R., Cheng, Y., Sun, Y.E., Colwell, C.S., 2015. Circadian rhythm disruption in a mouse model of Rett syndrome circadian disruption in RTT. Neurobiol. Dis. 77, 155–164.
Liebau, S., Proepper, C., Schmidt, T., Schoen, M., Bockmann, J., Boeckers, T.M., 2009. ProSAPiP2, a novel postsynaptic density protein that interacts with ProSAP2/Shank3. Biochem. Biophys. Res. Commun. 385, 460–465.
Lim, S., Sala, C., Yoon, J., Park, S., Kuroda, S., Sheng, M., Kim, E., 2001. Sharpin, a novel postsynaptic density protein that directly interacts with the shank family of proteins. Mol. Cell. Neurosci. 17, 385–397.
Linhoff, M.W., Garg, S.K., Mandel, G., 2015. A high-resolution imaging approach to investigate chromatin architecture in complex tissues. Cell 163, 246–255.
Lioy, D.T., Garg, S.K., Monaghan, C.E., Raber, J., Foust, K.D., Kaspar, B.K., Hirrlinger, P. G., Kirchhoff, F., Bissonnette, J.M., Ballas, N., Mandel, G., 2011. A role for glia in the progression of Rett's syndrome. Nature 475, 497–500.

Liu, P., Lacaria, M., Zhang, F., Withers, M., Hastings, P.J., Lupski, J.R., 2011. Frequency of nonallelic homologous recombination is correlated with length of homology: evidence that ectopic synapsis precedes ectopic crossing-over. Am. J. Hum. Genet. 89, 580–588.
Liu, X.S., Wu, H., Krzisch, M., Wu, X., Graef, J., Muffat, J., Hnisz, D., Li, C.H., Yuan, B., Xu, C., Li, Y., Vershkov, D., Cacace, A., Young, R.A., Jaenisch, R., 2018. Rescue of fragile X syndrome neurons by DNA methylation editing of the FMR1 gene. Cell 172 (979-992), e976.
Lombardi, L.M., Baker, S.A., Zoghbi, H.Y., 2015. MECP2 disorders: from the clinic to mice and back. J. Clin. Invest. 125, 2914–2923.
Lombardi, L.M., Zaghlula, M., Sztainberg, Y., Baker, S.A., Klisch, T.J., Tang, A.A., Huang, E.J., Zoghbi, H.Y., 2017. An RNA interference screen identifies druggable regulators of MeCP2 stability. Sci. Transl. Med. 9.
Loomes, R., Hull, L., Mandy, W.P.L., 2017. What is the male-to-Female ratio in autism Spectrum disorder? A systematic review and meta-analysis. J. Am. Acad. Child Adolesc. Psychiatry 56, 466–474.
Lossie, A.C., Whitney, M.M., Amidon, D., Dong, H.J., Chen, P., Theriaque, D., Hutson, A., Nicholls, R.D., Zori, R.T., Williams, C.A., Driscoll, D.J., 2001. Distinct phenotypes distinguish the molecular classes of Angelman syndrome. J. Med. Genet. 38, 834–845.
Lovaas, O.I., 1987. Behavioral treatment and normal educational and intellectual functioning in young autistic children. J. Consult. Clin. Psychol. 55, 3–9.
Lu, C., Chen, Q., Zhou, T., Bozic, D., Fu, Z., Pan, J.Q., Feng, G., 2016a. Micro-electrode array recordings reveal reductions in both excitation and inhibition in cultured cortical neuron networks lacking Shank3. Mol. Psychiatry 21, 159–168.
Lu, H., Ash, R.T., He, L., Kee, S.E., Wang, W., Yu, D., Hao, S., Meng, X., Ure, K., Ito-Ishida, A., Tang, B., Sun, Y., Ji, D., Tang, J., Arenkiel, B.R., Smirnakis, S.M., Zoghbi, H.Y., 2016b. Loss and gain of MeCP2 cause similar hippocampal circuit dysfunction that is rescued by deep brain stimulation in a rett syndrome mouse model. Neuron 91, 739–747.
Lu, W., Ziff, E.B., 2005. PICK1 interacts with ABP/GRIP to regulate AMPA receptor trafficking. Neuron 47, 407–421.
Luciani, J.J., de Mas, P., Depetris, D., Mignon-Ravix, C., Bottani, A., Prieur, M., Jonveaux, P., Philippe, A., Bourrouillou, G., de Martinville, B., Delobel, B., Vallee, L., Croquette, M.F., Mattei, M.G., 2003. Telomeric 22q13 deletions resulting from rings, simple deletions, and translocations: cytogenetic, molecular, and clinical analyses of 32 new observations. J. Med. Genet. 40, 690–696.
Lugtenberg, D., de Brouwer, A.P., Kleefstra, T., Oudakker, A.R., Frints, S.G., Schrander-Stumpel, C.T., Fryns, J.P., Jensen, L.R., Chelly, J., Moraine, C., Turner, G., Veltman, J.A., Hamel, B.C., de Vries, B.B., van Bokhoven, H., Yntema, H.G., 2006. Chromosomal copy number changes in patients with non-syndromic X linked mental retardation detected by array CGH. J. Med. Genet. 43, 362–370.
Luikenhuis, S., Giacometti, E., Beard, C.F., Jaenisch, R., 2004. Expression of MeCP2 in postmitotic neurons rescues Rett syndrome in mice. Proc Natl Acad Sci U S A 101, 6033–6038.
Luo, L., Callaway, E.M., Svoboda, K., 2018. Genetic dissection of neural circuits: a decade of progress. Neuron 98, 256–281.
Luo, L., Ambrozkiewicz, M.C., Benseler, F., Chen, C., Dumontier, E., Falkner, S., Furlanis, E., Gomez, A.M., Hoshina, N., Huang, W.H., Hutchison, M.A., Itoh-Maruoka, Y., Lavery, L.A., Li, W., Maruo, T., Motohashi, J., Pai, E.L., Pelkey, K.A., Pereira, A., Philips, T., Sinclair, J.L., Stogsdill, J.A., Traunmüller, L., Wang, J., Wortel, J., You, W., Abumaria, N., Beier, K.T., Brose, N., Burgess, H.A., Cepko, C.L., Cloutier, J.F., Eroglu, C., Goebbels, S., Kaeser, P.S., Kay, J.N., Lu, W., Mandai, K., McBain, C.J., Nave, K.A., Prado, M.A.M., Prado, V.F., Rothstein, J., Rubenstein, J.L. R., Saher, G., Sakimura, K., Sanes, J.R., Scheiffele, P., Takai, Y., Umemori, H., Verhage, M., Yuzaki, M., Zoghbi, H.Y., Kawabe, H., Craig, A.M., 2020. Optimizing nervous system-specific gene targeting with cre driver lines: prevalence of germline recombination and influencing factors. Neuron.
Lupski, J.R., 2015. Structural variation mutagenesis of the human genome: impact on disease and evolution. Environ. Mol. Mutagen. 56, 419–436.
Lyst, M.J., Bird, A., 2015. Rett syndrome: a complex disorder with simple roots. Nat. Rev. Genet. 16, 261–275.
Lyst, M.J., Ekiert, R., Ebert, D.H., Merusi, C., Nowak, J., Selfridge, J., Guy, J., Kastan, N. R., Robinson, N.D., de Lima Alves, F., Rappsilber, J., Greenberg, M.E., Bird, A., 2013. Rett syndrome mutations abolish the interaction of MeCP2 with the NCoR/SMRT co-repressor. Nat. Neurosci. 16, 898–902.
Magenis, R.E., Brown, M.G., Lacy, D.A., Budden, S., LaFranchi, S., 1987. Is Angelman syndrome an alternate result of del(15)(q11q13)? Am. J. Med. Genet. 28, 829–838.
Magoulas, P.L., Liu, P., Gelowani, V., Soler-Alfonso, C., Kivuva, E.C., Lupski, J.R., Potocki, L., 2014. Inherited dup(17)(p11.2p11.2): expanding the phenotype of the Potocki-Lupski syndrome. Am. J. Med. Genet. A 164A, 500–504.
Malcolm, S., Clayton-Smith, J., Nichols, M., Robb, S., Webb, T., Armour, J.A., Jeffreys, A. J., Pembrey, M.E., 1991. Uniparental paternal disomy in Angelman's syndrome. Lancet 337, 694–697.
Mandel-Brehm, C., Salogiannis, J., Dhamne, S.C., Rotenberg, A., Greenberg, M.E., 2015. Seizure-like activity in a juvenile Angelman syndrome mouse model is attenuated by reducing Arc expression. Proc Natl Acad Sci U S A 112, 5129–5134.
Margolis, S.S., Salogiannis, J., Lipton, D.M., Mandel-Brehm, C., Wills, Z.P., Mardinly, A. R., Hu, L., Greer, P.L., Bikoff, J.B., Ho, H.Y., Soskis, M.J., Sahin, M., Greenberg, M.E., 2010. EphB-mediated degradation of the RhoA GEF Ephexin5 relieves a developmental brake on excitatory synapse formation. Cell 143, 442–455.
Marin, O., 2016. Developmental timing and critical windows for the treatment of psychiatric disorders. Nat. Med. 22, 1229–1238.
Matharu, N., Rattanasopha, S., Tamura, S., Maliskova, L., Wang, Y., Bernard, A., Hardin, A., Eckalbar, W.L., Vaisse, C., Ahituv, N., 2019. CRISPR-mediated activation of a promoter or enhancer rescues obesity caused by haploinsufficiency. Science 363.
Matsuura, T., Sutcliffe, J.S., Fang, P., Galjaard, R.J., Jiang, Y.H., Benton, C.S., Rommens, J.M., Beaudet, A.L., 1997. De novo truncating mutations in E6-AP ubiquitin-protein ligase gene (UBE3A) in Angelman syndrome. Nat. Genet. 15, 74–77.
Maunakea, A.K., Nagarajan, R.P., Bilenky, M., Ballinger, T.J., D'Souza, C., Fouse, S.D., Johnson, B.E., Hong, C., Nielsen, C., Zhao, Y., Turecki, G., Delaney, A., Varhol, R., Thiessen, N., Shchors, K., Heine, V.M., Rowitch, D.H., Xing, X., Fiore, C., Schillebeeckx, M., Jones, S.J., Haussler, D., Marra, M.A., Hirst, M., Wang, T., Costello, J.F., 2010. Conserved role of intragenic DNA methylation in regulating alternative promoters. Nature 466, 253–257.
McGraw, C.M., Samaco, R.C., Zoghbi, H.Y., 2011. Adult neural function requires MeCP2. Science 333, 186.
Mei, Y., Monteiro, P., Zhou, Y., Kim, J.A., Gao, X., Fu, Z., Feng, G., 2016. Adult restoration of Shank3 expression rescues selective autistic-like phenotypes. Nature 530, 481–484.
Meng, L., Person, R.E., Beaudet, A.L., 2012. Ube3a-ATS is an atypical RNA polymerase II transcript that represses the paternal expression of Ube3a. Hum. Mol. Genet. 21, 3001–3012.
Meng, L., Person, R.E., Huang, W., Zhu, P.J., Costa-Mattioli, M., Beaudet, A.L., 2013. Truncation of Ube3a-ATS unsilences paternal Ube3a and ameliorates behavioral defects in the Angelman syndrome mouse model. PLoS Genet. 9, e1004039.
Meng, L., Ward, A.J., Chun, S., Bennett, C.F., Beaudet, A.L., Rigo, F., 2015. Towards a therapy for Angelman syndrome by targeting a long non-coding RNA. Nature 518, 409–412.
Meng, X., Wang, W., Lu, H., He, L.J., Chen, W., Chao, E.S., Fiorotto, M.L., Tang, B., Herrera, J.A., Seymour, M.L., Neul, J.L., Pereira, F.A., Tang, J., Xue, M., Zoghbi, H. Y., 2016. Manipulations of MeCP2 in glutamatergic neurons highlight their contributions to Rett and other neurological disorders. Elife 5.
Mercuri, E., Darras, B.T., Chiriboga, C.A., Day, J.W., Campbell, C., Connolly, A.M., Iannaccone, S.T., Kirschner, J., Kuntz, N.L., Saito, K., Shieh, P.B., Tulinius, M., Mazzone, E.S., Montes, J., Bishop, K.M., Yang, Q., Foster, R., Gheuens, S., Bennett, C. F., Farwell, W., Schneider, E., De Vivo, D.C., Finkel, R.S., Group, C.S., 2018. Nusinersen versus sham control in later-onset spinal muscular atrophy. N. Engl. J. Med. 378, 625–635.
Miao, S., Chen, R., Ye, J., Tan, G.H., Li, S., Zhang, J., Jiang, Y.H., Xiong, Z.Q., 2013. The Angelman syndrome protein Ube3a is required for polarized dendrite morphogenesis in pyramidal neurons. J. Neurosci. 33, 327–333.
Mierau, S.B., Patrizi, A., Hensch, T.K., Fagiolini, M., 2016. Cell-specific regulation of N-Methyl-D-Aspartate receptor maturation by Mecp2 in cortical circuits. Biol. Psychiatry 79, 746–754.
Mishra, A., Godavarthi, S.K., Jana, N.R., 2009. UBE3A/E6-AP regulates cell proliferation by promoting proteasomal degradation of p27. Neurobiol. Dis. 36, 26–34.
Miura, K., Kishino, T., Li, E., Webber, H., Dikkes, P., Holmes, G.L., Wagstaff, J., 2002. Neurobehavioral and electroencephalographic abnormalities in Ube3a maternal-deficient mice. Neurobiol. Dis. 9, 149–159.
Miyake, K., Hirasawa, T., Soutome, M., Itoh, M., Goto, Y., Endoh, K., Takahashi, K., Kudo, S., Nakagawa, T., Yokoi, S., Taira, T., Inazawa, J., Kubota, T., 2011. The protocadherins, PCDHB1 and PCDH7, are regulated by MeCP2 in neuronal cells and brain tissues: implication for pathogenesis of Rett syndrome. BMC Neurosci. 12, 81.
Miyamichi, K., Shlomai-Fuchs, Y., Shu, M., Weissbourd, B.C., Luo, L., Mizrahi, A., 2013. Dissecting local circuits: parvalbumin interneurons underlie broad feedback control of olfactory bulb output. Neuron 80, 1232–1245.
Moessner, R., Marshall, C.R., Sutcliffe, J.S., Skaug, J., Pinto, D., Vincent, J., Zwaigenbaum, L., Fernandez, B., Roberts, W., Szatmari, P., Scherer, S.W., 2007. Contribution of SHANK3 mutations to autism spectrum disorder. Am. J. Hum. Genet. 81, 1289–1297.
Molenhuis, R.T., Bruining, H., Brandt, M.J.V., van Soldt, P.E., Abu-Toamih Atamni, H.J., Burbach, J.P.H., Iraqi, F.A., Mott, R.F., Kas, M.J.H., 2018. Modeling the quantitative nature of neurodevelopmental disorders using Collaborative Cross mice. Mol. Autism 9, 63.
Molina, J., Carmona-Mora, P., Chrast, J., Krall, P.M., Canales, C.P., Lupski, J.R., Reymond, A., Walz, K., 2008. Abnormal social behaviors and altered gene expression rates in a mouse model for Potocki-Lupski syndrome. Hum. Mol. Genet. 17, 2486–2495.
Monk, D., Mackay, D.J.G., Eggermann, T., Maher, E.R., Riccio, A., 2019. Genomic imprinting disorders: lessons on how genome, epigenome and environment interact. Nat. Rev. Genet. 20, 235–248.
Monteiro, P., Feng, G., 2017. SHANK proteins: roles at the synapse and in autism spectrum disorder. Nat. Rev. Neurosci. 18, 147–157.
Moretti, P., Bouwknecht, J.A., Teague, R., Paylor, R., Zoghbi, H.Y., 2005. Abnormalities of social interactions and home-cage behavior in a mouse model of Rett syndrome. Hum. Mol. Genet. 14, 205–220.
Moretti, P., Levenson, J.M., Battaglia, F., Atkinson, R., Teague, R., Antalffy, B., Armstrong, D., Arancio, O., Sweatt, J.D., Zoghbi, H.Y., 2006. Learning and memory and synaptic plasticity are impaired in a mouse model of Rett syndrome. J. Neurosci. 26, 319–327.
Mullegama, S.V., Alaimo, J.T., Fountain, M.D., Burns, B., Balog, A.H., Chen, L., Elsea, S. H., 2017. RAI1 overexpression promotes altered circadian gene expression and dyssomnia in Potocki-Lupski syndrome. J. Pediatr. Genet. 6, 155–164.
Na, E.S., Nelson, E.D., Adachi, M., Autry, A.E., Mahgoub, M.A., Kavalali, E.T., Monteggia, L.M., 2012. A mouse model for MeCP2 duplication syndrome: MeCP2 overexpression impairs learning and memory and synaptic transmission. J. Neurosci. 32, 3109–3117.
Naisbitt, S., Kim, E., Tu, J.C., Xiao, B., Sala, C., Valtschanoff, J., Weinberg, R.J., Worley, P.F., Sheng, M., 1999. Shank, a novel family of postsynaptic density proteins

that binds to the NMDA receptor/PSD-95/GKAP complex and cortactin. Neuron 23, 569–582.
Nakamine, A., Ouchanov, L., Jimenez, P., Manghi, E.R., Esquivel, M., Monge, S., Fallas, M., Burton, B.K., Szomju, B., Elsea, S.H., Marshall, C.R., Scherer, S.W., McInnes, L.A., 2008. Duplication of 17(p11.2p11.2) in a male child with autism and severe language delay. Am. J. Med. Genet. A 146A, 636–643.
Nakatani, J., Tamada, K., Hatanaka, F., Ise, S., Ohta, H., Inoue, K., Tomonaga, S., Watanabe, Y., Chung, Y.J., Banerjee, R., Iwamoto, K., Kato, T., Okazawa, M., Yamauchi, K., Tanda, K., Takao, K., Miyakawa, T., Bradley, A., Takumi, T., 2009. Abnormal behavior in a chromosome-engineered mouse model for human 15q11-13 duplication seen in autism. Cell 137, 1235–1246.
Nan, X., Meehan, R.R., Bird, A., 1993. Dissection of the methyl-CpG binding domain from the chromosomal protein MeCP2. Nucleic Acids Res. 21, 4886–4892.
Nan, X., Campoy, F.J., Bird, A., 1997. MeCP2 is a transcriptional repressor with abundant binding sites in genomic chromatin. Cell 88, 471–481.
Nan, X., Ng, H.H., Johnson, C.A., Laherty, C.D., Turner, B.M., Eisenman, R.N., Bird, A., 1998. Transcriptional repression by the methyl-CpG-binding protein MeCP2 involves a histone deacetylase complex. Nature 393, 386–389.
Nawaz, Z., Lonard, D.M., Smith, C.L., Lev-Lehman, E., Tsai, S.Y., Tsai, M.J., O'Malley, B. W., 1999. The Angelman syndrome-associated protein, E6-AP, is a coactivator for the nuclear hormone receptor superfamily. Mol. Cell. Biol. 19, 1182–1189.
Nelson, E.D., Kavalali, E.T., Monteggia, L.M., 2006. MeCP2-dependent transcriptional repression regulates excitatory neurotransmission. Curr. Biol. 16, 710–716.
Nicholls, R.D., Knoll, J.H., Butler, M.G., Karam, S., Lalande, M., 1989. Genetic imprinting suggested by maternal heterodisomy in nondeletion Prader-Willi syndrome. Nature 342, 281–285.
Noble, M.E., Endicott, J.A., Johnson, L.N., 2004. Protein kinase inhibitors: insights into drug design from structure. Science 303, 1800–1805.
Noor, A., Dupuis, L., Mittal, K., Lionel, A.C., Marshall, C.R., Scherer, S.W., Stockley, T., Vincent, J.B., Mendoza-Londono, R., Stavropoulos, D.J., 2015. 15q11.2 duplication encompassing only the UBE3A gene is associated with developmental delay and neuropsychiatric phenotypes. Hum. Mutat. 36, 689–693.
Nott, A., Cheng, J., Gao, F., Lin, Y.T., Gjoneska, E., Ko, T., Minhas, P., Zamudio, A.V., Meng, J., Zhang, F., Jin, P., Tsai, L.H., 2016. Histone deacetylase 3 associates with MeCP2 to regulate FOXO and social behavior. Nat. Neurosci. 19, 1497–1505.
Novara, F., Simonati, A., Sicca, F., Battini, R., Fiori, S., Contaldo, A., Criscuolo, L., Zuffardi, O., Ciccone, R., 2014. MECP2 duplication phenotype in symptomatic females: report of three further cases. Mol. Cytogenet. 7, 10.
Nuber, U., Schwarz, S.E., Scheffner, M., 1998. The ubiquitin-protein ligase E6-associated protein (E6-AP) serves as its own substrate. Eur. J. Biochem. 254, 643–649.
O'Leary, H.M., Kaufmann, W.E., Barnes, K.V., Rakesh, K., Kapur, K., Tarquinio, D.C., Cantwell, N.G., Roche, K.J., Rose, S.A., Walco, A.C., Bruck, N.M., Bazin, G.A., Holm, I.A., Alexander, M.E., Swanson, L.C., Baczewski, L.M., Poon, C., Mayor Torres, J.M., Nelson 3rd, C.A., Sahin, M., 2018. Placebo-controlled crossover assessment of mecasermin for the treatment of Rett syndrome. Ann. Clin. Transl. Neurol. 5, 323–332.
Ogier, M., Wang, H., Hong, E., Wang, Q., Greenberg, M.E., Katz, D.M., 2007. Brain-derived neurotrophic factor expression and respiratory function improve after ampakine treatment in a mouse model of Rett syndrome. J. Neurosci. 27, 10912–10917.
Okamoto, P.M., Gamby, C., Wells, D., Fallon, J., Vallee, R.B., 2001. Dynamin isoform-specific interaction with the shank/ProSAP scaffolding proteins of the postsynaptic density and actin cytoskeleton. J. Biol. Chem. 276, 48458–48465.
Okamoto, N., Kubota, T., Nakamura, Y., Murakami, R., Nishikubo, T., Tanaka, I., Takahashi, Y., Hayashi, S., Imoto, I., Inazawa, J., Hosokai, N., Kohsaka, S., Uchino, S., 2007. 22q13 Microduplication in two patients with common clinical manifestations: a recognizable syndrome? Am. J. Med. Genet. A 143A, 2804–2809.
Oliver, C., Berg, K., Moss, J., Arron, K., Burbidge, C., 2011. Delineation of behavioral phenotypes in genetic syndromes: characteristics of autism spectrum disorder, affect and hyperactivity. J. Autism Dev. Disord. 41, 1019–1032.
Orefice, L.L., Zimmerman, A.L., Chirila, A.M., Sleboda, S.J., Head, J.P., Ginty, D.D., 2016. Peripheral mechanosensory neuron dysfunction underlies tactile and behavioral deficits in mouse models of ASDs. Cell 166, 299–313.
Papp, B., Pal, C., Hurst, L.D., 2003. Dosage sensitivity and the evolution of gene families in yeast. Nature 424, 194–197.
Park, H., Poo, M.M., 2013. Neurotrophin regulation of neural circuit development and function. Nat. Rev. Neurosci. 14, 7–23.
Park, J., Al-Ramahi, I., Tan, Q., Mollema, N., Diaz-Garcia, J.R., Gallego-Flores, T., Lu, H. C., Lagalwar, S., Duvick, L., Kang, H., Lee, Y., Jafar-Nejad, P., Sayegh, L.S., Richman, R., Liu, X., Gao, Y., Shaw, C.A., Arthur, J.S.C., Orr, H.T., Westbrook, T.F., Botas, J., Zoghbi, H.Y., 2013. RAS-MAPK-MSK1 pathway modulates ataxin 1 protein levels and toxicity in SCA1. Nature 498, 325–331.
Pasque, V., Plath, K., 2015. X chromosome reactivation in reprogramming and in development. Curr. Opin. Cell Biol. 37, 75–83.
Patrizi, A., Picard, N., Simon, A.J., Gunner, G., Centofante, E., Andrews, N.A., Fagiolini, M., 2016. Chronic administration of the N-Methyl-D-Aspartate receptor antagonist ketamine improves rett syndrome phenotype. Biol. Psychiatry 79, 755–764.
Peca, J., Feliciano, C., Ting, J.T., Wang, W., Wells, M.F., Venkatraman, T.N., Lascola, C. D., Fu, Z., Feng, G., 2011. Shank3 mutant mice display autistic-like behaviours and striatal dysfunction. Nature 472, 437–442.
Peixoto, R.T., Wang, W., Croney, D.M., Kozorovitskiy, Y., Sabatini, B.L., 2016. Early hyperactivity and precocious maturation of corticostriatal circuits in Shank3B(-/-) mice. Nat. Neurosci. 19, 716–724.
Pelka, G.J., Watson, C.M., Radziewic, T., Hayward, M., Lahooti, H., Christodoulou, J., Tam, P.P., 2006. Mecp2 deficiency is associated with learning and cognitive deficits and altered gene activity in the hippocampal region of mice. Brain 129, 887–898.
Peters, S.U., Hundley, R.J., Wilson, A.K., Warren, Z., Vehorn, A., Carvalho, C.M., Lupski, J.R., Ramocki, M.B., 2013. The behavioral phenotype in MECP2 duplication syndrome: a comparison with idiopathic autism. Autism Res. 6, 42–50.
Phelan, M.C., 2008. Deletion 22q13.3 syndrome. Orphanet J. Rare Dis. 3, 14.
Phelan, K., McDermid, H.E., 2012. The 22q13.3 deletion syndrome (Phelan-McDermid syndrome). Mol. Syndromol. 2, 186–201.
Phelan, K., Rogers, R.C., Boccuto, L., 1993. Phelan-McDermid syndrome. In: Adam, M.P., Ardinger, H.H., Pagon, R.A., Wallace, S.E., Bean, L.J.H., Stephens, K., Amemiya, A. (Eds.), GeneReviews((R)). Seattle (WA).
Phillips, M.L., Robinson, H.A., Pozzo-Miller, L., 2019. Ventral hippocampal projections to the medial prefrontal cortex regulate social memory. Elife 8.
Pohodich, A.E., Yalamanchili, H., Raman, A.T., Wan, Y.W., Gundry, M., Hao, S., Jin, H., Tang, J., Liu, Z., Zoghbi, H.Y., 2018. Forniceal deep brain stimulation induces gene expression and splicing changes that promote neurogenesis and plasticity. Elife 7.
Potocki, L., Neira-Fresneda, J., Yuan, B., 1993. Potocki-lupski syndrome. In: Adam, M.P., Ardinger, H.H., Pagon, R.A., Wallace, S.E., Bean, L.J.H., Stephens, K., Amemiya, A. (Eds.), Eds.), GeneReviews((R)). Seattle (WA).
Potocki, L., Chen, K.S., Park, S.S., Osterholm, D.E., Withers, M.A., Kimonis, V., Summers, A.M., Meschino, W.S., Anyane-Yeboa, K., Kashork, C.D., Shaffer, L.G., Lupski, J.R., 2000. Molecular mechanism for duplication 17p11.2- the homologous recombination reciprocal of the Smith-Magenis microdeletion. Nat. Genet. 24, 84–87.
Potocki, L., Bi, W., Treadwell-Deering, D., Carvalho, C.M., Eifert, A., Friedman, E.M., Glaze, D., Krull, K., Lee, J.A., Lewis, R.A., Mendoza-Londono, R., Robbins-Furman, P., Shaw, C., Shi, X., Weissenberger, G., Withers, M., Yatsenko, S.A., Zackai, E.H., Stankiewicz, P., Lupski, J.R., 2007. Characterization of Potocki-Lupski syndrome (dup(17)(p11.2p11.2)) and delineation of a dosage-sensitive critical interval that can convey an autism phenotype. Am. J. Hum. Genet. 80, 633–649.
Pristera, A., Blomeley, C., Lopes, E., Threlfell, S., Merlini, E., Burdakov, D., Cragg, S., Guillemot, F., Ang, S.L., 2019. Dopamine neuron-derived IGF-1 controls dopamine neuron firing, skill learning, and exploration. Proc Natl Acad Sci U S A 116, 3817–3826.
Przanowski, P., Wasko, U., Zheng, Z., Yu, J., Sherman, R., Zhu, L.J., McConnell, M.J., Tushir-Singh, J., Green, M.R., Bhatnagar, S., 2018. Pharmacological reactivation of inactive X-linked Mecp2 in cerebral cortical neurons of living mice. Proc Natl Acad Sci U S A 115, 7991–7996.
Pym, E., Sasidharan, N., Thompson-Peer, K.L., Simon, D.J., Anselmo, A., Sadreyev, R., Hall, Q., Nurrish, S., Kaplan, J.M., 2017. Shank is a dose-dependent regulator of Cav1 calcium current and CREB target expression. Elife 6.
Qualmann, B., Boeckers, T.M., Jeromin, M., Gundelfinger, E.D., Kessels, M.M., 2004. Linkage of the actin cytoskeleton to the postsynaptic density via direct interactions of Abp1 with the ProSAP/Shank family. J. Neurosci. 24, 2481–2495.
Ramamoorthy, S., Nawaz, Z., 2008. E6-associated protein (E6-AP) is a dual function coactivator of steroid hormone receptors. Nucl. Recept. Signal. 6, e006.
Ramocki, M.B., Tavyev, Y.J., Peters, S.U., 2010. The MECP2 duplication syndrome. Am. J. Med. Genet. A 152A, 1079–1088.
Randall, M., Egberts, K.J., Samtani, A., Scholten, R.J., Hooft, L., Livingstone, N., Sterling-Levis, K., Woolfenden, S., Williams, K., 2018. Diagnostic tests for autism spectrum disorder (ASD) in preschool children. Cochrane Database Syst. Rev. 7, CD009044.
Rao, N.R., Abad, C., Perez, I.C., Srivastava, A.K., Young, J.I., Walz, K., 2017. Rai1 haploinsufficiency is associated with social abnormalities in mice. Biology (Basel) 6.
Reim, D., Weis, T.M., Halbedl, S., Delling, J.P., Grabrucker, A.M., Boeckers, T.M., Schmeisser, M.J., 2016. The Shank3 interaction partner ProSAPiP1 regulates postsynaptic SPAR levels and the maturation of dendritic spines in hippocampal neurons. Front. Synaptic Neurosci. 8, 13.
Reiter, L.T., Seagroves, T.N., Bowers, M., Bier, E., 2006. Expression of the Rho-GEF Pbl/ECT2 is regulated by the UBE3A E3 ubiquitin ligase. Hum. Mol. Genet. 15, 2825–2835.
Rekdal, C., Sjottem, E., Johansen, T., 2000. The nuclear factor SPBP contains different functional domains and stimulates the activity of various transcriptional activators. J. Biol. Chem. 275, 40288–40300.
Renier, N., Adams, E.L., Kirst, C., Wu, Z., Azevedo, R., Kohl, J., Autry, A.E., Kadiri, L., Umadevi Venkataraju, K., Zhou, Y., Wang, V.X., Tang, C.Y., Olsen, O., Dulac, C., Osten, P., Tessier-Lavigne, M., 2016. Mapping of brain activity by automated volume analysis of immediate early genes. Cell 165, 1789–1802.
Renthal, W., Boxer, L.D., Hrvatin, S., Li, E., Silberfeld, A., Nagy, M.A., Griffith, E.C., Vierbuchen, T., Greenberg, M.E., 2018. Characterization of human mosaic Rett syndrome brain tissue by single-nucleus RNA sequencing. Nat. Neurosci. 21, 1670–1679.
Repetto, G.M., White, L.M., Bader, P.J., Johnson, D., Knoll, J.H., 1998. Interstitial duplications of chromosome region 15q11q13: clinical and molecular characterization. Am. J. Med. Genet. 79, 82–89.
Ricard, G., Molina, J., Chrast, J., Gu, W., Gheldof, N., Pradervand, S., Schutz, F., Young, J.I., Lupski, J.R., Reymond, A., Walz, K., 2010. Phenotypic consequences of copy number variation: insights from Smith-Magenis and Potocki-Lupski syndrome mouse models. PLoS Biol. 8, e1000543.
Roberts, S.E., Dennis, N.R., Browne, C.E., Willatt, L., Woods, G., Cross, I., Jacobs, P.A., Thomas, S., 2002. Characterisation of interstitial duplications and triplications of chromosome 15q11-q13. Hum. Genet. 110, 227–234.
Rotaru, D.C., van Woerden, G.M., Wallaard, I., Elgersma, Y., 2018. Adult Ube3a gene reinstatement restores the electrophysiological deficits of prefrontal cortex layer 5 neurons in a mouse model of angelman syndrome. J. Neurosci. 38, 8011–8030.

Rougeulle, C., Glatt, H., Lalande, M., 1997. The Angelman syndrome candidate gene, UBE3A/E6-AP, is imprinted in brain. Nat. Genet. 17, 14–15.
Roze, E., Cochen, V., Sangla, S., Bienvenu, T., Roubergue, A., Leu-Semenescu, S., Vidaihet, M., 2007. Rett syndrome: an overlooked diagnosis in women with stereotypic hand movements, psychomotor retardation, Parkinsonism, and dystonia? Mov. Disord. 22, 387–389.
Rubenstein, J.L., Merzenich, M.M., 2003. Model of autism: increased ratio of excitation/inhibition in key neural systems. Genes Brain Behav. 2, 255–267.
Runte, M., Huttenhofer, A., Gross, S., Kiefmann, M., Horsthemke, B., Buiting, K., 2001. The IC-SNURF-SNRPN transcript serves as a host for multiple small nucleolar RNA species and as an antisense RNA for UBE3A. Hum. Mol. Genet. 10, 2687–2700.
Runte, M., Kroisel, P.M., Gillessen-Kaesbach, G., Varon, R., Horn, D., Cohen, M.Y., Wagstaff, J., Horsthemke, B., Buiting, K., 2004. SNURF-SNRPN and UBE3A transcript levels in patients with Angelman syndrome. Hum. Genet. 114, 553–561.
Samaco, R.C., Mandel-Brehm, C., McGraw, C.M., Shaw, C.A., McGill, B.E., Zoghbi, H.Y., 2012. Crh and Oprm1 mediate anxiety-related behavior and social approach in a mouse model of MECP2 duplication syndrome. Nat. Genet. 44, 206–211.
Samaco, R.C., McGraw, C.M., Ward, C.S., Sun, Y., Neul, J.L., Zoghbi, H.Y., 2013. Female Mecp2(+/-) mice display robust behavioral deficits on two different genetic backgrounds providing a framework for pre-clinical studies. Hum. Mol. Genet. 22, 96–109.
Sanchez-Valle, A., Pierpont, M.E., Potocki, L., 2011. The severe end of the spectrum: hypoplastic left heart in Potocki-Lupski syndrome. Am. J. Med. Genet. A 155A, 363–366.
Sanders, S.J., Ercan-Sencicek, A.G., Hus, V., Luo, R., Murtha, M.T., Moreno-De-Luca, D., Chu, S.H., Moreau, M.P., Gupta, A.R., Thomson, S.A., Mason, C.E., Bilguvar, K., Celestino-Soper, P.B., Choi, M., Crawford, E.L., Davis, L., Wright, N.R., Dhodapkar, R.M., DiCola, M., DiLullo, N.M., Fernandez, T.V., Fielding-Singh, V., Fishman, D.O., Frahm, S., Garagaloyan, R., Goh, G.S., Kammela, S., Klei, L., Lowe, J. K., Lund, S.C., McGrew, A.D., Meyer, K.A., Moffat, W.J., Murdoch, J.D., O'Roak, B.J., Ober, G.T., Pottenger, R.S., Raubeson, M.J., Song, Y., Wang, Q., Yaspan, B.L., Yu, T. W., Yurkiewicz, I.R., Beaudet, A.L., Cantor, R.M., Curland, M., Grice, D.E., Gunel, M., Lifton, R.P., Mane, S.M., Martin, D.M., Shaw, C.A., Sheldon, M., Tischfield, J.A., Walsh, C.A., Morrow, E.M., Ledbetter, D.H., Fombonne, E., Lord, C., Martin, C.L., Brooks, A.I., Sutcliffe, J.S., Cook Jr, E.H., Geschwind, D., Roeder, K., Devlin, B., State, M.W., 2011. Multiple recurrent de novo CNVs, including duplications of the 7q11.23 Williams syndrome region, are strongly associated with autism. Neuron 70, 863–885.
Sandin, S., Lichtenstein, P., Kuja-Halkola, R., Larsson, H., Hultman, C.M., Reichenberg, A., 2014. The familial risk of autism. JAMA 311, 1770–1777.
Sarasua, S.M., Dwivedi, A., Boccuto, L., Rollins, J.D., Chen, C.F., Rogers, R.C., Phelan, K., DuPont, B.R., Collins, J.S., 2011. Association between deletion size and important phenotypes expands the genomic region of interest in Phelan-McDermid syndrome (22q13 deletion syndrome). J. Med. Genet. 48, 761–766.
Sato, M., Stryker, M.P., 2010. Genomic imprinting of experience-dependent cortical plasticity by the ubiquitin ligase gene Ube3a. Proc Natl Acad Sci U S A 107, 5611–5616.
Sato, D., Lionel, A.C., Leblond, C.S., Prasad, A., Pinto, D., Walker, S., O'Connor, I., Russell, C., Drmic, I.E., Hamdan, F.F., Michaud, J.L., Endris, V., Roeth, R., Delorme, R., Huguet, G., Leboyer, M., Rastam, M., Gillberg, C., Lathrop, M., Stavropoulos, D.J., Anagnostou, E., Weksberg, R., Fombonne, E., Zwaigenbaum, L., Fernandez, B.A., Roberts, W., Rappold, G.A., Marshall, C.R., Bourgeron, T., Szatmari, P., Scherer, S.W., 2012. SHANK1 deletions in males with autism Spectrum disorder. Am. J. Hum. Genet. 90, 879–887.
Satterstrom, F.K., Kosmicki, J.A., Wang, J., Breen, M.S., De Rubeis, S., An, J.Y., Peng, M., Collins, R., Grove, J., Klei, L., Stevens, C., Reichert, J., Mulhern, M.S., Artomov, M., Gerges, S., Sheppard, B., Xu, X., Bhaduri, A., Norman, U., Brand, H., Schwartz, G., Nguyen, R., Guerrero, E.E., Dias, C., Betancur, C., Cook, E.H., Gallagher, L., Gill, M., Sutcliffe, J.S., Thurm, A., Zwick, M.E., Børglum, A.D., State, M.W., Cicek, A.E., Talkowski, M.E., Cutler, D.J., Devlin, B., Sanders, S.J., Roeder, K., Daly, M.J., Buxbaum, J.D., Consortium, A.S, Consortium, i.-B, 2020. Large-scale exome sequencing study implicates both developmental and functional changes in the neurobiology of autism. Cell.
Scheffner, M., Huibregtse, J.M., Vierstra, R.D., Howley, P.M., 1993. The HPV-16 E6 and E6-AP complex functions as a ubiquitin-protein ligase in the ubiquitination of p53. Cell 75, 495–505.
Schmeisser, M.J., Ey, E., Wegener, S., Bockmann, J., Stempel, A.V., Kuebler, A., Janssen, A.L., Udvardi, P.T., Shiban, E., Spilker, C., Balschun, D., Skryabin, B.V., Dieck, S., Smalla, K.H., Montag, D., Leblond, C.S., Faure, P., Torquet, N., Le Sourd, A. M., Toro, R., Grabrucker, A.M., Shoichet, S.A., Schmitz, D., Kreutz, M.R., Bourgeron, T., Gundelfinger, E.D., Boeckers, T.M., 2012. Autistic-like behaviours and hyperactivity in mice lacking ProSAP1/Shank2. Nature 486, 256–260.
Scoles, D.R., Minikel, E.V., Pulst, S.M., 2019. Antisense oligonucleotides: a primer. Neurol. Genet. 5, e323.
Sebat, J., Lakshmi, B., Troge, J., Alexander, J., Young, J., Lundin, P., Maner, S., Massa, H., Walker, M., Chi, M., Navin, N., Lucito, R., Healy, J., Hicks, J., Ye, K., Reiner, A., Gilliam, T.C., Trask, B., Patterson, N., Zetterberg, A., Wigler, M., 2004. Large-scale copy number polymorphism in the human genome. Science 305, 525–528.
Sebat, J., Lakshmi, B., Malhotra, D., Troge, J., Lese-Martin, C., Walsh, T., Yamrom, B., Yoon, S., Krasnitz, A., Kendall, J., Leotta, A., Pai, D., Zhang, R., Lee, Y.H., Hicks, J., Spence, S.J., Lee, A.T., Puura, K., Lehtimaki, T., Ledbetter, D., Gregersen, P.K., Bregman, J., Sutcliffe, J.S., Jobanputra, V., Chung, W., Warburton, D., King, M.C., Skuse, D., Geschwind, D.H., Gilliam, T.C., Ye, K., Wigler, M., 2007. Strong association of de novo copy number mutations with autism. Science 316, 445–449.
Seranski, P., Hoff, C., Radelof, U., Hennig, S., Reinhardt, R., Schwartz, C.E., Heiss, N.S., Poustka, A., 2001. RAI1 is a novel polyglutamine encoding gene that is deleted in Smith-Magenis syndrome patients. Gene 270, 69–76.
Shahbazian, M.D., Antalffy, B., Armstrong, D.L., Zoghbi, H.Y., 2002. Insight into Rett syndrome: MeCP2 levels display tissue- and cell-specific differences and correlate with neuronal maturation. Hum. Mol. Genet. 11, 115–124.
Shaltiel, G., Maeng, S., Malkesman, O., Pearson, B., Schloesser, R.J., Tragon, T., Rogawski, M., Gasior, M., Luckenbaugh, D., Chen, G., Manji, H.K., 2008. Evidence for the involvement of the kainate receptor subunit GluR6 (GRIK2) in mediating behavioral displays related to behavioral symptoms of mania. Mol. Psychiatry 13, 858–872.
Shcheglovitov, A., Shcheglovitova, O., Yazawa, M., Portmann, T., Shu, R., Sebastiano, V., Krawisz, A., Froehlich, W., Bernstein, J.A., Hallmayer, J.F., Dolmetsch, R.E., 2013. SHANK3 and IGF1 restore synaptic deficits in neurons from 22q13 deletion syndrome patients. Nature 503, 267–271.
Shi, S.Q., Bichell, T.J., Ihrie, R.A., Johnson, C.H., 2015. Ube3a imprinting impairs circadian robustness in Angelman syndrome models. Curr. Biol. 25, 537–545.
Shimada, S., Okamoto, N., Ito, M., Arai, Y., Momosaki, K., Togawa, M., Maegaki, Y., Sugawara, M., Shimojima, K., Osawa, M., Yamamoto, T., 2013. MECP2 duplication syndrome in both genders. Brain Dev. 35, 411–419.
Silva-Santos, S., van Woerden, G.M., Bruinsma, C.F., Mientjes, E., Jolfaei, M.A., Distel, B., Kushner, S.A., Elgersma, Y., 2015. Ube3a reinstatement identifies distinct developmental windows in a murine Angelman syndrome model. J. Clin. Invest. 125, 2069–2076.
Sittig, L.J., Carbonetto, P., Engel, K.A., Krauss, K.S., Barrios-Camacho, C.M., Palmer, A. A., 2016. Genetic background limits generalizability of genotype-phenotype relationships. Neuron 91, 1253–1259.
Skene, P.J., Illingworth, R.S., Webb, S., Kerr, A.R., James, K.D., Turner, D.J., Andrews, R., Bird, A.P., 2010. Neuronal MeCP2 is expressed at near histone-octamer levels and globally alters the chromatin state. Mol. Cell 37, 457–468.
Skogstrand, K., Hagen, C.M., Borbye-Lorenzen, N., Christiansen, M., Bybjerg-Grauholm, J., Baekvad-Hansen, M., Werge, T., Borglum, A., Mors, O., Nordentoft, M., Mortensen, P.B., Hougaard, D.M., 2019. Reduced neonatal brain-derived neurotrophic factor is associated with autism spectrum disorders. Transl. Psychiatry 9, 252.
Slager, R.E., Newton, T.L., Vlangos, C.N., Finucane, B., Elsea, S.H., 2003. Mutations in RAI1 associated with Smith-Magenis syndrome. Nat. Genet. 33, 466–468.
Smith, A.C., McGavran, L., Robinson, J., Waldstein, G., Macfarlane, J., Zonona, J., Reiss, J., Lahr, M., Allen, L., Magenis, E., 1986. Interstitial deletion of (17) (p11.2p11.2) in nine patients. Am. J. Med. Genet. 24, 393–414.
Smith, A.C., Gropman, A.L., Bailey-Wilson, J.E., Goker-Alpan, O., Elsea, S.H., Blancato, J., Lupski, J.R., Potocki, L., 2002. Hypercholesterolemia in children with Smith-Magenis syndrome: del (17) (p11.2p11.2). Genet. Med. 4, 118–125.
Smith, S.E., Zhou, Y.D., Zhang, G., Jin, Z., Stoppel, D.C., Anderson, M.P., 2011. Increased gene dosage of Ube3a results in autism traits and decreased glutamate synaptic transmission in mice. Sci. Transl. Med. 3, 103ra197.
Soler-Alfonso, C., Motil, K.J., Turk, C.L., Robbins-Furman, P., Friedman, E.M., Zhang, F., Lupski, J.R., Fraley, J.K., Potocki, L., 2011. Potocki-Lupski syndrome: a microduplication syndrome associated with oropharyngeal dysphagia and failure to thrive. J. Pediatr. 158 (655-659), e652.
Sonzogni, M., Wallaard, I., Santos, S.S., Kingma, J., du Mee, D., van Woerden, G.M., Elgersma, Y., 2018. A behavioral test battery for mouse models of Angelman syndrome: a powerful tool for testing drugs and novel Ube3a mutants. Mol. Autism 9, 47.
Sonzogni, M., Hakonen, J., Bernabe Kleijn, M., Silva-Santos, S., Judson, M.C., Philpot, B. D., van Woerden, G.M., Elgersma, Y., 2019. Delayed loss of UBE3A reduces the expression of Angelman syndrome-associated phenotypes. Mol. Autism 10, 23.
Soorya, L., Kolevzon, A., Zweifach, J., Lim, T., Dobry, Y., Schwartz, L., Frank, Y., Wang, A.T., Cai, G., Parkhomenko, E., Halpern, D., Grodberg, D., Angarita, B., Willner, J.P., Yang, A., Canitano, R., Chaplin, W., Betancur, C., Buxbaum, J.D., 2013. Prospective investigation of autism and genotype-phenotype correlations in 22q13 deletion syndrome and SHANK3 deficiency. Mol. Autism 4, 18.
Sripathy, S., Leko, V., Adrianse, R.L., Loe, T., Foss, E.J., Dalrymple, E., Lao, U., Gatbonton-Schwager, T., Carter, K.T., Payer, B., Paddison, P.J., Grady, W.M., Lee, J. T., Bartolomei, M.S., Bedalov, A., 2017. Screen for reactivation of MeCP2 on the inactive X chromosome identifies the BMP/TGF-beta superfamily as a regulator of XIST expression. Proc Natl Acad Sci U S A 114, 1619–1624.
Steffenburg, S., Gillberg, C., Hellgren, L., Andersson, L., Gillberg, I.C., Jakobsson, G., Bohman, M., 1989. A twin study of autism in Denmark, Finland, Iceland, Norway and Sweden. J. Child Psychol. Psychiatry 30, 405–416.
Sugino, K., Hempel, C.M., Okaty, B.W., Arnson, H.A., Kato, S., Dani, V.S., Nelson, S.B., 2014. Cell-type-specific repression by methyl-CpG-binding protein 2 is biased toward long genes. J. Neurosci. 34, 12877–12883.
Sun, J., Zhu, G., Liu, Y., Standley, S., Ji, A., Tunuguntla, R., Wang, Y., Claus, C., Luo, Y., Baudry, M., Bi, X., 2015. UBE3A regulates synaptic plasticity and learning and memory by controlling SK2 channel endocytosis. Cell Rep. 12, 449–461.
Sun, A.X., Yuan, Q., Fukuda, M., Yu, W., Yan, H., Lim, G.G.Y., Nai, M.H., D'Agostino, G. A., Tran, H.D., Itahana, Y., Wang, D., Lokman, H., Itahana, K., Lim, S.W.L., Tang, J., Chang, Y.Y., Zhang, M., Cook, S.A., Rackham, O.J.L., Lim, C.T., Tan, E.K., Ng, H.H., Lim, K.L., Jiang, Y.H., Je, H.S., 2019. Potassium channel dysfunction in human neuronal models of Angelman syndrome. Science 366, 1486–1492.
Sutcliffe, J.S., Nakao, M., Christian, S., Orstavik, K.H., Tommerup, N., Ledbetter, D.H., Beaudet, A.L., 1994. Deletions of a differentially methylated CpG island at the SNRPN gene define a putative imprinting control region. Nat. Genet. 8, 52–58.

Sztainberg, Y., Chen, H.M., Swann, J.W., Hao, S., Tang, B., Wu, Z., Tang, J., Wan, Y.W., Liu, Z., Rigo, F., Zoghbi, H.Y., 2015. Reversal of phenotypes in MECP2 duplication mice using genetic rescue or antisense oligonucleotides. Nature 528, 123–126.
Sztainberg, Y., Zoghbi, H.Y., 2016. Lessons learned from studying syndromic autism spectrum disorders. Nat. Neurosci. 19, 1408–1417.
Tammimies, K., Marshall, C.R., Walker, S., Kaur, G., Thiruvahindrapuram, B., Lionel, A. C., Yuen, R.K., Uddin, M., Roberts, W., Weksberg, R., Woodbury-Smith, M., Zwaigenbaum, L., Anagnostou, E., Wang, Z., Wei, J., Howe, J.L., Gazzellone, M.J., Lau, L., Sung, W.W., Whitten, K., Vardy, C., Crosbie, V., Tsang, B., D'Abate, L., Tong, W.W., Luscombe, S., Doyle, T., Carter, M.T., Szatmari, P., Stuckless, S., Merico, D., Stavropoulos, D.J., Scherer, S.W., Fernandez, B.A., 2015. Molecular Diagnostic Yield of Chromosomal Microarray Analysis and Whole-Exome Sequencing in Children With Autism Spectrum Disorder. JAMA 314, 895–903.
Tang, S.S., Fernandez, D., Lazarou, L.P., Singh, R., Fallon, P., 2012. MECP2 triplication in 3 brothers - a rarely described cause of familial neurological regression in boys. Eur. J. Paediatr. Neurol. 16, 209–212.
Thibert, R.L., Larson, A.M., Hsieh, D.T., Raby, A.R., Thiele, E.A., 2013. Neurologic manifestations of Angelman syndrome. Pediatr. Neurol. 48, 271–279.
Thomas, N.S., Browne, C.E., Oley, C., Healey, S., Crolla, J.A., 1999. Investigation of a cryptic interstitial duplication involving the Prader-Willi/Angelman syndrome critical region. Hum. Genet. 105, 384–387.
Tillotson, R., Selfridge, J., Koerner, M.V., Gadalla, K.K.E., Guy, J., De Sousa, D., Hector, R.D., Cobb, S.R., Bird, A., 2017. Radically truncated MeCP2 rescues Rett syndrome-like neurological defects. Nature 550, 398–401.
Toro, R., Konyukh, M., Delorme, R., Leblond, C., Chaste, P., Fauchereau, F., Coleman, M., Leboyer, M., Gillberg, C., Bourgeron, T., 2010. Key role for gene dosage and synaptic homeostasis in autism spectrum disorders. Trends Genet. 26, 363–372.
Trappe, R., Laccone, F., Cobilanschi, J., Meins, M., Huppke, P., Hanefeld, F., Engel, W., 2001. MECP2 mutations in sporadic cases of Rett syndrome are almost exclusively of paternal origin. Am. J. Hum. Genet. 68, 1093–1101.
Treadwell-Deering, D.E., Powell, M.P., Potocki, L., 2010. Cognitive and behavioral characterization of the Potocki-Lupski syndrome (duplication 17p11.2). J. Dev. Behav. Pediatr. 31, 137–143.
Tronche, F., Kellendonk, C., Kretz, O., Gass, P., Anlag, K., Orban, P.C., Bock, R., Klein, R., Schutz, G., 1999. Disruption of the glucocorticoid receptor gene in the nervous system results in reduced anxiety. Nat. Genet. 23, 99–103.
Tropea, D., Giacometti, E., Wilson, N.R., Beard, C., McCurry, C., Fu, D.D., Flannery, R., Jaenisch, R., Sur, M., 2009. Partial reversal of Rett Syndrome-like symptoms in MeCP2 mutant mice. Proc Natl Acad Sci U S A 106, 2029–2034.
Tu, J.C., Xiao, B., Yuan, J.P., Lanahan, A.A., Leoffert, K., Li, M., Linden, D.J., Worley, P. F., 1998. Homer binds a novel proline-rich motif and links group 1 metabotropic glutamate receptors with IP3 receptors. Neuron 21, 717–726.
Tu, J.C., Xiao, B., Naisbitt, S., Yuan, J.P., Petralia, R.S., Brakeman, P., Doan, A., Aakalu, V.K., Lanahan, A.A., Sheng, M., Worley, P.F., 1999. Coupling of mGluR/Homer and PSD-95 complexes by the Shank family of postsynaptic density proteins. Neuron 23, 583–592.
Uchino, S., Wada, H., Honda, S., Nakamura, Y., Ondo, Y., Uchiyama, T., Tsutsumi, M., Suzuki, E., Hirasawa, T., Kohsaka, S., 2006. Direct interaction of post-synaptic density-95/Dlg/ZO-1 domain-containing synaptic molecule Shank3 with GluR1 alpha-amino-3-hydroxy-5-methyl-4-isoxazole propionic acid receptor. J. Neurochem. 97, 1203–1214.
Uemura, T., Mori, H., Mishina, M., 2004. Direct interaction of GluRdelta2 with Shank scaffold proteins in cerebellar Purkinje cells. Mol. Cell. Neurosci. 26, 330–341.
Ure, K., Lu, H., Wang, W., Ito-Ishida, A., Wu, Z., He, L.J., Sztainberg, Y., Chen, W., Tang, J., Zoghbi, H.Y., 2016. Restoration of Mecp2 expression in GABAergic neurons is sufficient to rescue multiple disease features in a mouse model of Rett syndrome. Elife 5.
Urraca, N., Cleary, J., Brewer, V., Pivnick, E.K., McVicar, K., Thibert, R.L., Schanen, N.C., Esmer, C., Lamport, D., Reiter, L.T., 2013. The interstitial duplication 15q11.2-q13 syndrome includes autism, mild facial anomalies and a characteristic EEG signature. Autism Res. 6, 268–279.
van der Zwaag, B., Franke, L., Poot, M., Hochstenbach, R., Spierenburg, H.A., Vorstman, J.A., van Daalen, E., de Jonge, M.V., Verbeek, N.E., Brilstra, E.H., van' t Slot, R., Ophoff, R.A., van Es, M.A., Blauw, H.M., Veldink, J.H., Buizer-Voskamp, J. E., Beemer, F.A., van den Berg, L.H., Wijmenga, C., van Amstel, H.K., van Engeland, H., Burbach, J.P., Staal, W.G., 2009. Gene-network analysis identifies susceptibility genes related to glycobiology in autism. PLoS One 4, e5324.
Van Esch, H., Bauters, M., Ignatius, J., Jansen, M., Raynaud, M., Hollanders, K., Lugtenberg, D., Bienvenu, T., Jensen, L.R., Gecz, J., Moraine, C., Marynen, P., Fryns, J.P., Froyen, G., 2005. Duplication of the MECP2 region is a frequent cause of severe mental retardation and progressive neurological symptoms in males. Am. J. Hum. Genet. 77, 442–453.
van Woerden, G.M., Harris, K.D., Hojjati, M.R., Gustin, R.M., Qiu, S., de Avila Freire, R., Jiang, Y.H., Elgersma, Y., Weeber, E.J., 2007. Rescue of neurological deficits in a mouse model for Angelman syndrome by reduction of alphaCaMKII inhibitory phosphorylation. Nat. Neurosci. 10, 280–282.
Verhoeven, W.M., Egger, J.I., Willemsen, M.H., de Leijer, G.J., Kleefstra, T., 2012. Phelan-McDermid syndrome in two adult brothers: atypical bipolar disorder as its psychopathological phenotype? Neuropsychiatr. Dis. Treat. 8, 175–179.
Villard, L., Kpebe, A., Cardoso, C., Chelly, P.J., Tardieu, P.M., Fontes, M., 2000. Two affected boys in a Rett syndrome family: clinical and molecular findings. Neurology 55, 1188–1193.
Vogel Ciernia, A., Pride, M.C., Durbin-Johnson, B., Noronha, A., Chang, A., Yasui, D.H., Crawley, J.N., LaSalle, J.M., 2017. Early motor phenotype detection in a female mouse model of Rett syndrome is improved by cross-fostering. Hum. Mol. Genet. 26, 1839–1854.
Vu, T.H., Hoffman, A.R., 1997. Imprinting of the Angelman syndrome gene, UBE3A, is restricted to brain. Nat. Genet. 17, 12–13.
Wallace, M.L., Burette, A.C., Weinberg, R.J., Philpot, B.D., 2012. Maternal loss of Ube3a produces an excitatory/inhibitory imbalance through neuron type-specific synaptic defects. Neuron 74, 793–800.
Walz, K., Caratini-Rivera, S., Bi, W., Fonseca, P., Mansouri, D.L., Lynch, J., Vogel, H., Noebels, J.L., Bradley, A., Lupski, J.R., 2003. Modeling del(17)(p11.2p11.2) and dup (17)(p11.2p11.2) contiguous gene syndromes by chromosome engineering in mice: phenotypic consequences of gene dosage imbalance. Mol. Cell. Biol. 23, 3646–3655.
Walz, K., Spencer, C., Kaasik, K., Lee, C.C., Lupski, J.R., Paylor, R., 2004. Behavioral characterization of mouse models for Smith-Magenis syndrome and dup(17)(p11.2p11.2). Hum. Mol. Genet. 13, 367–378.
Walz, K., Paylor, R., Yan, J., Bi, W., Lupski, J.R., 2006. Rai1 duplication causes physical and behavioral phenotypes in a mouse model of dup(17)(p11.2p11.2). J. Clin. Invest. 116, 3035–3041.
Wang, X., McCoy, P.A., Rodriguiz, R.M., Pan, Y., Je, H.S., Roberts, A.C., Kim, C.J., Berrios, J., Colvin, J.S., Bousquet-Moore, D., Lorenzo, I., Wu, G., Weinberg, R.J., Ehlers, M.D., Philpot, B.D., Beaudet, A.L., Wetsel, W.C., Jiang, Y.H., 2011. Synaptic dysfunction and abnormal behaviors in mice lacking major isoforms of Shank3. Hum. Mol. Genet. 20, 3093–3108.
Wang, X., Xu, Q., Bey, A.L., Lee, Y., Jiang, Y.H., 2014. Transcriptional and functional complexity of Shank3 provides a molecular framework to understand the phenotypic heterogeneity of SHANK3 causing autism and Shank3 mutant mice. Mol. Autism 5, 30.
Wang, J., Wegener, J.E., Huang, T.W., Sripathy, S., De Jesus-Cortes, H., Xu, P., Tran, S., Knobbe, W., Leko, V., Britt, J., Starwalt, R., McDaniel, L., Ward, C.S., Parra, D., Newcomb, B., Lao, U., Nourigat, C., Flowers, D.A., Cullen, S., Jorstad, N.L., Yang, Y., Glaskova, L., Vingeau, S., Kozlitina, J., Yetman, M.J., Jankowsky, J.L., Reichardt, S. D., Reichardt, H.M., Gartner, J., Bartolomei, M.S., Fang, M., Loeb, K., Keene, C.D., Bernstein, I., Goodell, M., Brat, D.J., Huppke, P., Neul, J.L., Bedalov, A., Pieper, A.A., 2015. Wild-type microglia do not reverse pathology in mouse models of Rett syndrome. Nature 521, E1–4.
Wang, X., Bey, A.L., Katz, B.M., Badea, A., Kim, N., David, L.K., Duffney, L.J., Kumar, S., Mague, S.D., Hulbert, S.W., Dutta, N., Hayrapetyan, V., Yu, C., Gaidis, E., Zhao, S., Ding, J.D., Xu, Q., Chung, L., Rodriguiz, R.M., Wang, F., Weinberg, R.J., Wetsel, W. C., Dzirasa, K., Yin, H., Jiang, Y.H., 2016. Altered mGluR5-Homer scaffolds and corticostriatal connectivity in a Shank3 complete knockout model of autism. Nat. Commun. 7, 11459.
Wang, W., Li, C., Chen, Q., van der Goes, M.S., Hawrot, J., Yao, A.Y., Gao, X., Lu, C., Zang, Y., Zhang, Q., Lyman, K., Wang, D., Guo, B., Wu, S., Gerfen, C.R., Fu, Z., Feng, G., 2017a. Striatopallidal dysfunction underlies repetitive behavior in Shank3-deficient model of autism. J. Clin. Invest. 127, 1978–1990.
Wang, Y., Liu, X., Zhou, L., Duong, D., Bhuripanyo, K., Zhao, B., Zhou, H., Liu, R., Bi, Y., Kiyokawa, H., Yin, J., 2017b. Identifying the ubiquitination targets of E6AP by orthogonal ubiquitin transfer. Nat. Commun. 8, 2232.
Wang, J.B., Aryal, M., Zhong, Q., Vyas, D.B., Airan, R.D., 2018. Noninvasive ultrasonic drug uncaging maps whole-brain functional networks. Neuron 100 (728-738), e727.
Wang, L., Adamski, C.J., Bondar, V.V., Craigen, E., Collette, J.R., Pang, K., Han, K., Jain, A., Jung, Sung Y., Liu, Z., Sifers, R.N., Holder Jr, J.L., Zoghbi, H.Y., 2019a. A kinome-wide RNAi screen identifies ERK2 as a druggable regulator of Shank3 stability. Mol. Psychiatry.
Wang, L., Pang, K., Han, K., Adamski, C.J., Wang, W., He, L., Lai, J.K., Bondar, V.V., Duman, J.G., Richman, R., Tolias, K.F., Barth, P., Palzkill, T., Liu, Z., Holder Jr, J.L., Zoghbi, H.Y., 2019b. An autism-linked missense mutation in SHANK3 reveals the modularity of Shank3 function. Mol. Psychiatry.
Watt, J.L., Olson, I.A., Johnston, A.W., Ross, H.S., Couzin, D.A., Stephen, G.S., 1985. A familial pericentric inversion of chromosome 22 with a recombinant subject illustrating a' pure' partial monosomy syndrome. J. Med. Genet. 22, 283–287.
Weeber, E.J., Jiang, Y.H., Elgersma, Y., Varga, A.W., Carrasquillo, Y., Brown, S.E., Christian, J.M., Mirnikjoo, B., Silva, A., Beaudet, A.L., Sweatt, J.D., 2003. Derangements of hippocampal calcium/calmodulin-dependent protein kinase II in a mouse model for Angelman mental retardation syndrome. J. Neurosci. 23, 2634–2644.
Wegiel, J., Schanen, N.C., Cook, E.H., Sigman, M., Brown, W.T., Kuchna, I., Nowicki, K., Wegiel, J., Imaki, H., Ma, S.Y., Marchi, E., Wierzba-Bobrowicz, T., Chauhan, A., Chauhan, V., Cohen, I.L., London, E., Flory, M., Lach, B., Wisniewski, T., 2012. Differences between the pattern of developmental abnormalities in autism associated with duplications 15q11.2-q13 and idiopathic autism. J Neuropathol Exp Neurol 71, 382–397.
Weissbourd, B., Ren, J., DeLoach, K.E., Guenthner, C.J., Miyamichi, K., Luo, L., 2014. Presynaptic partners of dorsal raphe serotonergic and GABAergic neurons. Neuron 83, 645–662.
Wen, Z., Cheng, T.L., Li, G.Z., Sun, S.B., Yu, S.Y., Zhang, Y., Du, Y.S., Qiu, Z., 2017. Identification of autism-related MECP2 mutations by whole-exome sequencing and functional validation. Mol. Autism 8, 43.
Wendholt, D., Spilker, C., Schmitt, A., Dolnik, A., Smalla, K.H., Proepper, C., Bockmann, J., Sobue, K., Gundelfinger, E.D., Kreutz, M.R., Boeckers, T.M., 2006. ProSAP-interacting protein 1 (ProSAPiP1), a novel protein of the postsynaptic density that links the spine-associated Rap-Gap (SPAR) to the scaffolding protein ProSAP2/Shank3. J. Biol. Chem. 281, 13805–13816.
Williams, C.A., 2005. Neurological aspects of the Angelman syndrome. Brain Dev. 27, 88–94.
Wilson, H.L., Wong, A.C., Shaw, S.R., Tse, W.Y., Stapleton, G.A., Phelan, M.C., Hu, S., Marshall, J., McDermid, H.E., 2003. Molecular characterisation of the 22q13 deletion syndrome supports the role of haploinsufficiency of SHANK3/PROSAP2 in the major neurological symptoms. J. Med. Genet. 40, 575–584.

Wyszynski, M., Kim, E., Dunah, A.W., Passafaro, M., Valtschanoff, J.G., Serra-Pages, C., Streuli, M., Weinberg, R.J., Sheng, M., 2002. Interaction between GRIP and liprin-alpha/SYD2 is required for AMPA receptor targeting. Neuron 34, 39–52.

Yan, J., Bi, W., Lupski, J.R., 2007. Penetrance of craniofacial anomalies in mouse models of Smith-Magenis syndrome is modified by genomic sequence surrounding Rai1: not all null alleles are alike. Am. J. Hum. Genet. 80, 518–525.

Yashiro, K., Riday, T.T., Condon, K.H., Roberts, A.C., Bernardo, D.R., Prakash, R., Weinberg, R.J., Ehlers, M.D., Philpot, B.D., 2009. Ube3a is required for experience-dependent maturation of the neocortex. Nat. Neurosci. 12, 777–783.

Yen, H.C., Elledge, S.J., 2008. Identification of SCF ubiquitin ligase substrates by global protein stability profiling. Science 322, 923–929.

Yi, J.J., Berrios, J., Newbern, J.M., Snider, W.D., Philpot, B.D., Hahn, K.M., Zylka, M.J., 2015. An autism-linked mutation disables phosphorylation control of UBE3A. Cell 162, 795–807.

Yi, F., Danko, T., Botelho, S.C., Patzke, C., Pak, C., Wernig, M., Sudhof, T.C., 2016. Autism-associated SHANK3 haploinsufficiency causes Ih channelopathy in human neurons. Science 352, aaf2669.

Yoo, T., Cho, H., Park, H., Lee, J., Kim, E., 2019a. Shank3 exons 14-16 deletion in glutamatergic neurons leads to social and repetitive behavioral deficits associated with increased cortical layer 2/3 neuronal excitability. Front. Cell. Neurosci. 13, 458.

Yoo, Y.E., Yoo, T., Lee, S., Lee, J., Kim, D., Han, H.M., Bae, Y.C., Kim, E., 2019b. Shank3 mice carrying the human Q321R mutation display enhanced self-grooming, abnormal electroencephalogram patterns, and suppressed neuronal excitability and seizure susceptibility. Front. Mol. Neurosci. 12, 155.

Young, D., Nagarajan, L., de Klerk, N., Jacoby, P., Ellaway, C., Leonard, H., 2007. Sleep problems in Rett syndrome. Brain Dev. 29, 609–616.

Yusufzai, T.M., Wolffe, A.P., 2000. Functional consequences of Rett syndrome mutations on human MeCP2. Nucleic Acids Res. 28, 4172–4179.

Yusupov, R., Roberts, A.E., Lacro, R.V., Sandstrom, M., Ligon, A.H., 2011. Potocki-Lupski syndrome: an inherited dup(17)(p11.2p11.2) with hypoplastic left heart. Am. J. Med. Genet. A 155A, 367–371.

Zeier, Z., Kumar, A., Bodhinathan, K., Feller, J.A., Foster, T.C., Bloom, D.C., 2009. Fragile X mental retardation protein replacement restores hippocampal synaptic function in a mouse model of fragile X syndrome. Gene Ther. 16, 1122–1129.

Zhang, H., Maximov, A., Fu, Y., Xu, F., Tang, T.S., Tkatch, T., Surmeier, D.J., Bezprozvanny, I., 2005. Association of CaV1.3 L-type calcium channels with Shank. J. Neurosci. 25, 1037–1049.

Zhang, F., Potocki, L., Sampson, J.B., Liu, P., Sanchez-Valle, A., Robbins-Furman, P., Navarro, A.D., Wheeler, P.G., Spence, J.E., Brasington, C.K., Withers, M.A., Lupski, J. R., 2010. Identification of uncommon recurrent Potocki-Lupski syndrome-associated duplications and the distribution of rearrangement types and mechanisms in PTLS. Am. J. Hum. Genet. 86, 462–470.

Zhou, Y., Kaiser, T., Monteiro, P., Zhang, X., Van der Goes, M.S., Wang, D., Barak, B., Zeng, M., Li, C., Lu, C., Wells, M., Amaya, A., Nguyen, S., Lewis, M., Sanjana, N., Zhou, Y., Zhang, M., Zhang, F., Fu, Z., Feng, G., 2016. Mice with Shank3 mutations associated with ASD and schizophrenia display both shared and distinct defects. Neuron 89, 147–162.

Ziff, E.B., 1997. Enlightening the postsynaptic density. Neuron 19, 1163–1174.

Zody, M.C., Garber, M., Adams, D.J., Sharpe, T., Harrow, J., Lupski, J.R., Nicholson, C., Searle, S.M., Wilming, L., Young, S.K., Abouelleil, A., Allen, N.R., Bi, W., Bloom, T., Borowsky, M.L., Bugalter, B.E., Butler, J., Chang, J.L., Chen, C.K., Cook, A., Corum, B., Cuomo, C.A., de Jong, P.J., DeCaprio, D., Dewar, K., FitzGerald, M., Gilbert, J., Gibson, R., Gnerre, S., Goldstein, S., Grafham, D.V., Grocock, R., Hafez, N., Hagopian, D.S., Hart, E., Norman, C.H., Humphray, S., Jaffe, D.B., Jones, M., Kamal, M., Khodiyar, V.K., LaButti, K., Laird, G., Lehoczky, J., Liu, X., Lokyitsang, T., Loveland, J., Lui, A., Macdonald, P., Major, J.E., Matthews, L., Mauceli, E., McCarroll, S.A., Mihalev, A.H., Mudge, J., Nguyen, C., Nicol, R., O'Leary, S.B., Osoegawa, K., Schwartz, D.C., Shaw-Smith, C., Stankiewicz, P., Steward, C., Swarbreck, D., Venkataraman, V., Whittaker, C.A., Yang, X., Zimmer, A. R., Bradley, A., Hubbard, T., Birren, B.W., Rogers, J., Lander, E.S., Nusbaum, C., 2006. DNA sequence of human chromosome 17 and analysis of rearrangement in the human lineage. Nature 440, 1045–1049.

Zoghbi, H.Y., Bear, M.F., 2012. Synaptic dysfunction in neurodevelopmental disorders associated with autism and intellectual disabilities. Cold Spring Harb. Perspect. Biol. 4.

Zoghbi, H.Y., Percy, A.K., Glaze, D.G., Butler, I.J., Riccardi, V.M., 1985. Reduction of biogenic amine levels in the Rett syndrome. N. Engl. J. Med. 313, 921–924.